Efficient Removal of Arsenic and Chromium from Water by Polymer Hydrogel Adsorbents

（高分子ゲル吸着剤を使用した水からのヒ素とクロムの効率的除去）

Yu Song

Hiroshima University

Graduate School of Advanced Science and Engineering

1-4-1 Kagamiyama, Higashihiroshima, Hiroshima, Japan

739-8527

Abstract

Heavy metal ions, especially arsenic (As) and chromium (Cr), pose a substantial threat to human health and ecosystem. To deal with this issue, various techniques for removing heavy metal ions from wastewater have been developed, including chemical precipitation, ion exchange, membrane separation, and notably, adsorption technologies. Adsorption stands out for its operational simplicity, cost-effectiveness, and the potential for using low-cost, high-efficiency, and easily regenerable adsorbent materials.

Among the adsorbents, hydrogels are particularly notable. Hydrogels boast high water content, adjustable swelling properties, superior mechanical performance, and the ease of modification. Their primary roles in water treatment include: (1) Maintain structural integrity like solid substances, (2) providing nanoscale channels for the unhindered diffusion of small, water-soluble molecules, and (3) offering additional active sites through hydrogen bonding, enhancing the interaction with water-soluble molecules. This research focuses on the development of cost-effective and highly efficient removal methods and change the existence state of adsorbates in the aqueous environment for heavy metal ions removal, The research encompassed:

(1) **Efficient removal of As** via oxidation of As (III) to As (V): A cationic polymer gel, supported with oxidizing agents such as $KMnO_4$ or $K_2Cr_2O_7$, has been developed to effectively remove arsenic. This gel demonstrates the capability to adsorb both arsenite (III) and arsenate (V) through an ion exchange process, wherein the oxidizing agent converts As (III) to the more adsorbable As (V) form. Theoretically, the concentration of the oxidant within these gels can attain a significant level of up to 73.7Mol%. The D-Mn gel, embedded with MnO_4^-, and the D-Cr gel, containing $Cr_2O_7^{2-}$, exhibit impressive maximum adsorption capacities for As (III)—reaching up to 163 mg g^{-1} and 263 mg g^{-1}, respectively, better than that of many other adsorbent materials. Moreover, these gels consistently maintain an As (III) removal rate of over

85% in neutral and mildly acidic aquatic environments. The results of this study suggest that D-Mn and D-Cr gels are highly effective for adsorbing As (III), making them suitable for application in the removal of arsenic from industrial wastewater. This innovative approach combines the unique properties of the DMAPAA-Q gel with powerful oxidizing agents to offer a promising solution for mitigating arsenic pollution in aquatic environments. The oxidation of As (III) to As (V), to enhance the removal efficiency, is one of the removal methods that change the existence state of adsorbates in the aqueous environment.

(2) **Efficient removal of Cr** via reduction of Cr (VI) to Cr (III): a novel approach using ascorbic acid as a reducing agent supported by a copolymer hydrogel is introduced. Theoretically speaking, the maximum proportion of the reducing agent, ascorbic acid, in the gel can reach up to 49Mol%. This method effectively targets the removal of hexavalent chromium, Cr (VI) and could integrates the reduction and adsorption processes into a single step, streamlining the traditional chromium removal techniques while also reducing the costs. The process involves the adsorption of Cr (VI) through an ion exchange mechanism, and the removal of Cr (III), reduced from Cr (VI) by L-ascorbic acid (VC), through surface complexation and the formation of insoluble hydroxides [$Cr(OH)_3$] inside the gel. The study comprehensively investigates the influence of various parameters on the reduction and removal efficiency of the DA/DQ and DA/DQ/VC gels. These parameters include solution pH, initial Cr (VI) concentration, the presence of co-existing anions, contact time, and temperature. Notably, the gels exhibit high adsorption efficiency within a pH range of 3 to 6, due to the enhancement of the electrostatic interaction between the adsorption sites protonated by H^+ and chromium anionic species. Moreover, the adsorption capacities of gels can reach above 90 mg g^{-1} at initial concentration of 100 mg L^{-1}, with solution pH 3.This method, leveraging the unique properties of the synthesized gels, offers a promising solution for the effective removal of hexavalent chromium from heavily contaminated wastewater. The reduction of Cr (VI) to Cr (III) is also one

of the removal methods that change the existence state of adsorbates in the aqueous environment.

(3) **Simultaneous removal of As and Cr** via formation of positively charged complex ions (PCCs): The development of functional materials with enhanced adsorption capabilities and recyclability is gaining sustained attentions, which often limits their practical applications. Addressing this challenge, this study introduces a novel approach using ionic hydrogels to efficiently adsorb both cations and anions simultaneously by converting them into a stable complex form. (P.S. The formation of positively charged complex ions is also one of the removal methods that change the existence state of adsorbates in the aqueous environment.) This method significantly simplifies the adsorption process while maintaining high adsorption efficiency. Our research delved into the adsorption mechanisms of these ionic hydrogels, with a specific focus on the complex formation between arsenic and chromium in diverse environmental conditions. We conducted a thorough investigation into how various physicochemical factors influence the gel's adsorption capacities. One of the key findings was the formation of a positively charged complex in aqueous mixtures of arsenic and chromium, demonstrating a remarkable capacity for simultaneous adsorption in the binary system. The study methodically analyzed the adsorption behavior of the gels, applying various adsorption isotherms and two kinetic models to fit the experimental data. This analysis revealed that the binary systems exhibited significantly higher adsorption capacities compared to the single systems. Additionally, we observed that changes in the pH of the environment affected the stability of the As-Cr complex, subsequently influencing the gel's adsorption capacity. An intriguing outcome of our research was the discovery that the presence of other co-existing anions or cations could impact arsenic and chromium removal. It was noted that other metal ions could form positively charged complexes, occupying the adsorption sites initially intended for the As-Cr complex. This finding opens new possibilities for the removal of a broader range of contaminants using the corresponding gel materials.

List of Contents

List of Figures

List of Tables

List of Schemes

Chapter 1 Introduction

1.1 Heavy metal environmental pollution from wastewater

The rapid development of economies, population growth, and urbanization have intensified water pollution challenges.[1] This is particularly acute in developing nations.[2] Many industrial wastewaters carry a large variety of pollutants into the water environment, which makes a great threat to the human health and ecological environment. Therefore, Heavy metal contamination in aquatic environments has emerged as a major concern.[3] Heavy metals, defined as metallic elements with a density above 5 g cm^{-3} and arsenic, chromium, etc. are the most common toxic heavy metals in industrial wastewater. Many studies have shown that excessive accumulation of heavy metals will affect the human brain, lung, kidney, liver, other organs, and they are harmful to nervous or immune system.[4]

In the 21st century, China which is the largest developing country in the world has been continuously committed to the advancement of industrialization. Its economy and various industries have rapidly developed, and China was named as the "world's factory". However, with the development of industrialization, many heavy metal-contained wastewater was discharged, causing environmental problems. Notable incidents include As contamination due to the illegal discharge of wastewater in Yunnan's Yangzonghai Lake in 2008, threatening the water safety of thousands,[5] and Serious Cr slag contamination accident occurred in Qujing in Yunnan province in 2011, since the industry illegally dumped untreated Cr slag into the mountains and Nanpan River.[6] These events highlight the serious health and ecological risks posed by such pollutants.

In response, China's "12th Five-Year Plan for Comprehensive Prevention and Control of Heavy Metal Pollution" marked a decisive step towards mitigating these issues in 2011, leading to notable reductions in heavy metal emissions.[7] Despite overall

improvements, persistent challenges remain. Hence, to further strengthen the control of heavy metal pollutant discharge, in 2022, China's Ministry of Ecology and Environment proposed the “Opinions on Further Strengthening the Prevention and Control of Heavy Metal Pollution”. This document indicated the implementation of total quantity control over the emissions of five key pollutants: lead, mercury, cadmium, chromium, and arsenic.[8] Therefore, the development of heavy metal removal processes that are highly efficient, cost-effective, and practical is currently a top priority. In this study, arsenic and chromium have been selected as the primary targets for removal.

1.2 Contamination of Arsenic

1.2.1 Sources, risk, and status of Arsenic

Arsenic is often found in minerals in combination with metals and sulfur, and less frequently as a pure elemental crystal. It is more commonly found in the environment because of industrial processes and natural occurrences.[9] For instance, it is often used in the production of pesticides, herbicides, and insecticides, and in semiconductor technology due to its efficient conductivity properties.

Arsenic is notoriously toxic, particularly trivalent arsenic. Prolonged exposure to arsenic compounds can cause various health problems and is known to be carcinogenic. Arsenic compounds can also contaminate water sources, leading to serious environmental and health issues, especially in areas with high natural arsenic levels or industrial pollution. As a result, the World Health Organization has established a strict limit for As in drinking water at 10 μg L^{-1}.[10] While it is reported that arsenic, in trace amounts, is significant in human metabolic processes, its presence in the body is inevitable due to natural consumption through drinking water and food. For instance, a person weighing 50 kg may contain about 5 mg of arsenic, equating to roughly 0.1 mg per kilogram of body weight. Despite this, the strong toxicity of arsenic cannot be

overlooked.[11] Prolonged exposure to water contaminated with high concentrations of arsenic can lead to serious health issues such as skin pigmentation, hyperkeratosis, ulceration, and skin cancer, as well as adversely affecting the liver, kidneys, heart, and lungs.[12]

As shown in **Fig. 1.1**, the natural contamination of As in groundwater has been reported worldwide, and the majority of these belong to South Asian and South American regions according to the research of Shaji, et al. China is also one of the most affected countries facing health issues because of arsenic contamination.[13] In China, there have been distressing incidents of environmental pollution around mines and mass poisoning due to arsenic contamination, which have escalated into social issues. Therefore, it is highly necessary to remove arsenic efficiently.

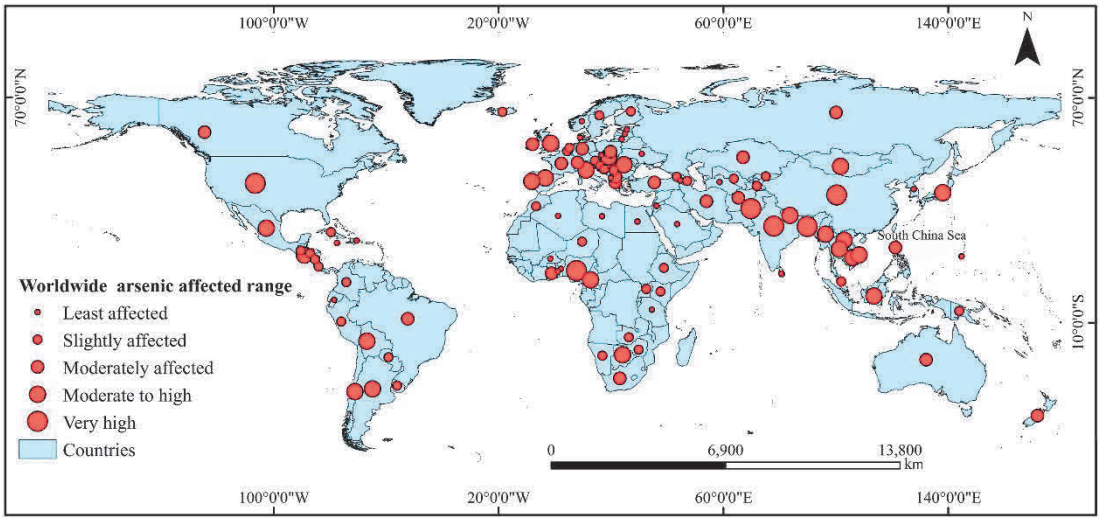

Fig. 1.1. Arsenic affected countries of the world with intensity shown by the size of the plots.[13]

1.2.2 Characteristics of Arsenic

Arsenic can form compounds in different oxidation states: -3, 0, +3, and +5. The main dissolved forms of arsenic are +3 and +5. Based on their dissociation constants, the dissociation states of these compounds as functions of pH are illustrated in **Fig. 1.2**.

As (V) exists as an anion across a broad pH range, whereas As (III) exists as H_3AsO_3 molecule in acidic environments and primarily exists as an anion at pH levels above 7. It is well-known that arsenic in its molecular state is extremely difficult to adsorb and separate, whereas arsenic in its ionic state can be removed through methods like electrostatic attraction and ion exchange. Therefore, to enhance the removal efficiency of trivalent arsenic, oxidation of arsenic is necessary.

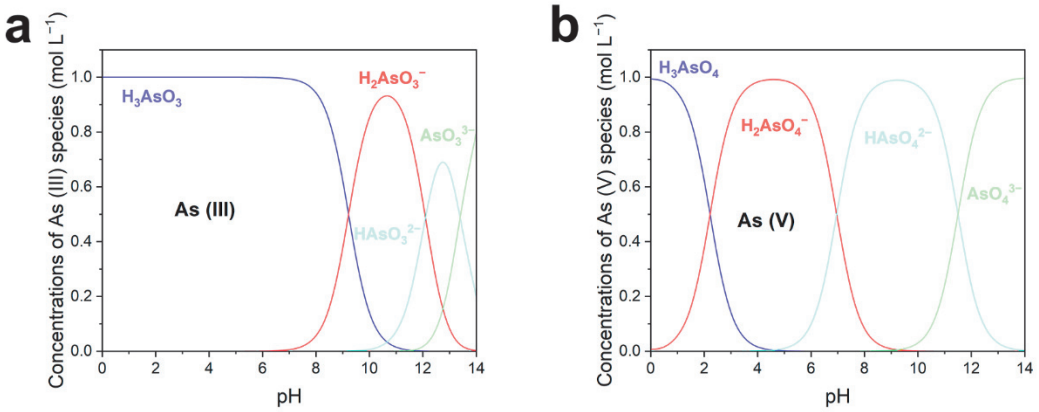

Fig. 1.2. Arsenic speciation (a) As (III) and (b) As (V) as a function of the solution pH.

1.3 Contamination of Cr

1.3.1 Sources, risk, and status of Cr

Chromium is one of the most hazardous metals that enter the environment through a variety of natural and artificial sources. Much of the environmental discharge of chromium are from industrial activities, from industrial processing and manufacturing of chemicals, minerals, steel, metal plating, leather tanning, textile dyeing, electroplating, and cement production, metallurgical and other works.[14] Chromium content in various industrial effluents sources and wastewater release is shown in **Table 1.1**. [15]

Chromium stands out as a major inorganic contaminant. Once entering the environment, Cr exists in two stable states: hexavalent chromium (Cr(VI)) and trivalent chromium (Cr (III)). Hexavalent chromium (Cr (VI)) is identified as one of

the most toxic pollutants in aquatic environments due to its high solubility, potent toxicity, mutagenicity, and carcinogenic properties. As a result, the World Health Organization has established a strict threshold for Cr in drinking water at 0.05 mg L^{-1}.[16] However, trivalent chromium is not just non-toxic but also an essential mineral for humans, with a daily requirement of 50 to 200 μg. A deficiency in trivalent chromium can lead to abnormalities in glucose metabolism, potentially causing diabetes. While trivalent chromium's toxicity is markedly reduced compared to hexavalent chromium, it's important to acknowledge that trivalent chromium can still be toxic at high concentrations.

As shown in **Fig. 1.3**, entering the 21st century, alongside China's escalating industrialization, the production of industrial wastewater has steadily risen, culminating in a peak in 2007.[17] Following this, the Chinese government-initiated measures to regulate industrial wastewater discharge. This regulatory focus was further highlighted during the "Twelfth Five-Year Plan" period (2011-2015), where stringent restrictions on the emission of heavy metal pollutants were underscored. Notably, among all heavy metals in industrial wastewater, chromium registers the highest discharge levels. Consequently, enhancing the removal efficiencies of both hexavalent and trivalent chromium has been a focus consistently promoted and supported by the government.

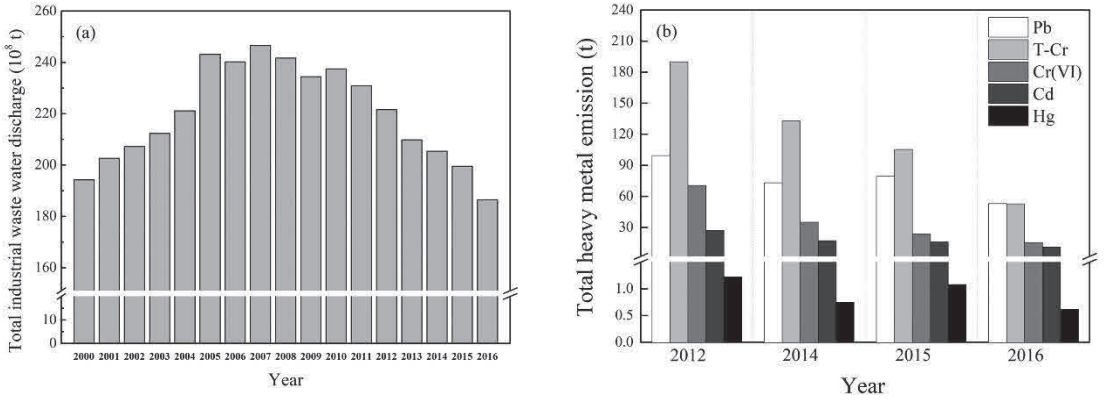

Fig. 1.3. (a) Total discharge of industrial wastewater and (b) main heavy metals.[17]

Table 1.1 Chromium content in various industrial effluents sources and wastewater release. [15]

NO.	Industrial effluents and wastewater release	Cr content (mg L^{-1}/mg kg^{-1})
1	Tannery effluents	0.7-345
2	Chromite	199-3970
3	Textile mills effluents	0.11-0.21
4	Chrome plating industry wastewater	5721.95
5	Steel industry slags	2915

1.3.2 Characteristics of Cr

Chromium exhibits a wide range of oxidation states, but the most stable and common are Cr (0), Cr (III), and Cr (VI). Based on the Cr (VI) dissociation constants, the dissociation states of these compounds as functions of pH are illustrated in **Fig. 1.4**.

In aquatic environments, Cr(VI) exists in various forms. **Fig. 1.4** demonstrates that $HCrO_4^-$ and $Cr_2O_7^{2-}$ are prevalent in the pH range of 2.0 to 6.0, CrO_4^{2-} dominates at pH levels greater than 6.0, and H_2CrO_4 becomes prominent at pH levels lower than 2.0. Notably, Cr(III) exhibits significantly lower toxicity and is prone to easy precipitation in natural settings.[18] Hence, there is an urgent requirement for the development and implementation of efficient chromium removal techniques to mitigate these environmental challenges.

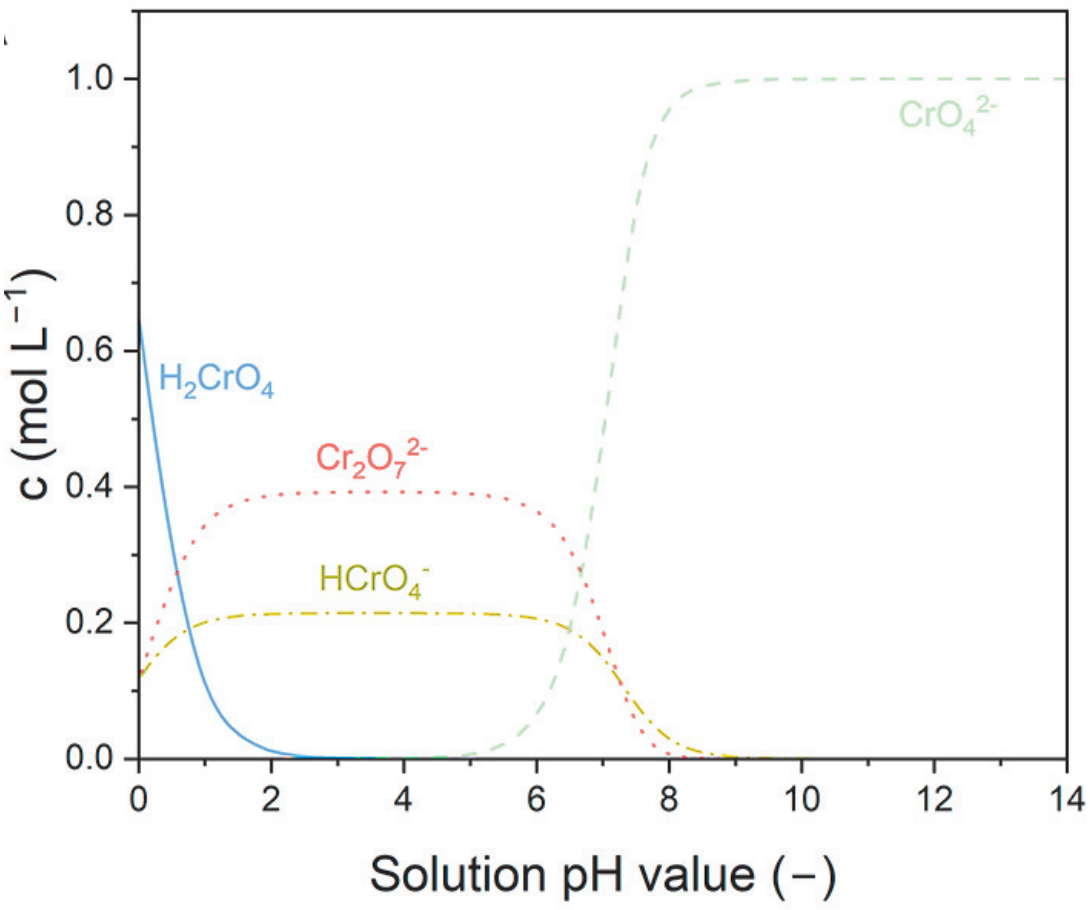

Fig. 1.4. Cr (VI) speciation as a function of the solution pH.

1.4 Conventional methods for removal of heavy metal

As global economic development progresses and environmental awareness intensifies, the issue of heavy metal pollution has garnered heightened attention from individuals, communities, and international entities alike. This growing concern has catalyzed a surge in both national and international research efforts, focused on developing effective strategies for the removal of heavy metal ions from wastewater.

1.4.1 Chemical precipitation

Chemical precipitation is a process that involves the addition of chemical agents

to water, reacting with heavy metal ions to form precipitates with low solubility, thereby facilitating their removal. This method is not only cost-effective but also widely employed in industrial wastewater treatment.[19] Chemical precipitation can be classified into several types, including hydroxide,[20,21] sulfide,[22] ferrite,[23] and chelate[24] precipitation. However, this method is characterized by slow metal precipitation and poor settling, alongside concerns about long-term environmental impacts.

1.4.2 Electrochemical treatment

Electrochemical treatment is a method leveraging electrodes in a reactor to enable electron transfer and electrochemical reactions for the recovery of heavy metals.[25] The effectiveness of an electrochemical reactor is influenced by factors like electrode material, electron mass transfer, current density, and the composition of the wastewater.[26] Prominent electrochemical treatment methods include electro-coagulation,[27] electrodeposition,[28] electroflotation,[29] electrodialysis,[30] and electrodionization.[31] However, this approach requires substantial capital investment and an expensive supply of electricity.

1.4.3 Ion-exchange

Ion exchange is a process that leverages the substitution of ions in a material with similar types of heavy metal ions found in wastewater, demonstrating high efficiency in metal ion removal. Typically, cation exchangers are employed for treating wastewater laden with heavy metal cations, whereas anion exchangers are apt for wastewater containing oxy heavy metal anion contaminants.[32] Predominant cation exchangers primarily comprise acid resins endowed with sulfonic acid groups ($-SO_3H$) and carboxylic acid groups (-COOH). Natural zeolites also exhibit inherent ion exchange capabilities. Predominant anion exchangers typically consist of alkaline

resins with tetrahedral ammonium salts, primary amine groups (-NH_2), secondary amine groups (-NHR), or tertiary amine groups (-NR_2).

The effectiveness of ion exchange resins is subject to a multitude of factors, including the pH level of the water, ambient environmental temperature, the initial concentration of heavy metal ions, the presence of other contaminants in the water, duration of the reaction, and the specific ion charge.[33] Notably, the regeneration phase of ion exchange resins necessitates the utilization of chemical eluents, leading to the generation of waste liquids and the potential risk of secondary pollution, thereby incrementally adding to the overall operational expenses. Moreover, this method is primarily suitable for treating low concentrations of metals.

1.4.4 Membrane filtration

Membrane separation, a pressure-driven separation technology, distinguishes particles based on size, solution concentration and pH, and applied pressure through a membrane material.[34] This technique is categorized into microfiltration, ultrafiltration, nanofiltration, and reverse osmosis, depending on the molecular weight cutoff.[35] The materials for membranes are primarily of two types: ceramic and polymer. Ceramic membranes, known for their structural robustness, are brittle and costly. Polymer membranes, in contrast, offer greater stability and chemical resistance. Consequently, polymer membranes are more commonly used in industrial wastewater treatment. Popular polymers employed include polyvinylidene fluoride (PVDF), polypropylene (PP), and polyethylene (PE).[36]

Membrane separation technology boasts advantages such as high efficiency, operational simplicity, and compactness.[37] However, challenges include a complex operational process, vulnerability to fouling, prolonged replacement cycles, and significant costs. These factors limit its extensive application in the treatment of heavy metal wastewater.

1.4.5 Adsorption

Adsorption utilizes the mutual forces between solid adsorbent materials and adsorbates in water, concentrating adsorbates on the adsorbent to achieve efficient separation.[38] This method is lauded for its design flexibility, ease of operation, cost-effectiveness, and reduced environmental impact, making it an effective strategy for handling heavy metal wastewater.[39] Additionally, the adsorption process is typically reversible, allowing for the regeneration of adsorbents through appropriate desorption methods for reuse.[40] Desorption and regeneration of adsorbent materials can be achieved through various approaches.[41]

Key factors influencing adsorption include the adsorbent's specific surface area, pore size distribution, and the quantity of active surface functional groups.[61]The adsorption process is fundamentally an interfacial interaction between solid and liquid phases. In physical adsorption, the material's specific surface area and pore structure are the primary determinants of performance. In chemical adsorption, the number of active surface functional groups significantly impacts adsorption efficiency. Research into the adsorption behavior between adsorbents and adsorbates is crucial in adsorption studies, providing valuable insights for designing and evaluating the performance of adsorbent materials.

1.5 Research on solid-Liquid interface adsorption mechanisms

1.5.1 Adsorption

The removal rate (R) and equilibrium adsorption capacity (Q_e) were determined as follows:

$$R=\frac{C_0-C_e}{C_0}\times 100\% \qquad (1.1)$$

$$Q_e = \frac{(C_0 - C_e)V}{M} \quad (1.2)$$

where C_0 (mg L^{-1}/mmol L^{-1}) and C_e (mg L^{-1}/mmol L^{-1}) are the initial and equilibrium concentrations, respectively, V (L) is the solution volume, and M (g) is the weight of the gel.

1.5.2 Adsorption isotherms

Adsorption isotherms are graphical representations depicting the equilibrium relationship between the quantity of adsorbate adsorbed onto a material and the residual concentration of the adsorbate in the liquid phase, under constant temperature conditions. These isotherms are vital tools for analyzing the effect of temperature on adsorption efficiency, examining the interactions between adsorbent materials and adsorbates, and forecasting the theoretical adsorption capacities of adsorbent materials.[42] Adsorption models, such as the Langmuir, Freundlich models, Dubinin-Radushkevich (D-R), and Temkin models, were used to study the adsorption isotherms.[43]

(1) Langmuir isotherm

One of the most applied adsorption isotherms models is Langmuir isotherm. The assumptions and deductions of the Langmuir models as follows: (a) monolayer adsorption; (b) the distribution of adsorption sites is homogeneous; (c) the adsorption energy is constant; (d) the interaction between adsorbate molecules is negligible.

The Langmuir equation can be written in the following linear form:

$$\frac{C_e}{Q_e} = \frac{C_e}{Q_m} + \frac{1}{K_L Q_m} \quad (1.3)$$

where C_e is the concentration of adsorbate at equilibrium (mg L^{-1}/mmol L^{-1}), Q_e is the adsorption capacity of adsorbates at equilibrium (mg g^{-1}-gel/mmol g^{-1}-gel), Q_m is the maximum adsorption capacity (mg g^{-1}-gel/mmol g^{-1}-gel), and K_L is the Langmuir constant (L mg^{-1}/L $mmol^{-1}$).

(2) Freundlich isotherm

The Freundlich isotherm model is one of the most widely used isotherm model in adsorption. In much research, the Freundlich isotherm was applied to represent the multi-layer adsorption on heterogamous surfaces.

The linear form of the Freundlich equation is expressed as follows:

$$\ln Q_e = \ln K_F + \frac{1}{n}\ln C_e \tag{1.4}$$

where K_F (mg g^{-1} (L $mg^{-1})^{1/n}$ / mmol g^{-1} (L $mmol^{-1})^{1/n}$) and n are Freundlich constants related to the adsorption capacity and favourability of adsorption, respectively.

(3) Dubinin-Radushkevich isotherm (D-R isotherm)

The D-R model was proposed as an empirical isotherm to represent the adsorption of vapours on solid. The D-R model assumes that the distribution of pores in adsorption follows the Gaussian energy distribution.

The Dubinin-Radushkevich isotherm is expressed as follows:

$$\ln Q_e = \ln Q_m - \beta\varepsilon^2 \tag{1.5}$$

$$\varepsilon = RT\ln\left(1+\frac{1}{C_e}\right) \tag{1.6}$$

$$E = \frac{1}{\sqrt{2\beta}} \tag{1.7}$$

where β (mol^2 kJ^{-2}) is the model constant and ε (kJ mol^{-1}) is the adsorption potential based on Polanyi's potential theory. The mean free energy E (kJ mol^{-1}) is frequently applied to determine whether the adsorption is dominated by physical (< 8 kJ mol^{-1}) or chemical processes (8 < E < 16 kJ mol^{-1}).

(4) Temkin isotherm

The Temkin model presumes that adsorption is a multi-layer process. Extremely high and low concentrations values of the adsorbate in liquid phase are ignored.

The Temkin model is presented as follows:

$$Q_e = \frac{RT}{b} \ln(AC_e) \tag{1.8}$$

where A (L g^{-1}) and b (J mol^{-1}) are constants.

1.5.3 Adsorption Dynamics

The adsorption process typically unfolds in three key stages:[44] (1) External diffusion or film diffusion stage, where the adsorbate from the solution enters the boundary layer of the adsorbent material through diffusion; (2) Surface or intraparticle diffusion stage, involving the migration of adsorbate, which has reached the boundary layer, across the surface or through the pores into the interior of the adsorbent; (3) The actual adsorption stage, during which the adsorbate that penetrates into the interior of the adsorbent interacts and accumulates on the material. As the adsorption stage often proceeds rapidly, the overall rate of adsorption is primarily governed by the initial two stages.

The adsorption rate is a vital measure for assessing the efficacy of adsorbent materials, thus making the exploration of adsorption kinetics critical for both evaluating adsorbent performance and designing effective adsorption systems. Kinetic models are frequently employed for non-linear data fitting to analyze the interactions between the adsorbent materials and adsorbates.

The kinetics of adsorption are commonly simulated using pseudo-first-order and pseudo-second-order kinetic models, which are instrumental in elucidating the adsorption mechanisms. These models are expressed through specific mathematical equations (1.9) and (1.10), providing a deeper understanding of the nature of adsorption processes.

$$ln(Q_e - Q_t) = lnQ_e - k_1 t \tag{1.9}$$

$$\frac{t}{Q_t} = \frac{1}{k_2 Q_e^{\,2}} + \frac{t}{Q_e} \tag{1.10}$$

where Q_e (mg g^{-1}/mmol g^{-1}) is the equilibrium adsorption capacity, Q_t (mg g^{-1}/mmol g^{-1}) is the adsorbed amount at time t, and k_1 (min^{-1}) and k_2 (g mg^{-1} min^{-1}/ g $mmol^{-1}$ min^{-1}) are the pseudo-first-order and pseudo-second-order rate constants, respectively.

1.5.4 Adsorption thermodynamics

The adsorption process, being a form of mass transfer, inevitably leads to energy changes. Consequently, temperature significantly influences the interactions between the adsorbent material and adsorbate.[45] These influences are quantifiable through thermodynamic parameters, which are crucial for understanding the spontaneity and heat exchange dynamics of the adsorption process. Key thermodynamic parameters,

including the standard Gibbs free energy change (ΔG, in kJ mol^{-1}), enthalpy change (ΔH, in kJ mol^{-1}), and entropy change (ΔS, in J mol^{-1} K^{-1}), are calculated to gain insights into these dynamics. These calculations help in evaluating the feasibility and thermodynamic nature of the adsorption process, providing a comprehensive understanding of the energy changes involved.

$$K_d = \frac{Q_e}{C_e} \tag{1.11}$$

$$\Delta G = \Delta H - T\Delta S \tag{1.12}$$

$$\Delta G = -RT\ln K_d \tag{1.13}$$

$$\ln K_d = \frac{\Delta S}{R} - \frac{\Delta H}{RT} \tag{1.14}$$

where K_d is the distribution adsorption coefficient, Q_e (mg g^{-1}/mmol g^{-1}) is the adsorption capacity per unit mass of the adsorbent, and C_e (mg L^{-1}/ mmol L^{-1}) is the equilibrium concentration.

1.6 Adsorbents

The advancement of adsorption technology hinges on the research and development of adsorbent materials. Classified by their chemical composition, adsorbent materials generally fall into categories such as carbon-based, non-metallic mineral, metallic, and polymeric materials. Each type offers distinct advantages, making them suitable for specific applications in removing contaminants from water bodies.

1.6.1 Carbon-based materials

Carbon-based materials are known for their high porosity and specific surface area. These materials, derived from coal or organic substances, undergo processes like high-temperature, high-pressure, or chemical treatments to achieve their desirable properties. In the water treatment, the most used carbonaceous adsorbents include activated carbon,[46] carbon nanotubes,[47] graphene,[48] and biochar.[49]

1.6.2 Non-metallic mineral materials

Non-metallic mineral materials, known for their high cation exchange capacity and relatively modest specific surface area in proportion to particle size, are abundant and cost-effective, making them excellent adsorbents. Key non-metallic mineral materials extensively studied in water treatment include zeolite,[50] diatomaceous earth,[51] kaolin,[52] and sepiolite.[53]

1.6.3 Metallic materials

The adsorption of heavy metal ions in water has been extensively explored with a variety of metallic materials, including metal oxides,[54] metal sulfides,[55] metal carbides,[56] and metal-organic frameworks (MOFs).[57] Each category of these materials offers unique advantages and mechanisms in addressing heavy metal pollution.

1.6.4 Polymer materials

Polymer materials, with their notable stability and adaptable structural properties, have gained widespread attention in various application areas.[58] These materials are generally classified into three main types: synthetic polymers, biomass, and composite

polymers, each offering unique benefits and functionalities.

Synthetic Polymers are produced through the polymerization of monomers, allowing for the selection of monomers with specific functional groups tailored to specific applications. Alternatively, modification can introduce desired functional groups into the polymers.[59] In the realm of water treatment, frequently studied synthetic polymers include fibers[60], gels[61], membranes[62], and resin microspheres[63]. Membranes and certain resin microspheres have even achieved commercial status. Membrane materials leverage differential permeability to various substances for selective filtration, relying on external driving forces like pressure or temperature gradients.

Biomass Polymers encompass all living matter and their derivatives, characterized by their ubiquity, richness, biodegradability, and biocompatibility.[64] In environmental functional material research, algae, microorganisms, and agricultural and forestry wastes are prominent sources.[65] Key active components such as amino acids, chitosan, starch, cellulose, lignin, and humic substances contain functional groups that facilitate chemical interactions and adsorption of heavy metals.[66]

Polymer Composite Materials merge the benefits of both synthetic and biomass polymers. Synthetic polymers provide stability, adjustability, and a designable framework, whereas biomass polymers offer abundance, biodegradability, and cost-effectiveness, encouraging the utilization of waste resources. The combination of these two types in composite materials holds promising prospects for diverse applications.[67]

In summary, polymeric materials, whether synthetic, biomass-based, or composite, present a versatile and dynamic field with immense potential for environmental and industrial applications, particularly in water treatment and heavy metal adsorption.

1.7 Hydrogels

Hydrogels, as cross-linked polymeric materials, exhibit reversible dry and swelling characteristics. These versatile materials can have their water content, internal cross-linking structure, pore size, and shape customized through the control of monomers and preparation conditions.[68]

1.7.1 Classification

Hydrogels are typically created using physical, or chemical cross-linking methods (as shown in **Fig. 1.5**). The former are materials cross-linked through hydrogen bonding, ionic bonding, coordination bonding, and can undergo reversible sol-gel transitions with external stimuli like heat. Examples include substances like agar and gelatin. The latter are cross-linked through covalent bonding due to chemical reactions, making them insoluble and chemically stable unless their structure is disrupted. High-absorbency polymers found in diapers and the material used in soft contact lenses are examples of chemical gels.[69]

Within hydrogel materials, the bound water serves three primary functions:[138] (1) it acts as a support medium, helping the hydrogel maintain a specific shape; (2) it provides nanoscale channels, enabling the free diffusion of small water-soluble molecules; and (3) it offers hydrogen bonding sites, facilitating additional active interactions between the hydrogel and molecules in solution. Consequently, hydrogels are highly effective for pollutant adsorption in aqueous environments.

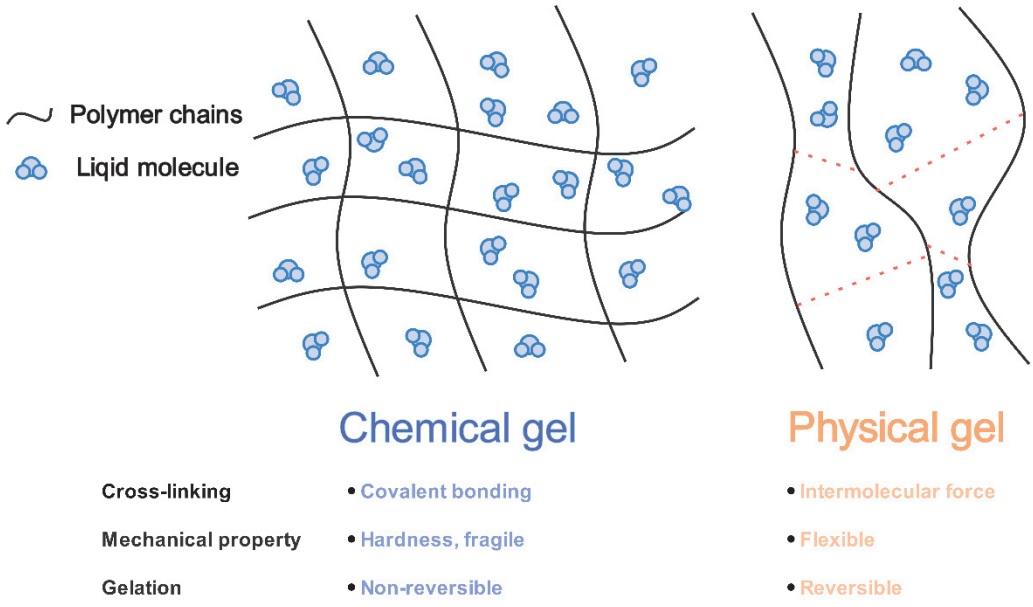

Fig. 1.5. Comparison of chemical and physical gels

1.7.2 Synthesis

The synthesis of polymer gels has a variety of synthesis methods, influenced by different cross-linking techniques and the objective of shaping the network structure. One of the most prevalent approaches is synthesis via radical polymerization. This entails the reaction of vinyl monomers and divinyl compounds with a radical initiator in a solvent, leading to polymerization. Commonly used cross-linkers include *N, N*'-Methylenebisacrylamide (MBAA) or Ethylene Glycol Dimethacrylate (EDMA), while initiators like Azobisisobutyronitrile (AIBN), Benzoyl Peroxide (BPO), or persulfates are standard choices. Notably, in instances where water serves as the solvent, a combination of Ammonium Persulfate (APS) as the initiator and Tetramethylethylenediamine (TEMED) as an accelerator is frequently employed.

1.7.3 Cross-linking structure of polymer gels

Polymer gels have a structure characterized by a three-dimensional network formed by cross-linked polymers. As a result, while polymer gels immerse in a solvent, polymer gels with a three-dimensional network structure swell to a certain extent due to interaction with the solvent, but only exhibit a finite degree of swelling. Additionally, within this three-dimensional network structure, an intricate microenvironment exists where closely packed polymer chains coexist with the solvent and solutes. This structure acts as a barrier to the external environment while simultaneously allowing the passage of necessary substances, thus playing a crucial role in controlling the internal microenvironment.

1.7.4 Swelling property of polymer gels

Traditional hydrogels are known for their considerable swelling capabilities, retaining substantial water within their three-dimensional networks without dissolving.[70] When a polymer gel is immersed in a solvent, it absorbs the solvent and swells, or expels the solvent and contracts, eventually reaching an equilibrium state at a certain volume. This equilibrium is known as swelling equilibrium. The swelling equilibrium of a gel is determined by the interaction between the gel and the solvent and is sensitive to external conditions, even within the same network structure. Additionally, attaching fixed ions to the network can significantly increase the degree of swelling. Furthermore, depending on the composition of the network and the solvent, some gels undergo a volume phase transition, where a slight change in external conditions can cause the volume to change by a factor of 10 to 1000.

1.8 Polymer gel in this study

Hydrogels can be classified not only based on their cross-linking methods but also according to their charge properties, falling into three categories: cationic hydrogels, anionic hydrogels, and nonionic hydrogels. In the following, the representative of each type to summarize the characteristics of these three types of gels and their roles in the context of this paper will be presented.

1.8.1 Cationic *polymer hydrogels*

Cationic polymer gels contain positively charged groups, often in the form of ammonium ions or similar cationic functional groups. They are highly hydrophilic and can adsorb large amounts of water relative to their own mass. For example, *N,N*-dimethylamino propylacrylamide, methyl chloride quaternary (DMAPAA-Q) gel.

The structure of this gel is shown in **Scheme 1.1**. DMAPAA-Q contains a quaternary amino group and Cl^- ions that are attracted to the vicinity of the quaternary amino group to maintain electrical balance. The presence of Cl^- allows the gel to adsorb harmful anions [As (III), As(V), Cr (VI)] or obtain useful anions (inorganic oxidants and reductants) via ion exchange.

1.8.2 Anionic *polymer hydrogels*

Anionic polymer gels contain negatively charged functional groups, such as carboxylate ($-COO^-$) or sulfonate ($-SO_3^-$) groups. For example, 2-Acrylamido-2-methyl-1-propanesulfonic acid sodium salt [AMPS (Na)] gel.

The structure of the AMPS(Na) gel is shown in **Scheme 1.1**. AMPS(Na) monomer contains a negatively charged sulfonic acid group and a sodium ion, can remove heavy metal cations [Cr (III)] via ion exchange adsorption method.

1.8.3 nonionic polymer hydrogels

Nonionic gels lack charged functional groups, which makes them neutral in charge. This absence of ionic groups often leads to different interaction mechanisms with their environment compared to ionic hydrogels. For example, *N, N*-dimethylaminopropylacrylamide (DMAPAA) gel.

The structure of this gel is shown in **Scheme 1.1**. The tertiary amine functional group in its structure can undergo protonation in an aqueous solution, which results in the quaternary ammonium ion carrying a positive charge. This allows the gel to adsorb anionic species via electrostatic attraction. Moreover, different pH environments will be formed on the surface and interior of the gel. While the surface will carry a positive charge due to protonation, the interior will contain a large amount of OH^- due to deprotonation, which enables the fixation of metal ions as hydroxides inside the gel.

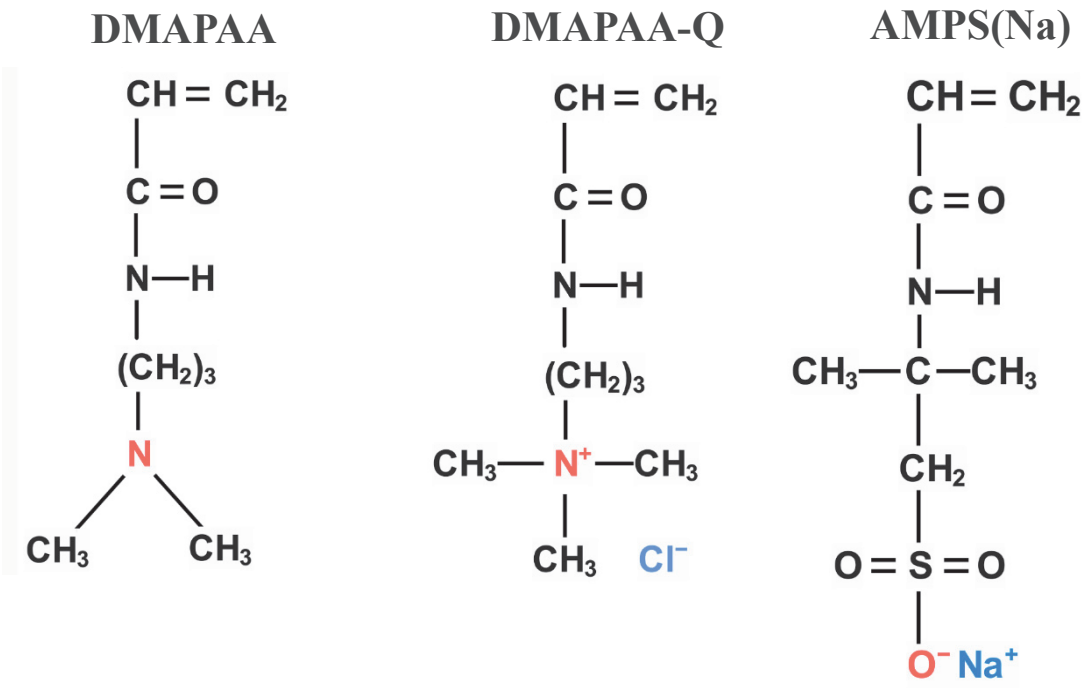

Scheme 1.1. Structural formula of DMAPAA, DMAPAAQ, and AMPS(Na) gels.

1.9 Insights and issues from previous research

Previous research has highlighted various issues in terms of processing efficiency, cost-effectiveness, and practicality, revealing that numerous research challenges remain. The insights gained include:

(1) Adsorption stands out as the most appropriate method for wastewater treatment due to its flexible design, ease of operation, cost-effectiveness, and minimal environmental impact.

(2) By utilizing the varying properties of adsorbates, environments conducive to adsorption can be created.

(3) Each adsorbent material has its strengths and weaknesses, necessitating improvement through various means.

(4) The synthesis of adsorbent materials with high adsorption performance is increasingly becoming complex, posing significant challenges to their practical

application.

1.10 Research purpose

Arsenic and chromium, prevalent as harmful ions in industrial wastewater, rank among the top five contaminants targeted for national regulation. Their presence in the environment poses grave risks to both human health and ecological systems. Adsorption emerges as an effective, economical, and eco-friendly strategy for mitigating the impact of these inorganic pollutants, with the selection of appropriate adsorbent materials being paramount. The ideal adsorbents are characterized by substantial adsorption capacities, necessitating an abundance of active functional groups readily accessible to the harmful ions.

Hydrogels are distinguished by several key features: (1) robust mechanical properties that facilitate their regeneration and recycling; (2) a three-dimensional network, established through chemical cross-linking, that entraps functional groups and comonomers, thereby preventing their leaching; (3) a versatile polymer framework with chemically adaptable active sites, enabling the incorporation of diverse and abundant functional groups; (4) high water content and swelling abilities, allowing for the unhindered diffusion of water-soluble molecules within the gel, which enhances the interaction and subsequent reaction between active sites and harmful ions. Consequently, hydrogels are recognized as exemplary materials for the adsorption of heavy metals.

This study addresses several critical concerns: (1) Trivalent arsenic predominantly exists as arsenous acid molecules in acidic and neutral water environments, posing challenges for its removal, in contrast to pentavalent arsenic, which primarily exists in anionic form above pH 2, rendering it more amenable to extraction; (2) Hexavalent chromium, apart from being highly toxic, is susceptible to remobilization under varying physicochemical conditions, thus exhibiting pronounced

mobility, unlike trivalent chromium, whose toxicity is a mere fraction (one percent) of its hexavalent counterpart and which is more readily immobilized; (3) Although the toxicity levels of pentavalent arsenic and trivalent chromium are markedly lower than those of trivalent arsenic and hexavalent chromium, their coexistence and the concurrent removal of anions and cations significantly challenge the efficacy of adsorbent materials. Therefore, Functionalizing hydrogels with suitable functional groups or modifying the state of the adsorbates to enhance the effective removal for heavy metal ion adsorption is the research purpose.

In response to the insights and issues from previous research and several critical concerns, we have arranged our study as follows:

(1) Trivalent arsenic should be oxidized first, and hexavalent chromium reduced, to enhance the overall adsorption efficiency.
(2) To reduce costs, the processes of oxidation-reduction and adsorption should be integrated into a single step.
(3) The hydrogel needs to be functionalized to acquire capabilities it inherently lacks.
(4) In the simultaneous removal of both anionic and cationic harmful ions, we aim to significantly improve the overall adsorption efficiency by altering the state of the adsorbate, rather than by functionalizing the gel.

1.11 Research contents

Building upon the context and significance previously outlined, this research predominantly concentrates on the selection of diverse functional groups for chemically modifying polymer hydrogel materials and modifying the state of adsorbates, thereby enhancing the adsorption efficiency. The study evaluates the adsorption capabilities of these materials in capturing heavy metal ions. The detailed aspects of the research are as follows:

(1) As (III) removal: *N*-[3-(dimethylamino)propyl]acrylamide, methyl chloride

quaternary (DMAPAAQ) is selected as the polymer monomer, and hydrogels are synthesized via free radical polymerization. Subsequently, these gels undergo chemical modification using oxidizing agents like potassium permanganate and potassium dichromate, which infuse a substantial number of oxidizing ion groups. This process results in the creation of D-Mn and D-Cr gels, featuring oxidizing ion functionalities. The study meticulously explores the adsorption efficiency of these gels for trivalent arsenic, employing systematic adsorption tests and comprehensive analyses of the adsorption behavior.

(2) Cr (VI) removal: Utilizing *N*, *N'*-Dimethylaminopropylacrylamide (DMAPAA) and DMAPAAQ as the polymer monomers, DA/DQ (DMAPAA/DMAPAAQ) copolymer hydrogels are fabricated through free radical polymerization. These gels are further modified with ascorbic acid (VC), a reducing agent, thereby integrating a plethora of ascorbic acid groups with reducing characteristics to create the reduced ion-functionalized DA/DQ/VC gels. Analytical techniques such as Fourier-transform infrared spectroscopy and X-ray photoelectron spectroscopy are employed to characterize the structural and functional attributes of the gels. A systematic investigation is conducted on their adsorption properties for hexavalent chromium, analyzing the adsorption dynamics in detail.

(3) As (V) and Cr (III) simultaneous removal: 2-acrylamido-2-methyl-1-propanesulfonic acid sodium salt [AMPS(Na)] is chosen as the polymer monomer for the synthesis of hydrogels through free radical polymerization. The adsorbates selected for study are pentavalent arsenic and trivalent chromium, which are converted into a positively charged complex ion by incorporating nitric acid. The structural and functional characteristics of these gels are evaluated using methods like Fourier-transform infrared spectroscopy and X-ray photoelectron spectroscopy. The research methodically examines the concurrent adsorption capacities of the gels for both pentavalent arsenic and trivalent chromium, delving into the nuances of their adsorption mechanisms.

1.12 References

(1) Liang, W.; Yang, M. Urbanization, economic growth and environmental pollution: Evidence from China. *Sustain. Comput.: Infor. Syst.* **2019**, *21*, 1-9.
(2) Charles, K. J.; Nowicki, S.; Bartram, J. K. A framework for monitoring the safety of water services: from measurements to security. *npj Clean Water* **2020**, *3* (1), 36.
(3) Hama Aziz, K. H.; Mustafa, F. S.; Omer, K. M.; Hama, S.; Hamarawf, R. F.; Rahman, K. O. Heavy metal pollution in the aquatic environment: efficient and low-cost removal approaches to eliminate their toxicity: a review. *RSC Adv.* **2023**, *13* (26), 17595-17610.
(4) Panda, B. P.; Mohanta, Y. K.; Parida, S. P.; Pradhan, A.; Mohanta, T. K.; Patowary, K.; Wan Mahari, W. A.; Lam, S. S.; Ghfar, A. A.; Guerriero, G.; et al. Metal pollution in freshwater fish: A key indicator of contamination and carcinogenic risk to public health. *Environ. Pollut.* **2023**, *330*, 121796.
(5) Chen, J.; Wang, S.; Zhang, S.; Yang, X.; Huang, Z.; Wang, C.; Wei, Q.; Zhang, G.; Xiao, J.; Jiang, F.; et al. Arsenic pollution and its treatment in Yangzonghai lake in China: In situ remediation. *Ecotoxicol. Environ. Saf.* **2015**, *122*, 178-185.
(6) Gao, Y.; Xia, J. Chromium contamination accident in China: viewing environment policy of China. *Environ. Sci. Technol.* **2011**, *45* (20), 8605-8606.
(7) Zhu, C.; Tian, H.; Cheng, K.; Liu, K.; Wang, K.; Hua, S.; Gao, J.; Zhou, J. Potentials of whole process control of heavy metals emissions from coal-fired power plants in China. *J. Clean. Prod.* **2016**, *114*, 343-351.
(8) Ministry of Ecology and Environment of the People Republic of China Website; https://www.mee.gov.cn/xxgk2018/xxgk/xxgk03/202203/t20220315_971552.html.
(9) Siddiqui, S. I.; Naushad, M.; Chaudhry, S. A. Promising prospects of nanomaterials for arsenic water remediation: A comprehensive review. *Process Saf. Environ. Prot.* **2019**, *126*, 60-97.
(10) Lee, C. G.; Alvarez, P. J. J.; Nam, A.; Park, S. J.; Do, T.; Choi, U. S.; Lee, S. H. Arsenic(V) removal using an amine-doped acrylic ion exchange fiber: Kinetic, equilibrium, and regeneration studies. *J. Hazard. Mater.* **2017**, *325*, 223-229.
(11) Fatoki, J. O.; Badmus, J. A. Arsenic as an environmental and human health antagonist: A review of its toxicity and disease initiation. *J. Hazard. Mater. Adv.* **2022**, *5*, 100052.
(12) Ungureanu, G.; Santos, S.; Boaventura, R.; Botelho, C. Arsenic and antimony in water and wastewater: overview of removal techniques with special reference to latest advances in adsorption. *J. Environ. Manage.* **2015**, *151*, 326-342.
(13) Shaji, E.; Santosh, M.; Sarath, K. V.; Prakash, P.; Deepchand, V.; Divya, B. V. Arsenic contamination of groundwater: A global synopsis with focus on the Indian Peninsula. *Geosci. Front.* **2021**, *12* (3), 101079.
(14) Sinha, V.; Pakshirajan, K.; Chaturvedi, R. Chromium tolerance, bioaccumulation and localization in plants: An overview. *J. Environ. Manage.* **2018**, *206*, 715-730.
(15) Prasad, S.; Yadav, K. K.; Kumar, S.; Gupta, N.; Cabral-Pinto, M. M. S.; Rezania, S.; Radwan, N.; Alam, J. Chromium contamination and effect on environmental health and its remediation: A sustainable approaches. *J. Environ. Manage.* **2021**, *285*, 112174.
(16) Georgaki, M.-N.; Charalambous, M.; Kazakis, N.; Talias, M. A.; Georgakis, C.; Papamitsou, T.; Mytiglaki, C. Chromium in Water and Carcinogenic Human Health Risk. *Environments* **2023**, *10* (2),

33.
(17) Li, Q.-g.; Liu, G.-h.; Qi, L.; Wang, H.-c.; Ye, Z.-f.; Zhao, Q.-l. Heavy metal-contained wastewater in China: Discharge, management and treatment. *Sci. Total Environ.* **2022**, *808*, 152091.
(18) Antoniadis, V.; Polyzois, T.; Golia, E. E.; Petropoulos, S. A. Hexavalent chromium availability and phytoremediation potential of Cichorium spinosum as affect by manure, zeolite and soil ageing. *Chemosphere* **2017**, *171*, 729-734.
(19) Azimi, A.; Azari, A.; Rezakazemi, M.; Ansarpour, M. Removal of Heavy Metals from Industrial Wastewaters: A Review. *ChemBioEng Rev.* **2017**, *4* (1), 37-59.
(20) Aziz, H. A.; Adlan, M. N.; Ariffin, K. S. Heavy metals (Cd, Pb, Zn, Ni, Cu and Cr(III)) removal from water in Malaysia: post treatment by high quality limestone. *Bioresour. Technol.* **2008**, *99* (6), 1578-1583.
(21) Fu, F.; Wang, Q. Removal of heavy metal ions from wastewaters: a review. *J. Environ. Manage.* **2011**, *92* (3), 407-418.
(22) Lewis, A. E. Review of metal sulphide precipitation. *Hydrometallurgy* **2010**, *104* (2), 222-234.
(23) Vicente-Martínez, Y.; Arroniz-Lázaro, A.; Hernández-Córdoba, M.; López-García, I. Use of in-situ synthesized magnetic ferrite to remove heavy metals from waters. *Green Anal. Chem.* **2024**, *8,* 100089.
(24) Navarro, R. R.; Wada, S.; Tatsumi, K. Heavy metal precipitation by polycation-polyanion complex of PEI and its phosphonomethylated derivative. *J. Hazard. Mater.* **2005**, *123* (1-3), 203-209.
(25) Trellu, C.; Mousset, E.; Pechaud, Y.; Huguenot, D.; van Hullebusch, E. D.; Esposito, G.; Oturan, M. A. Removal of hydrophobic organic pollutants from soil washing/flushing solutions: A critical review. *J. Hazard. Mater.* **2016**, *306*, 149-174.
(26) Sousa, R. M. S.; Mendes, L. W.; Antunes, J. E. L.; Oliveira, L. M. d. S.; Sousa, A. M. d. C. B.; Gomes, R. L. F.; Lopes, A. C. d. A.; Araújo, F. F.; Melo, V. M. M.; Araujo, A. S. F. Diversity and structure of bacterial community in rhizosphere of lima bean. *Appl. Soil Ecol.* **2020**, *150*, 103490.
(27) Zhang, C.; Jiang, Y.; Li, Y.; Hu, Z.; Zhou, L.; Zhou, M. Three-dimensional electrochemical process for wastewater treatment: A general review. *Chem. Eng. J.* **2013**, *228*, 455-467.
(28) Doggaz, A.; Attour, A.; Le Page Mostefa, M.; Côme, K.; Tlili, M.; Lapicque, F. Removal of heavy metals by electrocoagulation from hydrogenocarbonate-containing waters: Compared cases of divalent iron and zinc cations. *J. Water Process. Eng.* **2019**, *29*, 100796.
(29) Qasem, N. A. A.; Mohammed, R. H.; Lawal, D. U. Removal of heavy metal ions from wastewater: a comprehensive and critical review. *npj Clean Water* **2021**, *4* (1), 36.
(30) Khelifa, A.; Aoudj, S.; Moulay, S.; De Petris-Wery, M. A one-step electrochlorination/electroflotation process for the treatment of heavy metals wastewater in presence of EDTA. *Chem.l Eng. Process.: Process Intensif.* **2013**, *70*, 110-116.
(31) Arana Juve, J.-M.; Christensen, F. M. S.; Wang, Y.; Wei, Z. Electrodialysis for metal removal and recovery: A review. *Chem. Eng. J.* **2022**, *435*, 134857.
(32) Chauhan, M. S.; Rahul, A. K.; Shekhar, S.; Kumar, S. Removal of heavy metal from wastewater using ion exchange with membrane filtration from Swarnamukhi river in Tirupati. *Mater. Today: Proc.* **2023**, *78*, 1-6.
(33) Gode, F.; Pehlivan, E. Removal of chromium(III) from aqueous solutions using Lewatit S 100: the effect of pH, time, metal concentration and temperature. *J. Hazard. Mater.* **2006**, *136* (2), 330-337.
(34) Xiang, H.; Min, X.; Tang, C.-J.; Sillanpää, M.; Zhao, F. Recent advances in membrane filtration for heavy metal removal from wastewater: A mini review. *J. Water Process Eng.* **2022**, *49*, 103023.

(35) Divakar, S.; Padaki, M.; Balakrishna, R. G. Review on Liquid-Liquid Separation by Membrane Filtration. *ACS Omega* **2022**, *7* (49), 44495-44506.
(36) Liu, F.; Hashim, N. A.; Liu, Y.; Abed, M. R. M.; Li, K. Progress in the production and modification of PVDF membranes. *J. Membr. Sci.* **2011**, *375* (1-2), 1-27.
(37) Li, B.; Qi, B.; Guo, Z.; Wang, D.; Jiao, T. Recent developments in the application of membrane separation technology and its challenges in oil-water separation: A review. *Chemosphere* **2023**, *327*, 138528.
(38) Zhang, Y.; Liu, D.; Guo, W.; Ding, Y. Enhanced Selective Adsorption of Lanthanum(III) by Dual-Site Polymeric Ion-Imprinted Nanoparticles from Aqueous Media. *ACS Appl. Polym. Mater.* **2023**, *5* (5), 3315-3324.
(39) Demirbas, A. Heavy metal adsorption onto agro-based waste materials: a review. *J. Hazard. Mater.* **2008**, *157* (2-3), 220-229.
(40) Burakov, A. E.; Galunin, E. V.; Burakova, I. V.; Kucherova, A. E.; Agarwal, S.; Tkachev, A. G.; Gupta, V. K. Adsorption of heavy metals on conventional and nanostructured materials for wastewater treatment purposes: A review. *Ecotoxicol. Environ. Saf.* **2018**, *148*, 702-712.
(41) Baskar, A. V.; Bolan, N.; Hoang, S. A.; Sooriyakumar, P.; Kumar, M.; Singh, L.; Jasemizad, T.; Padhye, L. P.; Singh, G.; Vinu, A.; et al. Recovery, regeneration and sustainable management of spent adsorbents from wastewater treatment streams: A review. *Sci. Total. Environ.* **2022**, *822*, 153555.
(42) Foo, K. Y.; Hameed, B. H. Insights into the modeling of adsorption isotherm systems. *Chem. Eng. J.* **2010**, *156* (1), 2-10.
(43) Wang, J.; Guo, X. Adsorption isotherm models: Classification, physical meaning, application and solving method. *Chemosphere* **2020**, *258*, 127279.
(44) Qiu, H.; Lv, L.; Pan, B.-c.; Zhang, Q.-j.; Zhang, W.-m.; Zhang, Q.-x. Critical review in adsorption kinetic models. *J. Zhejiang Univ.-SC. A* **2009**, *10* (5), 716-724.
(45) Ahmad, N.; Bano, D.; Jabeen, S.; Ahmad, N.; Iqbal, A.; Waris; Anwer, A. H.; Jeong, C. Insight into the adsorption thermodynamics, kinetics, and photocatalytic studies of polyaniline/SnS_2 nanocomposite for dye removal. *J. Hazard. Mater. Adv.* **2023**, *10*, 100321.
(46) Heidarinejad, Z.; Dehghani, M. H.; Heidari, M.; Javedan, G.; Ali, I.; Sillanpää, M. Methods for preparation and activation of activated carbon: a review. *Environ. Chem. Lett.* **2020**, *18* (2), 393-415.
(47) Li, Y. H.; Zhao, Y. M.; Hu, W. B.; Ahmad, I.; Zhu, Y. Q.; Peng, X. J.; Luan, Z. K. Carbon nanotubes - the promising adsorbent in wastewater treatment. *J. Phys.: Con. Ser.* **2007**, *61*, 698-702.
(48) Avouris, P.; Dimitrakopoulos, C. Graphene: synthesis and applications. *Mater. Today* **2012**, *15* (3), 86-97.
(49) Pandey, D.; Daverey, A.; Arunachalam, K. Biochar: Production, properties and emerging role as a support for enzyme immobilization. *J. Clean. Prod.* **2020**, *255*, 120267.
(50) Zou, W.; Han, R.; Chen, Z.; Jinghua, Z.; Shi, J. Kinetic study of adsorption of Cu(II) and Pb(II) from aqueous solutions using manganese oxide coated zeolite in batch mode. *Colloids Surf. A: Physicochem. Eng. Asp.* **2006**, *279* (1-3), 238-246.
(51) Danil de Namor, A. F.; El Gamouz, A.; Frangie, S.; Martinez, V.; Valiente, L.; Webb, O. A. Turning the volume down on heavy metals using tuned diatomite. A review of diatomite and modified diatomite for the extraction of heavy metals from water. *J. Hazard. Mater.* **2012**, *241-242*, 14-31.
(52) Tehrani-Bagha, A. R.; Nikkar, H.; Mahmoodi, N. M.; Markazi, M.; Menger, F. M. The sorption of cationic dyes onto kaolin: Kinetic, isotherm and thermodynamic studies. *Desalination* **2011**, *266* (1-3),

274-280.
(53) Hossain, M.; Qin, B.; Li, B.; Duan, X. Synthesis, characterization, properties and applications of two-dimensional magnetic materials. *Nano Today* **2022**, *42*, 101338.
(54) Chen, L.; Xin, H.; Fang, Y.; Zhang, C.; Zhang, F.; Cao, X.; Zhang, C.; Li, X. Application of Metal Oxide Heterostructures in Arsenic Removal from Contaminated Water. *J. Nanomater.* **2014**, *2014*, 1-10.
(55) Zhang, X.; Zeng, L.; Wang, Y.; Tian, J.; Wang, J.; Sun, W.; Han, H.; Yang, Y. Selective separation of metals from wastewater using sulfide precipitation: A critical review in agents, operational factors and particle aggregation. *J. Environ. Manage.* **2023**, *344*, 118462.
(56) Gogotsi, Y.; Anasori, B. The Rise of MXenes. *ACS Nano* **2019**, *13* (8), 8491-8494.
(57) Zhou, H. C.; Long, J. R.; Yaghi, O. M. Introduction to metal-organic frameworks. *Chem. Rev.* **2012**, *112* (2), 673-674.
(58) Wang, K.; Amin, K.; An, Z.; Cai, Z.; Chen, H.; Chen, H.; Dong, Y.; Feng, X.; Fu, W.; Gu, J.; et al. Advanced functional polymer materials. *Mater. Chem. Front.* **2020**, *4* (7), 1803-1915.
(59) Panchal, S. S.; Vasava, D. V. Biodegradable Polymeric Materials: Synthetic Approach. *ACS Omega* **2020**, *5* (9), 4370-4379.
(60) Xu, G.; Wang, L.; Xie, Y.; Tao, M.; Zhang, W. Highly selective and efficient adsorption of Hg(2+) by a recyclable aminophosphonic acid functionalized polyacrylonitrile fiber. *J. Hazard. Mater.* **2018**, *344*, 679-688.
(61) Li, Z.; Wang, Y.; Wu, N.; Chen, Q.; Wu, K. Removal of heavy metal ions from wastewater by a novel HEA/AMPS copolymer hydrogel: preparation, characterization, and mechanism. *Environ. Sci. Pollut. Res. Int.* **2013**, *20* (3), 1511-1525.
(62) Feng, Q.; Wu, D.; Zhao, Y.; Wei, A.; Wei, Q.; Fong, H. Electrospun AOPAN/RC blend nanofiber membrane for efficient removal of heavy metal ions from water. *J. Hazard. Mater.* **2018**, *344*, 819-828.
(63) Li, Q.; Song, H.; Han, R.; Wang, G.; Li, A. Efficient removal of Cu(II) and citrate complexes by combined permanent magnetic resin and its mechanistic insights. *Chem. Eng. J.* **2019**, *366*, 1-10.
(64) Wang, Z.; Ganewatta, M. S.; Tang, C. Sustainable polymers from biomass: Bridging chemistry with materials and processing. *Prog. Polym. Sci.* **2020**, *101*, 101197.
(65) Arif, Z. U.; Khalid, M. Y.; Sheikh, M. F.; Zolfagharian, A.; Bodaghi, M. Biopolymeric sustainable materials and their emerging applications. *J. Environ. Chem. Eng.* **2022**, *10* (4), 108159.
(66) Bilal, M.; Shah, J. A.; Ashfaq, T.; Gardazi, S. M.; Tahir, A. A.; Pervez, A.; Haroon, H.; Mahmood, Q. Waste biomass adsorbents for copper removal from industrial wastewater--a review. *J. Hazard. Mater.* **2013**, *263* (2), 322-333.
(67) Sionkowska, A. Current research on the blends of natural and synthetic polymers as new biomaterials: Review. *Prog. Polym. Sci.* **2011**, *36* (9), 1254-1276.
(68) Ho, T. C.; Chang, C. C.; Chan, H. P.; Chung, T. W.; Shu, C. W.; Chuang, K. P.; Duh, T. H.; Yang, M. H.; Tyan, Y. C. Hydrogels: Properties and Applications in Biomedicine. *Molecules* **2022**, *27* (9), 2902.
(69) Ma, J.; Sun, Y.; Zhang, M.; Yang, M.; Gong, X.; Yu, F.; Zheng, J. Comparative Study of Graphene Hydrogels and Aerogels Reveals the Important Role of Buried Water in Pollutant Adsorption. *Environ. Sci. Technol.* **2017**, *51* (21), 12283-12292.
(70) Ahmed, E. M. Hydrogel: Preparation, characterization, and applications: A review. *J. Adv. Res.* **2015**, *6* (2), 105-121.

Chapter 2: Efficient removal of As (III)

2.1 Introduction

In the recent years, the reports of As contamination exceeding the environmental and wastewater standards in the industrial wastewater have been increasing worldwide.[1-6] According to the latest fact sheets of WHO,[7] tens of millions of people have consumed the high-concentration As-contaminated groundwater;[8-9] health problems, such as skin cancer caused by the As contaminants have become a major social problem.[2, 10-11] Therefore, the development of advanced materials or technologies for the efficient treatment of As wastewater continues to be a global research priority. Various removal methods have been developed and applied to treat the As wastewater, such as co-precipitation for the removal of arsenous acid using Fe (III) and Mn oxide, adsorption methods using various adsorbents and minerals, and ion exchange methods.[12-14] Among them, adsorption is widely used because of its technological simplicity, high efficiency, and low secondary pollution risk.[15] However, some conventional adsorbents have many drawbacks, such as high cost, few adsorbent sites, and small absorption capacity, which limits their application in the water treatment. Moreover, some conventional adsorbents have a low removal efficiency towards the highly toxic As (III), which further limits their application in the water treatment.[16]

Among the many adsorbents developed and used for the As (III) removal, the application of polymer sorbents has been the most popular approach for the As (III) removal from the industrial wastewater owing to their environmental safety, superior chemical modifiability, many adsorbent sites, and outstanding renewability.[17-19] There are two main types of polymer adsorbents, one of which adsorbs via electrostatic interactions through its cationic functional groups, while the other adsorbs by a

functional group that has a high affinity for As. Among the cationic polymers,[20] the polymers with amino groups are particularly well known. For example, *N*-[3-(dimethylamino)propyl] acrylamide, methyl chloride quaternary (DMAPAAQ) is a well-known quaternary ammonium salt-type cationic monomer. The quaternary amino group of DMAPAAQ is positively charged, which could attract counter anion Cl^- to maintain the charge balance [21]. Therefore, it is possible to either load the necessary anions or remove the harmful anions by exchanging the Cl^- ions with them.

The main forms of As in the groundwater are arsenate (V) and arsenite (III), which exist as molecules and exhibit negatively charged ionic states at acidic and neutral water environment as shown in **Fig. 2.1**.[22] The As in the groundwater often exists as arsenous acid as the groundwater is in a reducing environment. It is known that As (III) has a lower adsorption capacity than As (V). For example, activated alumina (Al_2O_3), Fe compounds, such as Fe hydroxide, and Ce oxide are known as As removers.[23] However, the As ions are hardly adsorbed on the activated Al_2O_3. In addition, it is generally considered that the trivalent As (H_3AsO_3) is more toxic than the pentavalent As (H_3AsO_4) form. As illustrated in **Fig. 2.1**, the anions of H_3AsO_4 exist over a wide pH range, whereas H_3AsO_3 does not dissociate in the acidic range and its anions exist only above pH 7, owing to which, it is less adsorbed. Therefore, it is necessary to oxidise the arsenite into arsenate to increase the removal efficiency. In other words, to increase the removal efficiency of the trivalent As, both an increase in the number of adsorption sites and the oxidation of As is essential.

Although the As adsorption method is used to remove As (III), most adsorbents have a very low As removal efficiency because they have few adsorption sites and a small absorption capacity. This restricts its application in the water treatment. To resolve these problems, we propose a polymer gel adsorbent with a dense network structure and many adsorption sites. In the present work, a polymer hydrogel was prepared by radical polymerisation of DMAPAA-Q by carrying an oxidizing agent ($KMnO_4$, $K_2Cr_2O_7$) to enhance the adsorption capacity of As by changing the valence.

The synthesised D-Mn gel (DMAPAAQ gel carrying MnO_4^-) and D-Cr gel (DMAPAAQ gel carrying $Cr_2O_7^{2-}$) were systematically characterised before and after the As adsorption. Their As (III) removal performances were evaluated via a batch adsorption experiment. The adsorption kinetics and isotherms were also investigated in detail.

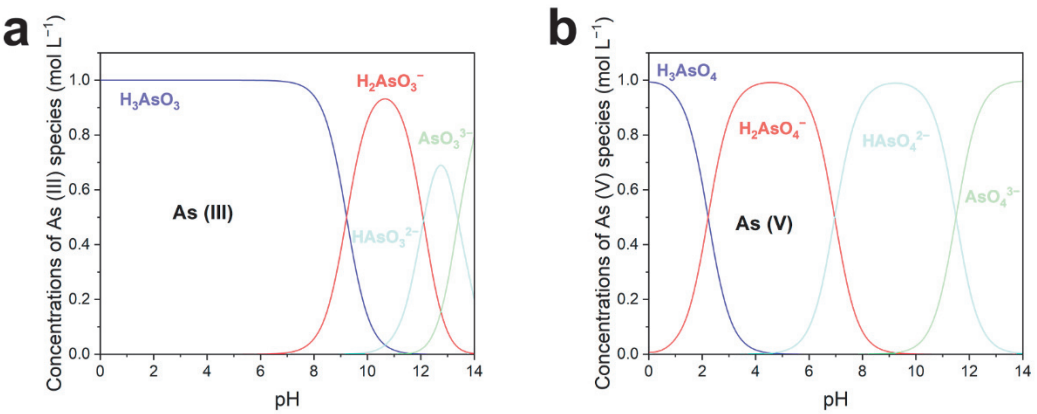

Fig. 2.1. Arsenic speciation as a function of the solution pH.[24]

2.2 Materials and methods

2.2.1 Reagents

DMAPAAQ monomer was obtained by KJ Chemicals Co., Japan. Potassium dichromate ($K_2Cr_2O_7$) and *N,N,N',N'*- tetramethylethylenediamine (TEMED) were obtained from Nacalai Tesque, Inc. Japan, *N,N'*-methylenebisacrylamide (MBAA), ammoniumperoxodisulfate (APS), and potassium permanganate ($KMnO_4$) were obtained from Sigma Aldrich Co., USA. All the reagents were reagent grade and used as received. Aqueous solutions were prepared using distilled water (DW).

2.2.2 Synthesis of DMAPAAQ hydrogel

In a 10 mL volumetric flask, 4.1342 g of DMAPAAQ (monomer), 0.1156 g of MBAA (cross-linking agent), and 0.0349 g of TEMED (accelerator) were dissolved in

distilled water. APS (initiator, 0.0685 g) was dissolved in distilled water in a 5 mL volumetric flask (as shown in **Table 2.1**). N_2 purge was performed for 30 min on each solution and the device to remove O_2 to prevent the inhibition of radical polymerisation in the flask containing distilled water. After N_2 purging, the initiator solution and monomer solution were mixed and stirred for 20 s. The obtained mixture was then injected into a gel-plate formation kit (AE-6401 1-mm Dual Mini Gel Cast, ATTO Corp.). DMAPAA-Q and MBAA were polymerized at 25 °C for 24 h, following which, the gel was peeled off from the glass plate and cut into a 10 mm × 10 mm × 1 mm plate. The gel was washed with methanol for 24 h using a Soxhlet extractor to remove the unreacted monomers. After washing, the gel was dried at 25 °C for several days and then thoroughly dried in an oven at 50 °C.

Table 2.1. Synthetic condition of DMAPAAQ hydrogel.

Component	Function	Molecular weight ($g\ mol^{-1}$)	Concentration ($mol\ m^{-3}$)	Mass (g)
DMAPAAQ	Monomer	206.71	1000	4.1342
MBAA	Linker	154.17	50	0.1156
TEMED	Accelerator	116.21	20	0.0349
APS	Initiator	228.19	20	0.0685

2.2.3 Synthesis of the D-Mn gel and D-Cr gel

A 0.01 mol L^{-1} solution was prepared by dissolving 0.079 g $KMnO_4$ in 50 ml distilled water. The DMAPAA-Q gel (0.2 g) was immersed in the prepared $KMnO_4$ solution, and the mixture was kept at 25 °C for 24 h. The gel was then washed with ion-exchanged water for 24 h to remove the excess ions from the surface of the gel. The ion-exchanged water was then replaced several times in a fixed time interval (every 4~6 h). After washing, the gel was completely dried in a drying oven at 50 °C.

A 0.01 mol L^{-1} solution was prepared by dissolving 0.1471 g of $K_2Cr_2O_7$ in 50 mL distilled water. In the prepared $K_2Cr_2O_7$ solution, 0.2 g of DMAPAAQ gel was immersed, and the mixture was kept at 25 °C for 24 h. The gel was then washed with ion-exchanged water for 24 h to remove the excess ions on its surface. The ion-exchanged water was replaced several times at fixed time intervals in 24 h (every 4~6 h). After washing, the gel was completely dried in an oven at 50 °C.

2.2.4 Batch adsorption experiments

The batch adsorption experiments were performed in plastic vials (10 mL) with 2 g L^{-1} adsorbent dosage to investigate the effects of pH, reaction time, temperature, co-existing anions, and the effect of co-existing competing anions on As removal in the synthetic As (III) solution.

The effect of pH on the As (III) removal was explored at different initial pH levels (ranging from 2-6). The concentration of As (III) was 10 mg L^{-1}, and the dosage of the D-Mn or D-Cr gels was 2 g L^{-1}, respectively. The effect of the co-existing ions was investigated as follows: 20 mg of a given gel was added to 10 mL of As (III) solution(10 mg L^{-1}) containing the ions HCO_3^-, SO_4^{2-}, and PO_4^{3-}, Cl^-, wherein the initial concentrations of the co-existing ions were 0, 0.1, 1, and 10 mM.

The adsorption isotherms were measured to determine the As adsorption capacities of the adsorbents in the As (III) solutions with initial concentrations ranging from 10-1000 mg L^{-1} for 24 h. After reaching equilibrium, the D-Mn and D-Cr gels were separated to measure the residual concentration of As. The removal rate (R) and equilibrium adsorption capacity Q_e were determined as formula (1.1) and (1.2). The Langmuir equations are expressed as equation (1.3).

The kinetics of As (III) adsorption was simulated using two mathematical models, namely the pseudo-first-order and pseudo-second-order kinetic models, which can be expressed as the equations (1.9) and (1.10). Thermodynamic experiments were

conducted by varying the initial concentration from 20 mg L^{-1} to 100 mg L^{-1} for 24 h at three different initial temperatures (10 °C, 25 °C, and 40 °C). The thermodynamic parameters for As (III) adsorption were quantified to explore the degree of spontaneity and heat exchange during the adsorption process. The standard Gibbs free energy ΔG (kJ mol^{-1}), enthalpy change ΔH (kJ mol^{-1}), and entropy change ΔS (J mol^{-1} K^{-1}) were calculated as equations (1.11) - (1.14):

All the aqueous samples were filtered through a 0.22 μm membrane, and the concentration of the residual As was analysed by the Inductively coupled plasma atomic emission spectroscopy (ICP-AES).

2.3 Results and discussion

2.3.1 Effect of pH of the As solution on the gel adsorption

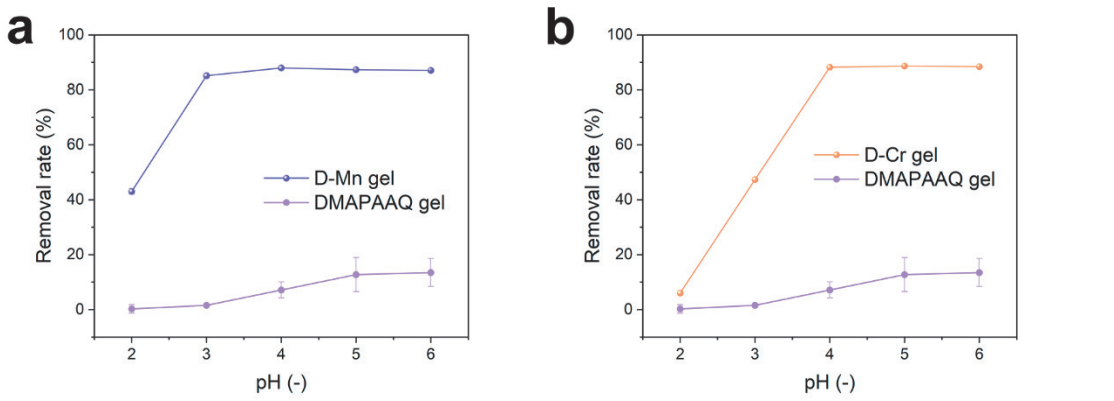

Fig. 2.2. Effect of pH on the As(III) removal rate of the (a) D-Mn and (b) D-Cr gels.

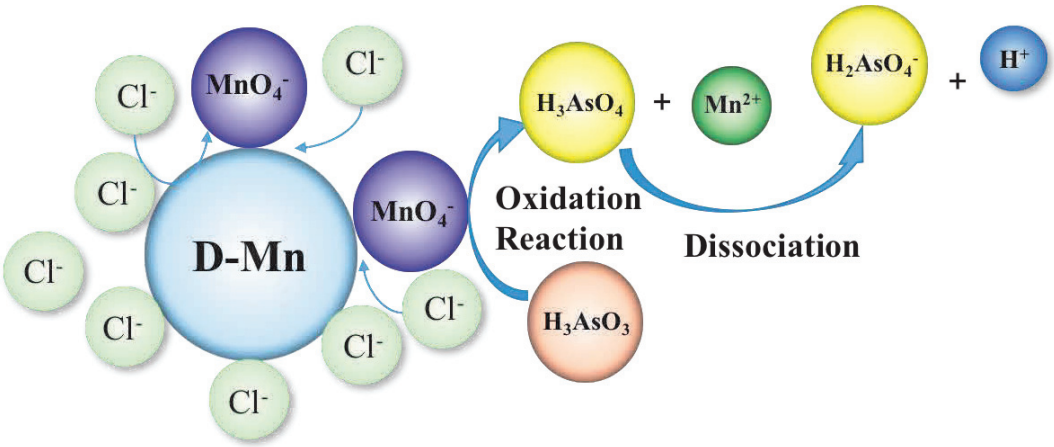

Scheme 2.1. Schematic representation of the effect of high Cl^- ion concentration on

the As adsorption of the D-Mn gel.

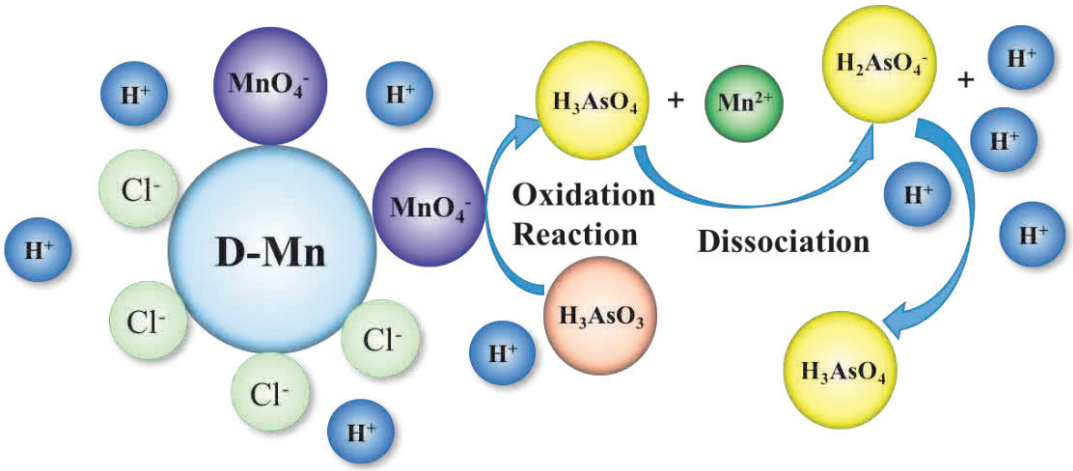

Scheme 2.2. Schematic representation of the effect of high H^+ ion concentration on the As adsorption of the D-Mn gel.

For the adsorption of As (III) in the aqueous environments, pH is a crucial parameter that affects the surface charge of the adsorbent as well as the conversion of the As species (as shown in **Fig. 2.2**). Generally, different forms of As (III) are present in the aqueous environments. H_3AsO_3 is dominant under the acidic conditions (pH < 7), while the anions, such as $H_2AsO_3^-$, $HAsO_3^{2-}$, and AsO_3^{3-} are dominant in the alkaline environments. [24] To determine the effect of the external pH on the As removal property of the gel, the As (III) adsorption by the D-Mn and D-Cr gels was first investigated in the pH range of 2−6 (**Fig. 2.2**). As shown in **Figs. 2.2**a and **Fig. 2.2**b, the DMAPAAQ gel removes a comparatively lesser amount of As (the removal rate of the DMAPAAQ < ~10%) than that of the D-Mn and D-Cr gels due to the formation of H_3AsO_3 under the acidic conditions, which could interfere in the ion exchange between the Cl^- and As-based anions. **Fig. 2.2** shows that the As (III) removal rate of the D-Mn and D-Cr gels could still be maintained at a high level between pH 4 and 6. The adsorption process took place inside the gel, on which the effect of the external environment was minimal. Under the acidic conditions, the redox reaction between MnO_4^- /$Cr_2O_7^{2-}$and As (III) in the gel is more likely to occur. Meanwhile a greater

number of As (V) anions are produced by redox reactions, which eases the As adsorption via the exchange of Cl^- and As (V) anions in the gels. **Fig. 2.2a** also shows that the As removal rate of the D-Mn gel was significantly higher than that of the DMAPAAQ gel. This was because the Mn oxide supported in the gel oxidized As (III) into As (V), and also adsorbed the oxidation product, i.e., As (V).

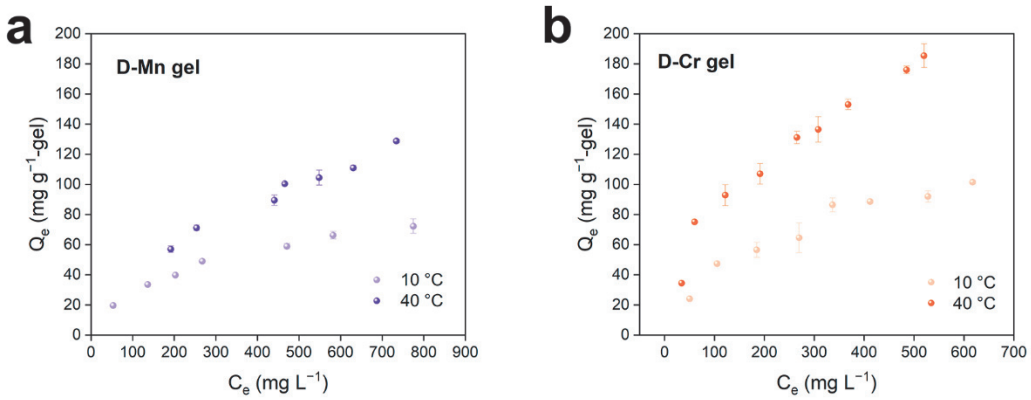

Fig. 2.3 Isotherms of the As(III) adsorption in the (a) D-Mn and (b) D-Cr gels at different temperatures.

In addition, it was confirmed that the removal rate increased remarkably with the increasing pH, becoming nearly constant for pH > 3. However, when pH < 2, the As removal rate decreased significantly. This phenomenon could be attributed to two reasons: (1) large amounts of Cl^- ions derived from the HCl were used to adjust the pH, suppressing the formation of the oxidation product As (V) on the gel, as shown in **Scheme 2.1**; (2) when a large amount of H^+ ions suppressed the dissociation of H_3AsO_4 and H_3AsO_3, the exchange of Cl^- and As (III) and As (V) was inhibited, thereby reducing the adsorption removal rate, as shown in **Scheme 2.2**.

2.3.2 Adsorption isotherm

Fig. 2.3 shows the isotherms of As (III) adsorption by D-Mn and D-Cr gels at

10 °C and 40 °C, respectively, for 24 h (24 h is enough to ensure that the adsorption can reach the equilibrium state). The maximum amount of As adsorbed in the gel increased with the increasing temperature, as did the amount of As adsorbed in general. This enhancement in the adsorption process could be attributed to the progress of the redox reaction facilitated by the increase in temperature. The maximum adsorbed amount in the gel and the equilibrium adsorption constant could be calculated from the slope of the straight line and the intercept, respectively, according to the Langmuir isotherm adsorption formula (3.3), as shown in **Fig. 2.4**a and **Fig. 2.4**b.

Fig. 2.4 shows the corresponding simulated results. The adsorption isothermal data were simulated using the Langmuir models. The parameters are listed in **Table 2.1** and **Table 2.2**.

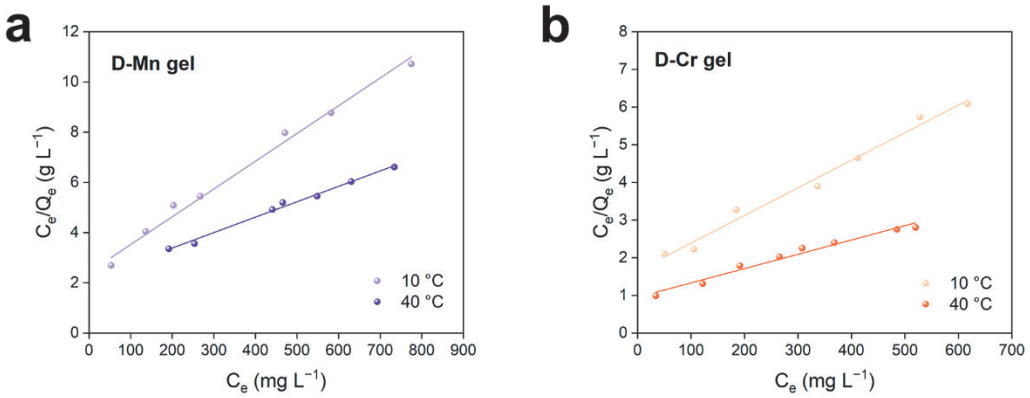

Fig. 2.4. Langmuir isotherm plots for the As(III) adsorption in (a) D-Mn and (b) D-Cr gels at different temperatures.

Table 2.1. Langmuir model parameters for As (III) adsorption in D-Mn gel.

Temperature(°C)	Q_{max} (mg g^{-1}-gel)	K_L (L mg^{-1})	R^2
10	90	0.0046	0.9902
40	163	0.0028	0.9938

Table 2.2. Langmuir model parameters for the adsorption of As (III) in D-Cr gel.

Temperature(°C)	Q_{max} (mg g^{-1}-gel)	K_L (L mg^{-1})	R^2
10	137	0.0044	0.9855
40	263	0.0040	0.9758

As mentioned above, the maximum amounts of As adsorbed by the two gels are 163 mg g^{-1}-gel and 263 mg g^{-1}-gel, which are considerably better than the maximum adsorbed amounts reported in previous studies, as listed in **Table 2.3**.

Table 2.3. Comparison of the maximum As (III) removal capacity with other related adsorbents

Adsorbent	Adsorbent dosage (g L^{-1})	Max. adsorption capacity (mg g^{-1})	References
D-Cr gel	**2**	**263**	**This work**
D-Mn gel	**2**	**163**	**This work**
Fe(III)/La(III)-chitosan	-	109	19
ZrPACM-43	13	41.48	25
Ceria-GO composite	0.5	185	26
Hydrous Cerium Oxide	0.5	170	27
CuO nanoparticles	0.08	39	28
TiO_2 nanoparticles	1	31.35	29
Fe_3O_4-graphene composite	2	0.313	11

2.3.3 Adsorption Kinetics

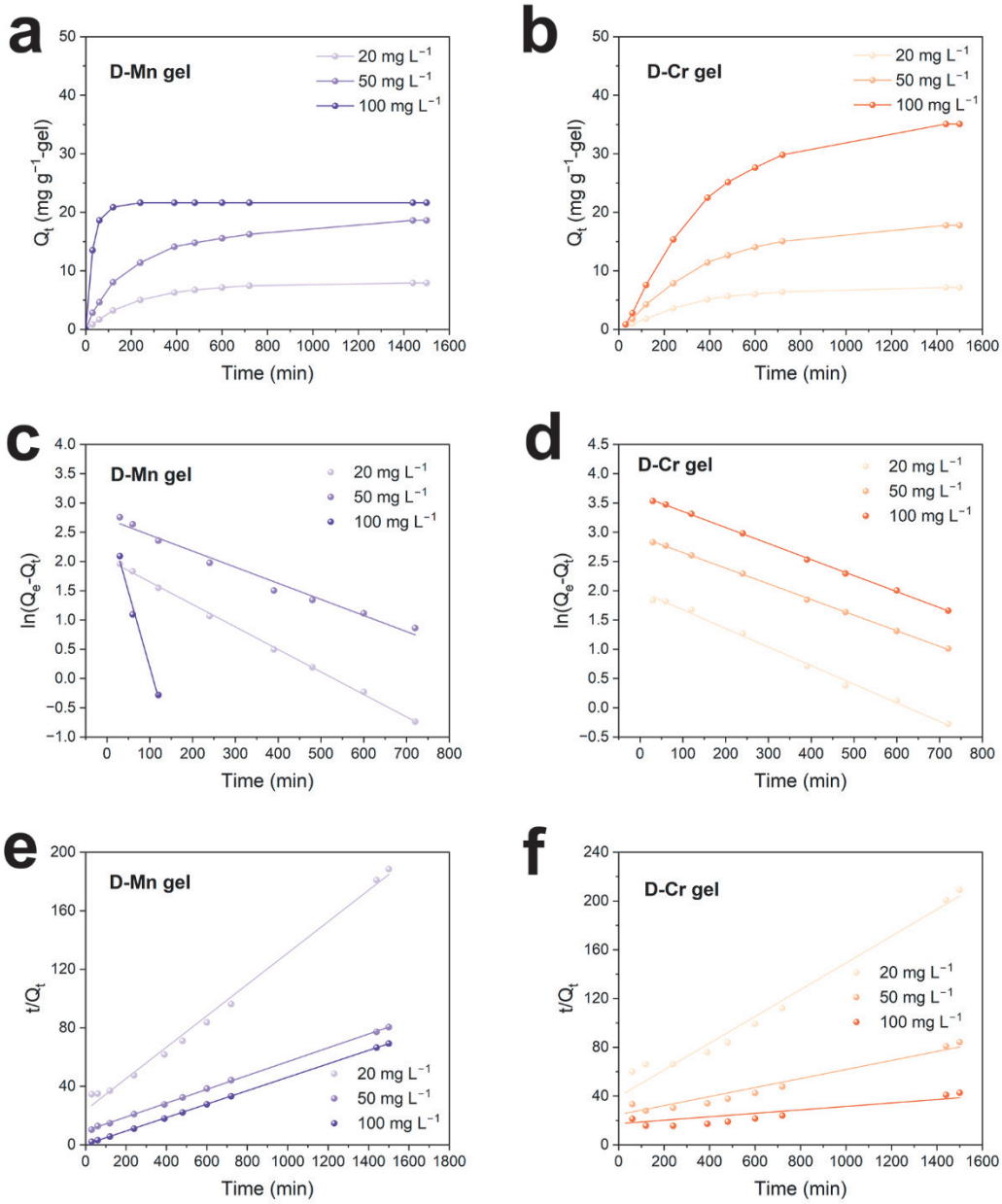

Fig. 2.5. Adsorption kinetics of (a) D-Mn and (b) D-Cr gels; plots of the pseudo-first-order dynamic model of (c) D-Mn and (d) D-Cr gels; plots of the pseudo-second-order dynamic model of (e) D-Mn and (f) D-Cr gels.

The initial concentrations for the kinetic studies were set at 20 mg L^{-1}, 50 mg L^{-1}, and 100 mg L^{-1}. The adsorbent dosage was set to 2 g L^{-1}, and the contact time range

was set at 30−1650 min. **Fig. 2.5**a shows that the reaction reached equilibrium after 20 h for the initial concentrations of 20 mg L^{-1} and 50 mg L^{-1}. However, at an initial concentration of 100 mg L^{-1}, the adsorbed amount increased rapidly in the first hour, and the reaction reached equilibrium within the following 3 h. The figure suggests that the reaction rate increased significantly with the increasing initial concentration. Therefore, the MnO_4^- ions were converted into MnO_2 at low As (III) concentrations, and MnO_2 could itself continuously adsorb As (III) after the redox reaction. Meanwhile, the MnO_4^- ions underwent a vigorous redox reaction and were directly reduced to Mn^{4+} in a highly concentrated As solution. This is because the oxidized trivalent As became pentavalent and was rapidly adsorbed by the amino group of the gel at that time.

Unlike the D-Mn gel, there was no significant change in the adsorption rate of the D-Cr gel at the different initial As (III) concentrations (as shown in **Fig. 2.5**b). This suggests that an increase in the initial concentration of the As solution did not change the reaction rate of the D-Cr gel. To elucidate the mechanism of As adsorption by the D-Mn and D-Cr gels, the adsorption behaviour was analysed using the pseudo-first-order and pseudo-second-order dynamics equations, as shown in **Figs. 2.5**c, d, e, and f. Since both the D-Mn and D-Cr gels showed higher correlations with the pseudo-second-order dynamics model than with the pseudo-first-order model, As adsorption by the D-Mn and D-Cr gels was considered to be dominated by chemisorption. The parameters are listed in **Tables 2.4** and **2.5**.

Table 2.4. Kinetic parameters of As (III) adsorption by the D-Mn gel.

Initial	Pseudo-first-order equation			Pseudo-second-order equation		
Concentration	k_1 (min^{-1})	Q_e (mg g^{-1})	R^2	k_2 (g $mg^{-1}min^{-1}$)	Q_e (mg g^{-1})	R^2
20 mg L^{-1}	0.0027	5.45	0.9659	0.00097	8.98	0.9983
50 mg L^{-1}	0.0027	10.91	0.9755	0.00056	20.75	0.9982
100 mg L^{-1}	–	–	–	0.00680	21.79	0.9999

Table 2.5. Kinetic parameters of As (III) adsorption by the D-Cr gel.

Initial	Pseudo-first-order equation			Pseudo-second-order equation		
Concentration	k_1 (min^{-1})	Q_e (mg g^{-1})	R^2	k_2 (g $mg^{-1}min^{-1}$)	Q_e (mg g^{-1})	R^2
20 mg L^{-1}	0.0030	7.23	0.9898	0.00043	9.08	0.9955
50 mg L^{-1}	0.0039	16.27	0.9942	0.00029	20.20	0.9968
100 mg L^{-1}	0.0044	27.46	0.9927	0.00023	34.01	0.9968

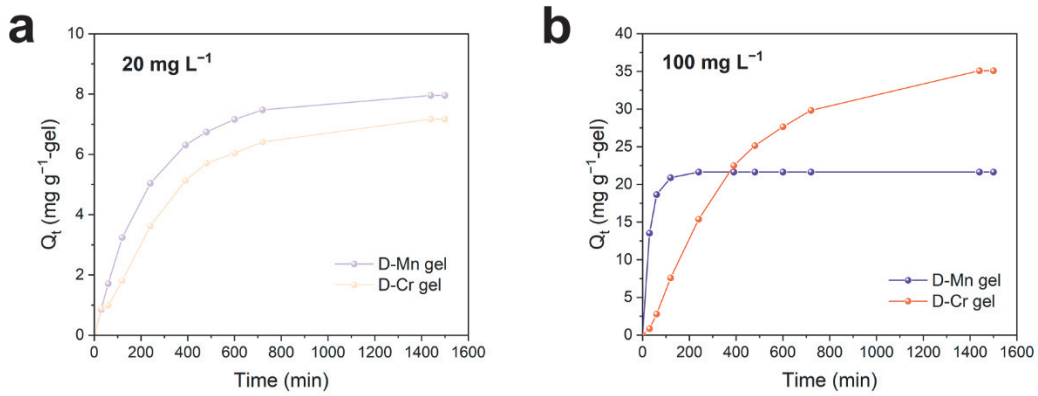

Fig. 2.6. Comparison of the adsorption kinetics of the D-Mn and D-Cr gels at the initial As(III) concentration of (a) 20 mg L^{-1} and (b) 100 mg L^{-1}, respectively.

Fig. 2.6 shows the changes in the amount of As adsorbed on the gel with time at initial concentrations of 20 mg L^{-1} and 100 mg L^{-1}. This figure shows that the adsorption performance of the D-Mn gel is superior to that of the D-Cr gel at the low As concentrations, which could be attributed to the ability of the MnO_4^- ions to form MnO_2 after the redox reaction, and continuously adsorb As even at low As concentrations. Meanwhile, the adsorption capacity of the D-Cr gel is much higher than that of the D-Mn gel, but the rate at which the latter reaches equilibrium is higher in the high-concentration As solutions. This is because the oxidizing property of the MnO_4^- ion is higher than that of the $Cr_2O_7^{2-}$ ion in a neutral environment (standard oxidation reduction potential: $KMnO_4$ (+1.51 V) > $K_2Cr_2O_7$ (+1.35 V)).

2.3.4 Adsorption Thermodynamics

The mechanisms of the As (III) adsorption on the gels were investigated by calculating the thermodynamic parameters, such as adsorption enthalpy (ΔH), adsorption free energy (ΔG), and adsorption entropy (ΔS).

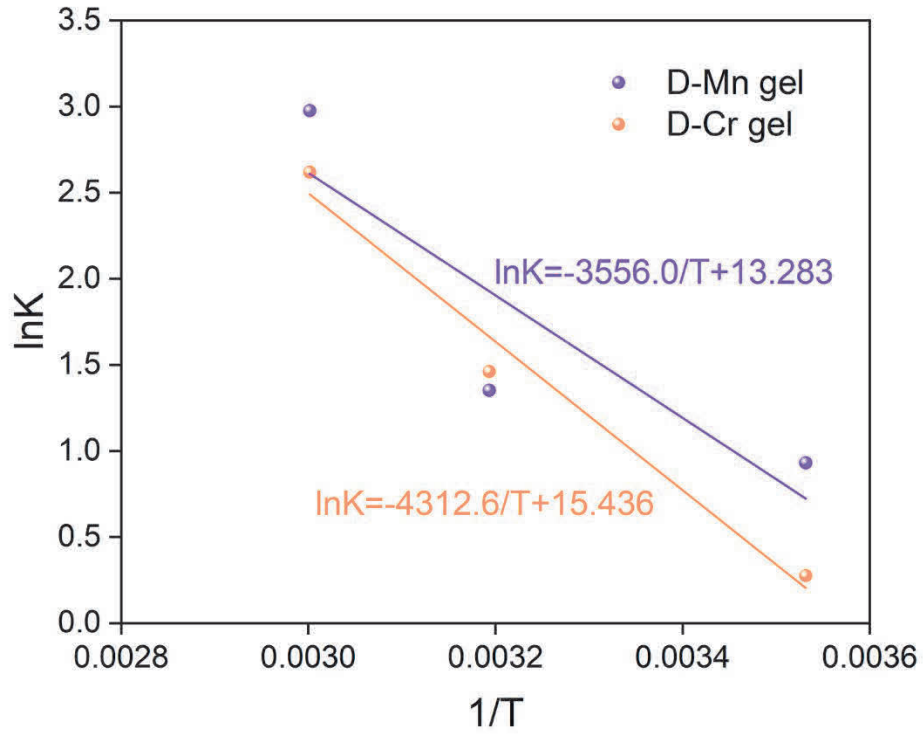

Fig. 2.7. Effect of temperature on the distribution of the adsorption coefficient of the D-Mn and D-Cr gels.

Table 2.6. Thermodynamic parameters of As adsorption in the D-Mn gel.

T (K)	$\ln K_d$	ΔG (kJ mol^{-1})	ΔH (kJ mol^{-1})	ΔS (kJ mol^{-1} K^{-1})
283.15	0.93258781	-1.5815	29.565	0.110
313.15	1.35287955	-4.8815	29.565	0.110
333.15	2.97647589	-7.0815	29.565	0.110

Table 2.7. Thermodynamic parameters of As adsorption in the D-Cr gel.

T (K)	$\ln K_d$	ΔG (kJ mol^{-1})	ΔH (kJ mol^{-1})	ΔS (kJ $mol^{-1} K^{-1}$)
283.15	0.2777234	-0.3872	35.856	0.128
313.15	1.46240344	-4.2272	35.856	0.128
333.15	2.61940407	-6.7872	35.856	0.128

Thermodynamic analyses of the adsorption experiments were conducted to elucidate the associated adsorption mechanisms. Experiments were conducted at the temperatures of 10, 40, and 60 °C to confirm the effect of temperature on the amount of As adsorbed in the gel (**Fig. 2.7**). The figure was obtained by plotting the results calculated by the thermodynamic equation, and then, using other thermodynamic equations, the ΔH and ΔS values can be calculated. The results of the calculations are listed in **Tables 2.6** and **2.7**, wherein $\Delta G < 0$ suggests that the adsorption process could be performed naturally. The higher the reaction temperature, the greater is the decrease in ΔG. Therefore, as the temperature increased, the spontaneous reaction was facilitated to a certain extent. Since both ΔH and ΔS are > 0, the adsorption process could be interpreted as an endothermic chemisorption.

2.3.5 Effect of co-existing ions on the As removal property of the D-Mn and D-Cr gels.

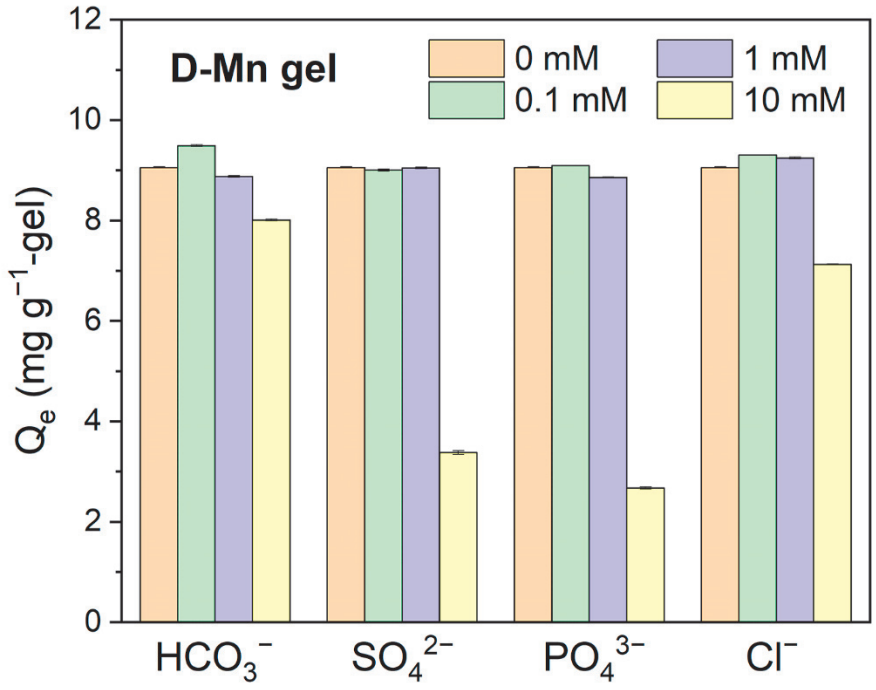

Fig. 2.8. Effect of co-existing ions on the As removal property of the D-Mn gel.

In wastewater treatment, various anions like HCO_3^-, SO_4^{2-}, PO_4^{3-}, and Cl^- are present in the aqueous solutions. To determine the effect of the coexistence of other anions on the As adsorption, a coexisting ion adsorption experiment was conducted at an initial As (III) concentration of 10 mg L^{-1}.

Fig. 2.8 shows that the amount of As adsorbed by the D-Mn gel varies considerably depending on the type of the co-existing ions. The influence on the As adsorption increased in the following order: $PO_4^{3-} > SO_4^{2-} > HCO_3^-$; therefore, the valence of the co-existing anions is considered to be strongly related to the amount of adsorbed As. **Fig. 2.8** shows that the adsorption capacity decreased with increasing valence of the co-existing anions. The gel also exhibited good stability with negligible

change in adsorption at anion concentrations of 0, 0.1, and 1 mM. Therefore, this gel appears to be suitable for removing the trivalent As in the presence of the monovalent anions.

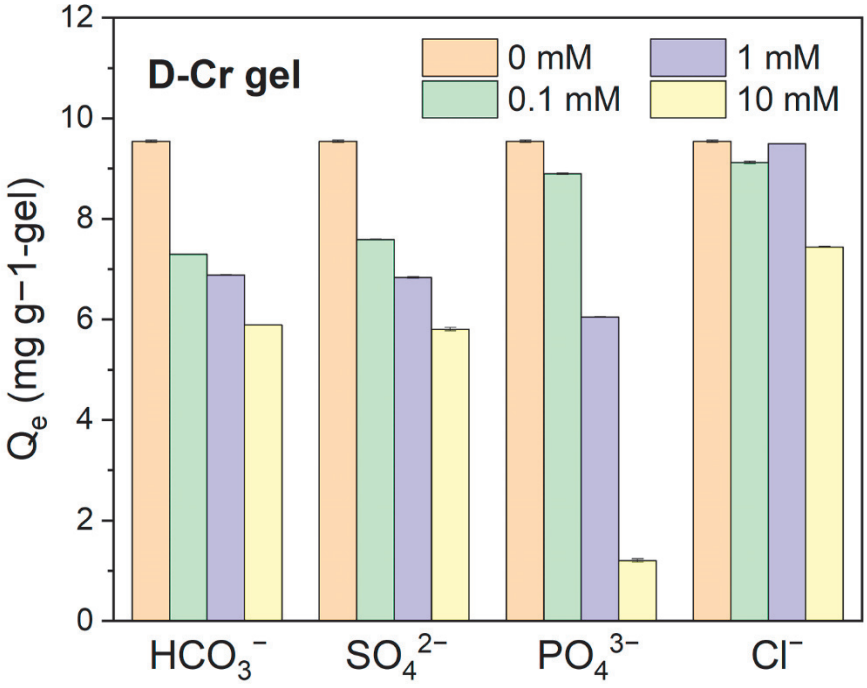

Fig. 2.9. Effect of co-existing ions on As removal by the D-Cr gel.

Similar to **Fig. 2.8**, **Fig. 2.9** shows that the As adsorption capacity was significantly different in the co-existence of different ions. The valence of the co-existing anions appears to be closely related to the amount of As adsorbed: the adsorption capacity of the gel decreased with increasing valence of the co-existing anions. However, unlike that of the D-Mn gel, the adsorption capacity of the D-Cr gel gradually decreased with the increasing concentration of the co-existing ions, indicating that its stability is inferior to that of the D-Mn gel. However, in the presence of divalent anions, the D-Cr gel showed a larger adsorption capacity than the D-Mn gel. Therefore, the D-Cr gel is considered suitable for removing the trivalent As in the

presence of the monovalent or divalent anions.

2.4. Conclusion

In summary, the polymer gel adsorbents (DMAPAAQ) carrying an oxidant ($KMnO_4$/$K_2Cr_2O_7$) were successfully synthesized (D-Mn and D-Cr gels). We demonstrated that a DMAPAAQ gel carrying an oxidant could significantly enhance the adsorption of As (III). Owing to the redox reaction with MnO_4^- and $Cr_2O_7^{2-}$ inside the gel, As (III) was oxidized to As (V), which increased the adsorption efficiency. As was also adsorbed onto MnO_2 in the gel. The maximum adsorption capacities for As (III) of D-Mn and D-Cr gels reach 163 and 263 mg g^{-1}-gel, respectively. The maximum adsorption capacities of the D-Mn and D-Cr gels were also larger than those of the other inorganic As adsorbents. The As adsorption in the D-Mn and D-Cr gels was dominated by chemisorption, as revealed by the adsorption kinetic analysis. The D-Mn gel appears to be suitable for removing As (III) in the presence of the monovalent anions, while the D-Cr gel is considered suitable for removing As (III) in the presence of monovalent or divalent anions.

2.5 References

(1) Ahmed, W.; Mehmood, S.; Núñez-Delgado, A.; Ali, S.; Qaswar, M.; Shakoor, A.; Maitlo, A.A.; Chen, D.-Y. Adsorption of Arsenic (III) from Aqueous Solution by a Novel Phosphorus-Modified Biochar Obtained from Taraxacum Mongolicum Hand-Mazz: Adsorption Behavior and Mechanistic Analysis. *J. Environ. Manage.* **2021**, *292*, 112764.

(2) Saif, S.; Adil, S.F.; Khan, M.; Hatshan, M.R.; Khan, M.; Bashir, F. Adsorption Studies of Arsenic(V) by CuO Nanoparticles Synthesized by Phyllanthus Emblica Leaf-Extract-Fueled Solution Combustion Synthesis. *Sustainability* **2021**, *13*, 2017.

(3) Brammer, H.; Ravenscroft, P. Arsenic in Groundwater: A Threat to Sustainable Agriculture in South and South-East Asia. *Environ Int.* **2009**, *35*, 647–654.

(4) Faria, M.C.S.; Rosemberg, R.S.; Bomfeti, C.A.; Monteiro, D.S.; Barbosa, F.; Oliveira, L.C.A.; Rodriguez, M.; Pereira, M.C.; Rodrigues, J.L. Arsenic Removal from Contaminated Water by Ultrafine δ-FeOOH Adsorbents. *Chem. Eng. J.* **2014**, *237*, 47–54.

(5) Mohan, D.; Pittman, C.U. Arsenic Removal from Water/Wastewater Using Adsorbents—A Critical Review. *J. Hazard. Mater.* **2007**, *142*, 1–53.

(6) Sorg, T.J.; Chen, A.S.C.; Wang, L. Arsenic Species in Drinking Water Wells in the USA with High Arsenic Concentrations. *Water Res.* **2014**, *48*, 156–169.

(7) World Health Organization (WHO) Home Page. Available online: https://www.who.int/news-room/fact-sheets/detail/arsenic (accessed on 15 January 2018).

(8) Sarmah, S.; Saikia, J.; Phukan, A.; Goswamee, R.L. Adsorption of As (V) from Water over a Hydroxyl-Alumina Modified Paddy Husk Ash Surface and Its Sludge Immobilization. *Water Air Soil Pollut.* **2019**, *230*, 32.

(9) Amini, M.; Abbaspour, K.C.; Berg, M.; Winkel, L.; Hug, S.J.; Hoehn, E.; Yang, H.; Johnson, C.A. Statistical Modeling of Global Geogenic Arsenic Contamination in Groundwater. *Environ. Sci. Technol.* **2008**, *42*, 3669–3675.

(10) Chi, Z.; Zhu, Y.; Liu, W.; Huang, H.; Li, H. Selective Removal of As (III) Using Magnetic Graphene Oxide Ion-Imprinted Polymer in Porous Media: Potential Effect of External Magnetic Field. *J. Environ. Chem. Eng.* **2021**, *9*, 105671.

(11) Guo, L.; Ye, P.; Wang, J.; Fu, F.; Wu, Z. Three-Dimensional Fe3O4-Graphene Macroscopic Composites for Arsenic and Arsenate Removal. *J. Hazard. Mater.* **2015**, *298*, 28–35.

(12) Yan, B.; Liang, T.; Yang, X.; Gadgil, A.J. Superior Removal of As (III) and As (V) from Water with Mn-Doped β-FeOOH Nanospindles on Carbon Foam. *J. Hazard. Mater.* **2021**, *418*, 126347.

(13) Ha, H.T.; Phong, P.T.; Minh, T.D. Synthesis of Iron Oxide Nanoparticle Functionalized Activated Carbon and Its Applications in Arsenic Adsorption. *J. Anal. Methods Chem.* **2021**, *2021*, 1–9.

(14) Kanel, S.R.; Nepal, D.; Manning, B.; Choi, H. Transport of Surface-Modified Iron Nano-particle in Porous Media and Application to Arsenic (III) Remediation. *J. Nanopart. Res.* **2007**, *9*, 725–735.

(15) Rahdar, S.; Taghavi, M.; Khaksefidi, R.; Ahmadi, S. Adsorption of Arsenic (V) from Aqueous Solution Using Modified Saxaul Ash: Isotherm and Thermodynamic Study. *Appl. Water Sci.* **2019**, *9*, 87.

(16) Joshi, S.; Sharma, M.; Kumari, A.; Shrestha, S.; Shrestha, B. Arsenic Removal from Water by Adsorption onto Iron Oxide/Nano-Porous Carbon Magnetic Composite. *Appl. Sci.* **2019**, *9*, 3732.

(17) Qureshi, M.; Stecher, G.; Huck, C.; Bonn, G. Preparation of Polymer Based Sorbents for Solid Phase Extraction of Polyphenolic Compounds. *Open Chem.* **2011**, *9*, 206–212.
(18) Beaugeard, V.; Muller, J.; Graillot, A.; Ding, X.; Robin, J.-J.; Monge, S. Acidic Polymeric Sorbents for the Removal of Metallic Pollution in Water: A Review. *Reactive Funct. Polym.* **2020**, *152*, 104599.
(19) Önnby, L.; Pakade, V.; Mattiasson, B.; Kirsebom, H. Polymer Composite Adsorbents Using Particles of Molecularly Imprinted Polymers or Aluminium Oxide Nanoparticles for Treatment of Arsenic Contaminated Waters. *Water Res.* **2012**, *46*, 4111–4120.
(20) Kim, H.-C.; Shang, X.; Huang, J.-H.; Dempsey, B.A. Treating Laundry Waste Water: Cationic Polymers for Removal of Contaminants and Decreased Fouling in Microfiltration. *J. Membr. Sci.* **2014**, *456*, 167–174.
(21) Safi, S.R.; Senmoto, K.; Gotoh, T.; Iizawa, T.; Nakai, S. The Effect of γ-FeOOH on Enhancing Arsenic Adsorption from Groundwater with DMAPAAQ + FeOOH Gel Composite. *Sci. Rep.* **2019**, *9*, 11909.
(22) Zhang, J.; Ding, T.; Zhang, Z.; Xu, L.; Zhang, C. Enhanced Adsorption of Trivalent Arsenic from Water by Functionalized Diatom Silica Shells. *PLoS One* **2015**, *10*, e0123395.
(23) Mishra, P.K.; Rai, P.K. Ultrafast Removal of Arsenic Using Solid Solution of Aero-Gel Based Ce1-XTixO2-Y Oxide Nanoparticles. *Chemosphere* **2019**, *217*, 483–495.
(24) Wen, Z.; Lu, J.; Zhang, Y.; Cheng, G.; Huang, S.; Chen, J.; Xu, R.; Ming, Y.; Wang, Y.; Chen, R. Facile Inverse Micelle Fabrication of Magnetic Ordered Mesoporous Iron Cerium Bimetal Oxides with Excellent Performance for Arsenic Removal from Water. *J. Hazard. Mater.* **2020**, *383*, 121172.

Chapter 3: Efficient Removal of Cr (VI)

3.1 Introduction

High-concentration Cr-contaminated wastewater, which exceeds wastewater emission standards, causes serious environmental and public health problems, such as cancer, hemolysis, and renal damage.[1] The primary constituent of heavy metal pollutants in industrial wastewater is hexavalent chromium, Cr (VI), which is primarily produced by the metal polishing, plating, textile dyeing, alloying, chromic salt, and leather processing industries.[2,3] Many methods aimed at treating Cr in wastewater, such as ion exchange,[4] adsorption,[5] reduction, and chemical precipitation,[6] have been applied to remove Cr (VI). Adsorption is widely used to remove contaminants, such as heavy metals and organic pollutants, owing to its operational simplicity, high efficiency, and relatively low expense.[7] Conventional Cr wastewater treatment is conducted via a reduction process that converts Cr (VI) into less toxic trivalent chromium, Cr (III), followed by adsorption, which removes the Cr (III).[8] However, the combination of these methods has certain disadvantages. The reducing agents cause secondary environmental pollution and involve multiple processes that significantly limit their practical application in industrial wastewater treatment.[3]

Therefore, researchers are increasingly focusing on developing advanced materials for the more efficient removal of Cr (VI).[9–11] In the past several years, many adsorbents have been fabricated and used for Cr (VI) adsorption. One group is polymer adsorbents, which are the most popular due to their ability to adsorb Cr (VI) from industrial wastewater. They are environmentally friendly and chemically modifiable whilst having many adsorbent sites and outstanding renewable advantages.[12,13] There are two main types of macromolecule adsorbents: one adsorbs via interactions between the hydrophobic groups of adsorbents and adsorbates, whereas the other adsorbs via

interactions between polar functional groups in adsorbents and hydrophilic groups in adsorbates that have a high affinity for Cr (VI), such as *N*-[3-(Dimethylamino) propyl] acrylamide methyl chloride quaternary monomer (DMAPAA-Q) (DQ) and *N, N*-dimethylamino propylacrylamide monomer (DMAPAA) (DA).[14] DQ, a cationic monomer with a positively charged quaternary amino group, is used as a polymer flocculant, an antistatic agent, and in cosmetics.[14] To maintain the charge balance of the DQ monomer, the positively charged quaternary amino group of DQ attracts the counter anion Cl^-. This property allows the loading and removal of necessary and harmful anions, respectively, via a mutual ion exchange of Cl^- ions.[14] DA is a cationic monomer with a functional amino group. The difference between DQ and DA is that the DA amino group is a tertiary amino group that becomes positively charged following protonation whilst simultaneously adsorbing heavy metal cations via chelation and anions through electrostatic interaction.[15,16]

Although polymer adsorbents possess many excellent properties, significant challenges are encountered during their use for Cr (VI) removal due to Cr properties. Cr exists in various oxidation states, the most common being Cr (III) and Cr (VI).[17] External environmental changes, such as pH changes, result in the release of adsorbed Cr (VI) into the environment, causing secondary pollution due to its high mobility.[18] In contrast, the toxicity of Cr (III) is only 1% of that of Cr (VI).[19] A small amount of Cr (VI), an essential trace element, is not harmful to the human body.[20] Moreover, it combines easily with OH^- to form insoluble chromium hydroxide ($Cr(OH)_3$), making its removal safer and more efficient. Therefore, DA, where adsorbates form the insoluble hydroxide internally with OH^- after protonation, and DQ, which carries the reductant and adsorbs the Cr anions via an ion exchange method, were selected to form a copolymer hydrogel adsorbent (**Scheme 3.1**) synthesized via in situ polymerization to improve the safe and efficient removal of Cr.

In this study, a reductant (ascorbic acid)-functionalized polymer gel adsorbent, prepared using DQ and DA, which are cationic polymers with many adsorption sites,

was synthesized to treat Cr-containing wastewater. A series of Cr adsorption experiments using the gels were conducted to detailly study the effects of aqueous physicochemical factors, including solution pH, initial Cr (VI) concentration (using adsorption isotherms such as Langmuir and Freundlich models), contact time (using adsorption kinetics such as pseudo-first-order and pseudo-second-order models), temperature (using adsorption thermodynamics), and co-existing anions on the removal process of Cr (VI).

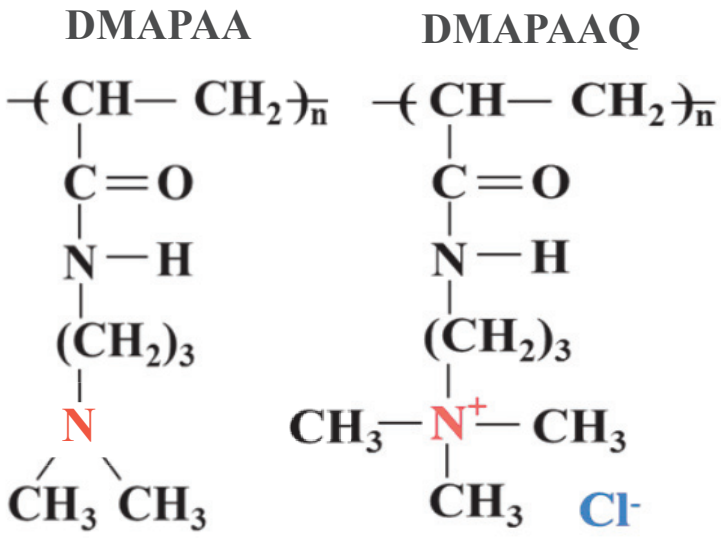

Scheme 3.1. Structural formula of DMAPAA/DMAPAAQ copolymer hydrogel.

3.2 Materials and method

3.2.1 Materials

DA and DQ monomers were purchased from KJ Chemicals Co., Tokyo, Japan. Potassium dichromate ($K_2Cr_2O_7$) and *N, N, N', N'*- tetrathylethylenediamine (TEMED) were purchased from Nacalai Tesque, Inc. (Kyoto, Japan), and *N, N'*-methylenebisacrylamide (MBAA), ammonium peroxodisulfate (APS), and L-ascorbic acid (VC) were purchased from Sigma Aldrich Co., (St. Louis, MO, USA). All reagents were of reagent grade and used as received. Aqueous solutions were prepared

using distilled water (DW).

3.2.2 Synthesis of DA/DQ (500:500) hydrogel

A monomer solution containing 2.5839 g of DQ (monomer), 1.9529 g of DA (monomer), 0.1927 g of MBAA (cross-linking agent), and 0.0581 g of TEMED (accelerator) was mixed with DW in a 20 mL volumetric flask whilst being magnetically stirred. Subsequently, 0.1141 g of APS (the initiator) was dissolved and mixed with DW in a 5 mL volumetric flask, creating the initiator solution (**Table 3.1**). The monomer and initiator solutions were infused with N_2 for 30 min to expel O_2 to prevent the inhibition of radical polymerization. Next, the initiator solution was added to the monomer solution and stirred for 20 s, and the mixture was injected into six tubes (diameter: 7 mm × 9 mm). The monomers (DQ, DA) and linker (MBAA) were copolymerized at 25 °C for 24 h, after which the gel was extracted from the tubes and cut into multiple 5 mm-high circular columns. A Soxhlet extractor (Asahi Glassplant Inc., Arao City, Japan) was used to wash the gels with methanol to remove unreacted components and eliminate the possibility of other substances affecting the adsorption results. After washing, the gel was air-dried at 25 °C for several days and subsequently dried in an oven at 50 °C for 24 h. Finally, the gels were crushed into powder using a Wonder Crusher WC-3 (Osaka Chemical Co., Ltd., Osaka City, Japan).

Table 3.1. Preparation of DA/DQ gel.

Component	Function	Molecular Weight (g mol^{-1})	Concentration (mol m^{-3})	Mass (g)
DMAPAAQ	Monomer	206.71	500	2.5839
DMAPAA	Monomer	156.23	500	1.9529
MBAA	Linker	154.17	50	0.1156
TEMED	Accelerator	116.21	20	0.0349
APS	Initiator	228.19	20	0.0685

3.2.3 Preparation of the ascorbic acid functionalized DA/DQ (DA/DQ/VC) gel

Ascorbic acid (0.8975 g) was dissolved with DW in a 250 mL volumetric flask to obtain a 0.01 mol L^{-1} solution and stirred for 15 min. Next, 2 g of DA/DQ gel was dispersed in the prepared ascorbic acid solution (250 mL), and the mixture was stirred at 25 °C for 24 h before the gel was dried in an oven at 50 °C for 24 h.

3.2.4 Batch Adsorption Experiments

A Cr (VI) sample solution was prepared by dissolving $K_2Cr_2O_7$ in the DW. Batch adsorption experiments were conducted in 40 mL plastic vials with 0.5 g L^{-1} gel adsorbent to investigate the influences of solution pH, contact time, temperature, and co-existing anions on Cr removal in the synthetic Cr (VI) solution by the two gels. Initially, Cr (VI) removal experiments were performed to explore the effect of pH (2–12) on Cr (VI) removal using an initial Cr (VI) concentration of 100 mg L^{-1} at 25 °C for 24 h. The initial pH of the synthetic Cr (VI) solution was adjusted with NaOH and HCl solutions (1 mol L^{-1}). Many adsorption models, such as the Langmuir, Freundlich, pseudo-first-order, and pseudo-second-order models, were used to further elucidate the mechanism underlying Cr adsorption by the gels. The effects of the initial Cr (VI) concentrations ranged from 20 to 500 mg L^{-1} for 24 h. The contact time varied from

0.5 to 6 h at different Cr (VI) initial concentrations, and temperatures of 25 °C, 35 °C, and 45 °C were investigated using the models.

The effects of co-existing ions were investigated by adding 20 mg of a given gel to 40 mL of Cr (VI) solution (initial Cr concentration: 1 mmol L^{-1}) containing HCO_3^-, SO_4^{2-}, PO_4^{3-}, and Cl^- ions in the binary system, with Cr and one of the co-existing anions (initial concentrations of the co-existing ions were 0, 0.1, 1, and 5 mmol L^{-1}, respectively).

3.2.5 Characterizations

An inductively coupled plasma atomic emission spectroscopy (ICP-AES, SPS-3500, Shimadzu Corp., Japan) was applied to measure the Cr concentration. After adsorption, all Cr solutions were filtered using a 0.22-μm membrane to prevent the gels from affecting the measurement results of the Cr equilibrium concentration, and all data were obtained from the calculation of the average of three measurements. X-ray photoelectron spectroscopy (XPS, ESCA-3400, Shimadzu Corp., Japan) was applied to record the surface element information. The structural information of gels was detected using Fourier transform infrared spectroscopy (FTIR, IRTracer−100, Shimadzu Corp., Japan) with a wavelength of 4000-400cm^{-1}.

3.3 Results and discussion

3.3.1 Effect of the solution pH

Various forms of Cr (VI) are present as solution pH value changes in aquatic environments (**Fig. 3.1**a), and solution pH changes could affect Cr removal by changing the surface charge of the adsorbent.[21] $HCrO_4^-$ and $Cr_2O_7^{2-}$ were dominant at pH 2−6, whereas CrO_4^{2-} and H_2CrO_4 were dominant at pH > 6.0 and pH < 2.0, respectively.

The effect of initial pH on Cr (VI) removal by DA/DQ and DA/DQ/VC gels was investigated, and the results are shown in **Fig. 3.1**b. Cr (VI) removal rate using both gels increased and reached a peak value at pH 3, which may be attributed to increasing amino group protonation; this was accompanied by decreasing pH and facilitated Cr adsorption via electrostatic attraction.[3] However, as the degree of dissociation of chromic acid decreased, H_2CrO_4 molecules appeared at pH < 2.0, weakening the electrostatic attraction between the adsorption site and Cr (VI) and making adsorption more difficult.[21] Moreover, both DA/DQ and DA/DQ/VC gels removed Cr (VI) via ion exchange adsorption, promoting their maintenance of a high Cr (VI) adsorption capacity with increasing pH and weak amino group protonation in a pH range of 3–6. However, at pH > 6 or in neutral and alkaline environments, the adsorption capacity of both gels decreased rapidly with increasing pH due to the exchange of large amounts of OH^- ions between Cr (VI) and Cl^- in DQ, which made the protonation of the amino group in DA difficult and consequently weakened the electrostatic attraction between Cr (VI) and $-NH^+$ adsorption sites. The DA/DQ/VC gel, which carried ascorbic acid with dissociated H^+, enhanced protonation of the amino group and increased the adsorption sites at the ascorbic acid functionalization stage, which helped maintain a higher removal efficiency than the DA/DQ gel at pH 7-10. However, at pH > 10, in the DA/DQ/VC gel, approximately 50% of the adsorption sites of positively charged quaternary amino groups were occupied by ascorbic acid. Therefore, this gel had a lower adsorption performance than the DA/DQ gel due to the difficulties in the ion exchange and oxidation-reduction reactions between Cr and the reductant in a strongly alkaline environment.

In addition, where 50% of the adsorption sites of positively charged quaternary amino groups were occupied by ascorbic acid, the adsorption capacity of the DA/DQ/VC gel was still more improved than that of the DA/DQ gel at pH < 10, confirming the adsorption method using DA/DQ/VC gel, which could improve the adsorption of Cr by reducing Cr (VI) to Cr (III), to be feasible.

To analyze the effect of K^+ in the Cr sample solution on the adsorption capacity of the gel, the Cr sample was prepared by dissolving $K_2Cr_2O_7$ powder in water for anions such as $Cr_2O_7^{2-}$ and cations such as K^+, to be present in the solution. The DA/DQ gel adsorbed $Cr_2O_7^{2-}$ anions via ion exchange and electrostatic attraction; thus, K^+ had no significant effect on its adsorption performance. The DA/DQ/VC gel had a diversified adsorption method that simultaneously removed anions and cations, suggesting that K^+ affects the Cr^{3+} adsorption capacity of the gel. However, even under the influence of K^+, the adsorption performance of the DA/DQ/VC gel was stronger than that of the DA/DQ gel. Therefore, without the influence of the cation, the removal performance of the DA/DQ/VC gel will be further improved.

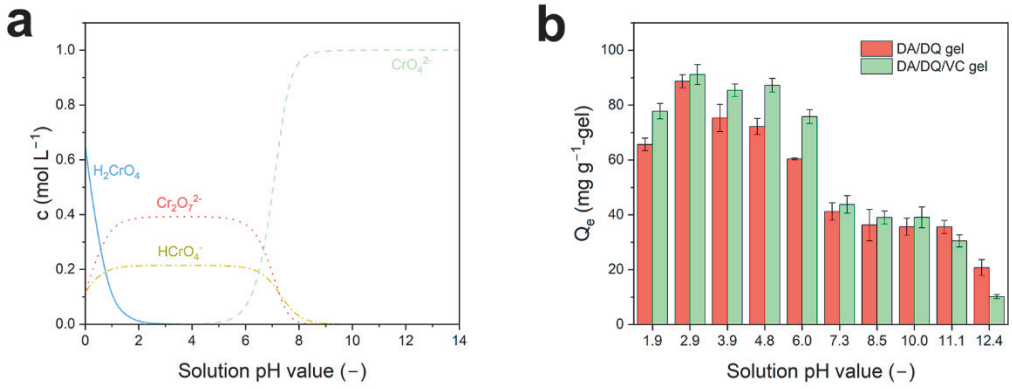

Fig. 3.1. (a) Chromium (Cr) speciation in different solution pH values. (b) Effect of pH value on the hexavalent chromium, Cr (VI), adsorption capacity of the (DA/DQ) and DA/DQ/L-ascorbic acid (DA/DQ/VC) gels.

3.3.2 Effect of initial Cr (VI) concentration (adsorption isotherms)

The adsorption isotherms for Cr removal by the gels are shown in **Fig. 3.2**. The Langmuir and Freundlich models were used to determine the amount of Cr removed by the DA/DQ and DA/DQ/VC gels (**Figs. 3a-d**).

The adsorption capacity of the DA/DQ/VC gel was better than that of the DA/DQ gel at each temperature (25, 35, and 45 °C), and the maximum adsorption

capacity of the DA/DQ/VC gel was higher than that of the DA/DQ gel (**Fig. 3.2**); this was because increased adsorption of Cr (III) from the total Cr increased the Cr adsorption efficiency and the difficulty in moving freely in cation form if Cr (III) is fixed inside the gel (via the formation of insoluble hydroxide). The ion exchange adsorption method had a strong adsorption capacity at low Cr concentrations; however, the mobility of Cr (IV) was relatively high. Changing external conditions would induce the movement of Cr (IV) from the gel back into the solution, resulting in difficulties in the practical water treatment application.

According to Yuwei and Jianlong,[22] the Freundlich model assumes that the adsorbent surface is energetically heterogeneous. The Langmuir model assumes that the adsorbent surface is structurally homogeneous.[23] The Freundlich model fits the total Cr (VI) removed by the DA/DQ gel more effectively (R^2 = 0.9926) than the Langmuir model (R^2 = 0.9346) at 25 °C, resulting in a higher correlation coefficient (**Table 3.2**). The DA/DQ/VC gel also fits the Freundlich model (R^2 = 0.9886) more closely than the Langmuir model (R^2 = 0.9169) at 25 °C (**Table 3.3**). The adsorption of both gels strongly correlated with the Freundlich model, which confirmed that the adsorption model of the two gels was not a single ion exchange or electrostatic interaction, but an effect of multiple interactions. As described in the Introduction, the DA/DQ gel removes Cr (VI) in two ways: the electrostatic attraction method, in which protonated tertiary amino groups attract the anions in DA and the ion exchange method in DQ.[3,14] However, the DA/DQ/VC gel had a slightly different mechanism: the ascorbic acid in the gel underwent a redox reaction with Cr (VI), whereas the reduced Cr (III) was fixed inside the gel via complex reactions, such as chelation and the formation of dissolved hydroxides. Unreduced Cr (VI) was also adsorbed by electrostatic attraction and ion exchange methods like those in the DA/DQ gel.

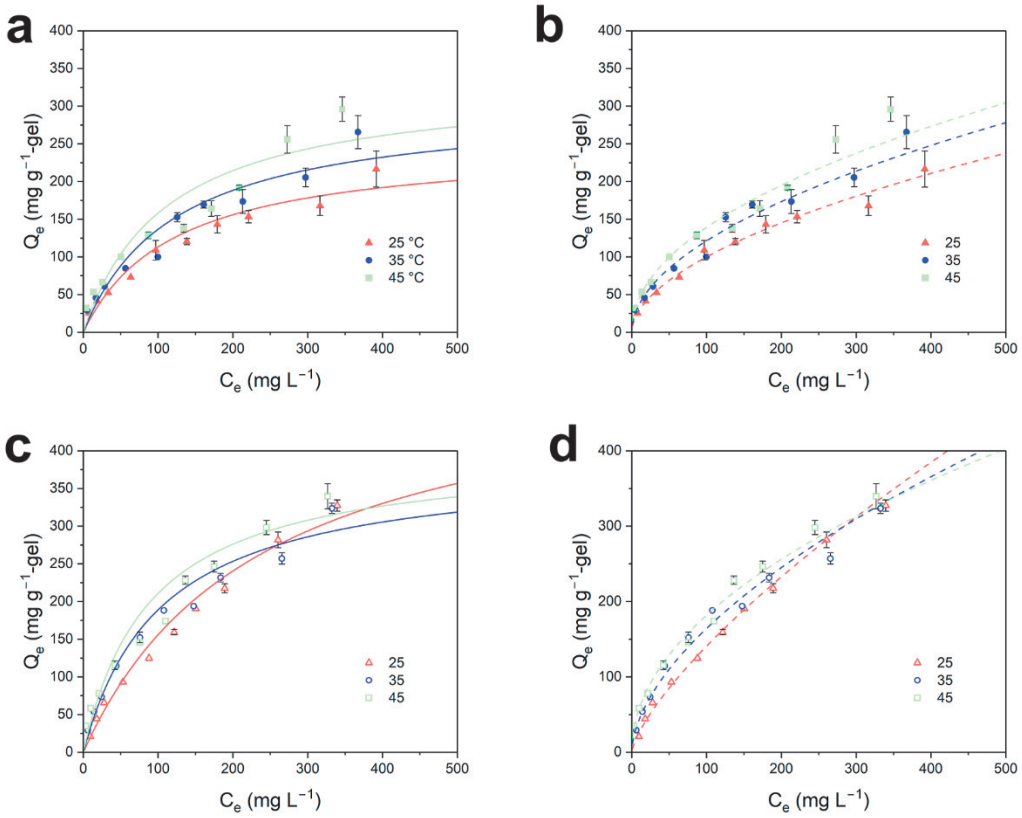

Fig. 3.2. Adsorption isotherms and Langmuir isotherms fitted to the Cr (VI) removal by (a) DA/DQ and (c) DA/DQ/VC gels; Adsorption isotherms and Freundlich isotherms fitted to the Cr (VI) removal by (b) DA/DQ and (d) DA/DQ/VC gels.

Table 3.2. Parameters of Langmuir and Freundlich model by DA/DQ gel at 25, 35, and 45 °C.

Tem. (°C)	Langmuir model			Freundlich model		
	Q_m (mg g^{-1})	K_L (L mg^{-1})	R^2	K_F (mg g^{-1}(L mg^{-1})$^{1/n}$)	1/n	R^2
25	250	0.0083	0.9346	8.37	0.54	0.9926
35	303	0.0082	0.8695	11.30	0.52	0.9812
45	333	0.0090	0.8305	14.81	0.49	0.9789

Table 3.3. Parameters of Langmuir and Freundlich model by DA/DQ/VC gel at 25, 35, and 45 °C.

Tem. (°C)	Langmuir model			Freundlich model		
	Q_m (mg g^{-1})	K_L (L mg^{-1})	R^2	K_F (mg g^{-1}(L mg^{-1})$^{1/n}$)	1/n	R^2
25	526	0.0042	0.9169	4.98	0.73	0.9886
35	384	0.0096	0.9521	11.52	0.58	0.9895
45	400	0.0111	0.9092	18.67	0.49	0.9923

3.3.3 Effect of contact time on Cr adsorption (adsorption kinetics)

The kinetics of Cr (VI) adsorption was simulated using the pseudo-first-order and pseudo-second-order kinetic models. [24] The effect of contact time on Cr removal by the gels was evaluated using initial Cr concentrations of 20 and 100 mg L^{-1}, respectively. Pseudo-first-order and pseudo-second-order models used to fit the amount of Cr removed by DA/DQ and DA/DQ/VC gels are shown in **Figs. 3.3**a, and **3.3**b. Due to ascorbic acid occupying nearly half of the adsorption sites of DQ (49 Mol%), the adsorption capacity of the DA/DQ/VC gel at low Cr concentrations was not as effective as that of the DA/DQ gel. Thus, although the maximum adsorption capacity of DA/DQ/VC was greater than that of DA/DQ, its adsorption performance would be drastically reduced at relatively low Cr concentrations. However, decreasing the dosage of the DA/DQ/VC gel (lowered to 0.25 g L^{-1} or less) may improve the adsorption of Cr.

The constants of both kinetic models are shown in **Tables 3.4** and **3.5**. The correlation coefficient of the pseudo-second-order model (DA/DQ: R^2 = 0.9993, DA/DQ/VC: R^2 = 0.9950) was much larger than that of the pseudo-first-order model (DA/DQ: R^2 = 0.9517, DA/DQ/VC: R^2 = 0.9296) at high Cr concentrations (100 mg L^{-1}). These results revealed that Cr removal using both DA/DQ gel and DA/DQ/VC gels fit the pseudo-second-order model when treating high-concentration Cr-

contaminated wastewater, suggesting that chemisorption plays a role in Cr removal using adsorbent. In addition, DA/DQ/VC gel adsorption at low concentrations (20 mg L^{-1}) was dominated by physisorption and chemisorption and highly correlated with both models.

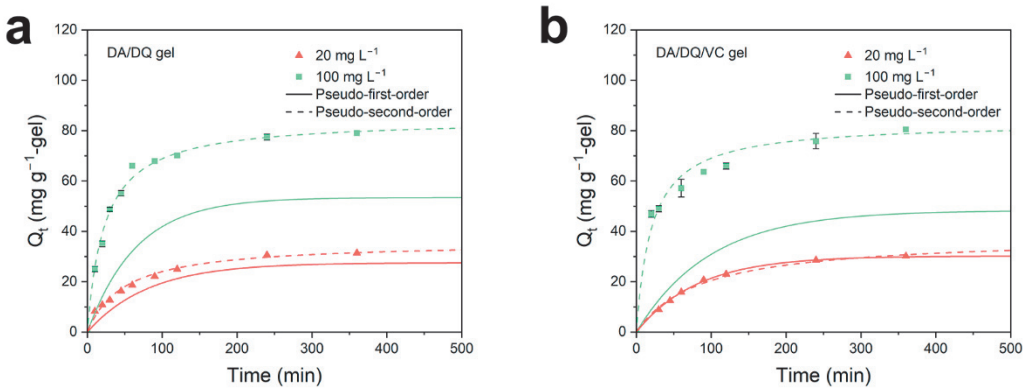

Fig. 3.3. (a) Plots of the pseudo-first-order and pseudo-second-order dynamic model of the DA/DQ gel at 20 and 100 mg L^{-1} initial Cr concentration; (b) Plots of the pseudo-first-order and pseudo-second-order dynamic model of the DA/DQ/VC gel at 20 and 100 mg L^{-1} initial Cr concentration.

Table 3.4. Kinetic parameters of Cr adsorption using the DA/DQ gel.

Initial	Pseudo-first-order model			Pseudo-second-order model		
concentration	k_1 (min^{-1})	Q_e (mg g^{-1})	R^2	k_2 (g mg^{-1} min^{-1})	Q_e (mg g^{-1})	R^2
20 mg L^{-1}	0.0123	27.53	0.9857	0.0006	35.84	0.9958
100 mg L^{-1}	0.0153	53.44	0.9517	0.0005	84.75	0.9993

Table 3.5. Kinetic parameters of Cr adsorption using the DA/DQ/VC gel.

Initial	Pseudo-first-order model			Pseudo-second-order model		
concentration	k_1 (min^{-1})	Q_e (mg g^{-1})	R^2	k_2 (g mg^{-1} min^{-1})	Q_e (mg g^{-1})	R^2
20 mg L^{-1}	0.0123	30.21	0.9991	0.0003	38.02	0.9948
100 mg L^{-1}	0.0102	48.30	0.9296	0.0006	83.33	0.9950

3.3.4 Effect of temperature (adsorption thermodynamics)

Temperature changes affect the movement of molecules, atoms, and ions, among others, and subsequently, affect the adsorption efficiency of the gel.[14] The thermodynamic parameters of Cr (VI) adsorption were quantified to investigate the effect of temperature on Cr removal via adsorption using DA/DQ/VC gel. The Gibbs free energy ΔG (kJ mol^{-1}), enthalpy change ΔH (kJ mol^{-1}), and entropy change ΔS (kJ mol^{-1} K^{-1}) were calculated. [25–27] The results calculated using equations (1.11) and (1.14) were plotted, and equations (1.12) and (1.13) were used to calculate ΔH, ΔS, and ΔG and obtain the values used in **Fig. 3.4**. The calculated thermodynamic parameters are presented in **Tables 3.6** and **3.7**. Previous discussions have shown that DA/DQ/VC gel removes reduced Cr (III) via chelation and the formation of insoluble hydroxides and Cr (VI) via ion exchange. Ion exchange, which involves the formation of ionic bonds, is an exothermic reaction.[14] However, these calculations showed that the removal process was endothermic (ΔH > 0), indicating that the heat absorbed by this process was primarily due to the redox reaction and adsorption of Cr (III). Furthermore, the DA/DQ gel may involve electrostatic interactions. The thermodynamic parameters (**Tables 3.6** and **3.7**) show that the Cr removal by both the DA/DQ and DA/DQ/VC gels was irreversible and spontaneous.

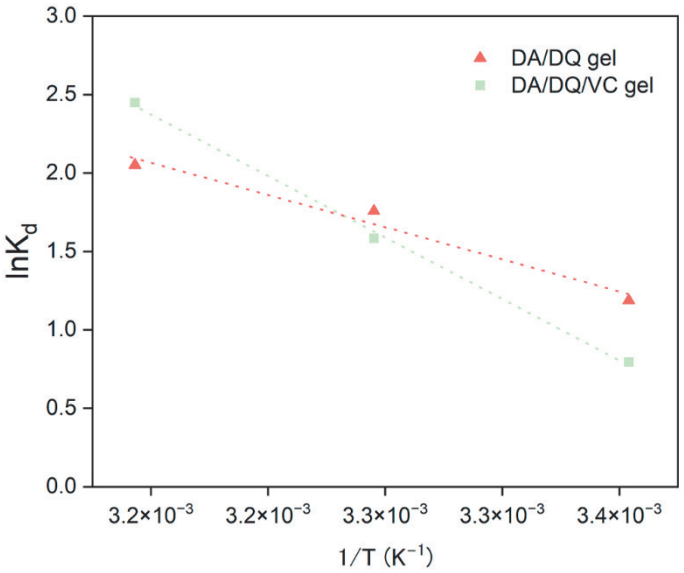

Fig. 3.4. Effect of temperature on the distribution of the adsorption coefficient of the DA/DQ/VC gel.

Table 3.6. Thermodynamic parameters of DA/DQ gel at 20 mg L^{-1} initial Cr concentration.

T (K)	lnK_d	ΔH (kJ mol^{-1})	ΔS (kJ mol^{-1} K^{-1})	ΔG (kJ mol^{-1})
298.15	1.19	34.13	0.13	-3.14
308.15	1.76	34.13	0.13	-4.39
318.15	2.05	34.13	0.13	-5.64

Table 3.7. Thermodynamic parameters of DA/DQ/VC gel at 20 mg L^{-1} initial Cr concentration.

T (K)	lnK_d	ΔH (kJ mol^{-1})	ΔS (kJ mol^{-1} K^{-1})	ΔG (kJ mol^{-1})
298.15	0.79	65.17	0.23	-1.92
308.15	1.58	65.17	0.23	-4.17
318.15	2.45	65.17	0.23	-6.42

3.3.5 Effect of co-existing anions on Cr (VI)-removing capabilities of the gels

The presence of various anions in the aqueous solution may interfere with Cr (VI) removal during wastewater treatment.[28–31] Therefore, the effect of other anions, such as HCO_3^-, SO_4^{2-}, PO_4^{3-}, and Cl^-, on Cr adsorption was investigated, and the results are presented in **Fig. 3.5**.

First, the adsorption capacity of the two gels decreased with increasing coexisting anion concentrations, and the higher the coexisting anion valence, the greater the decrease in gel adsorption capacity. This can be attributed to either the hindrance of exchanges between $HCrO_4^-$, $Cr_2O_7^{2-}$, or CrO_4^{2-} and Cl^- in DQ due to the presence of large amounts of co-existing anions, or the occupation of a part of the $-NH^+$ adsorption sites on DA by co-existing anions from the electrostatic attraction, which would decrease the adsorption capacity of the two gels.

Second, the influence of co-existing anions on the Cr-removing capability of DA/DQ/VC gel was much lower than that on the Cr-removing capability of DA/DQ gel because the low-valent co-existing anions exerted only a minor effect on the adsorption capacity of the gel, even at co-existing anion concentrations of 5 mM. This result revealed that the method of Cr (III) removal via chelation and the formation of insoluble hydroxides was more stable and less susceptible to co-existing anions than the method of Cr (IV) adsorption via electrostatic attraction.

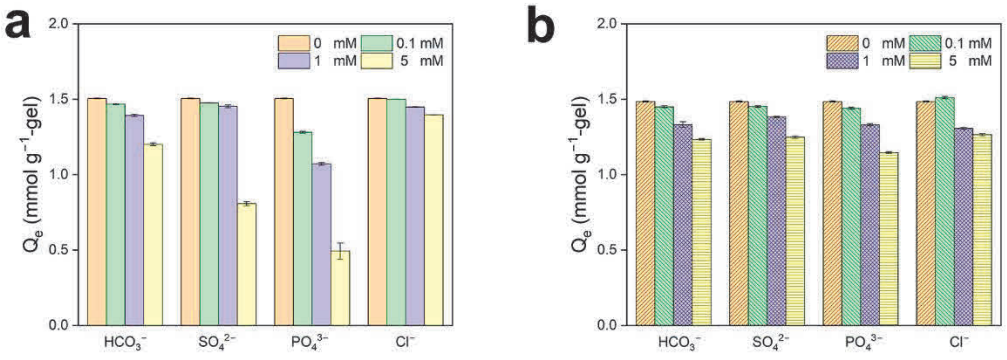

Fig. 3.5. Effect of various co-existing anions on Cr removal by (a) DA/DQ and (b) DA/DQ/VC gels.

3.3.6 Characterization (removal mechanisms)

To clarify the possible removal mechanisms of the gels, the FTIR spectra of DA/DQ and DA/DQ/VC gels were recorded before and after adsorption at 4000-400 cm^{-1}(**Figs. 3.6**a and **3.6**b). In the DA/DQ/VC gel spectra after Cr adsorption, a peak at 1715 cm^{-1} was observed and potentially derived from C=C, indicating that VC was successfully loaded on the DA/DQ gel. The intensity of peaks at 1070 and 1170 cm^{-1} of the DA/DQ/VC gel was stronger than that of the DA/DQ gel, which might be attributed to the increase of pronated amino groups into $–N^+$ due to the dissociation of VC.[9] In addition, the weak peaks at 930 and 875 cm^{-1} of the DA/DQ gel were attributed to the Cr-O stretch vibrations of CrO_4^{2-} and $HCrO_4^-$,[32] which indicated that Cr (VI) species were adsorbed by the DA/DQ gel.

The Cr removal models of DA/DQ and DA/DQ/VC gels after adsorption were also investigated using XPS spectroscopy. Cr peaks were observed in the wide spectra of DA/DQ and DA/DQ/VC gels (**Fig. 3.6**c). The Cr 2p high-resolution spectrum of DA/DQ/VC gel is shown in **Fig. 3.6**d**;** the Cr 2p1/2 and Cr 2p3/2 peaks were divided into double peaks, which could be ascribed to Cr (VI) and Cr (III), respectively. This result suggested that Cr (III), reduced by VC, was removed by the DA/DQ/VC gel.

Overall, the proposed mechanisms for Cr removal by the DA/DQ/VC gel (**Scheme 3.2**) include the ion exchange adsorption method–Cr (VI) anions ($HCrO_4^-$ and $Cr_2O_7^{2-}$, etc.) were removed on the positively charged quaternary amino groups ($-N^+(CH_3)_3Cl^-$) of the DQ monomer via a mutual exchange of Cl^- ions; the electrostatic interaction method–Cr (VI) anions were adsorbed on the protonated amino groups ($-N(CH_3)_2H^+$) in the DA monomer; chelation method–Cr (VI) anions were reduced to Cr^{3+} via oxidation-reduction reaction with reductant VC in the DA/DQ/VC gel. Thus, the reduced Cr^{3+} cations could be adsorbed on the protonated amino groups ($-N(CH_3)_2H^+$) of the DA monomer via chelation; and the insoluble hydroxide formation method–Cr (III) cation could form the insoluble chromium hydroxide ($Cr(OH)_3$) with OH^- inside the gel.

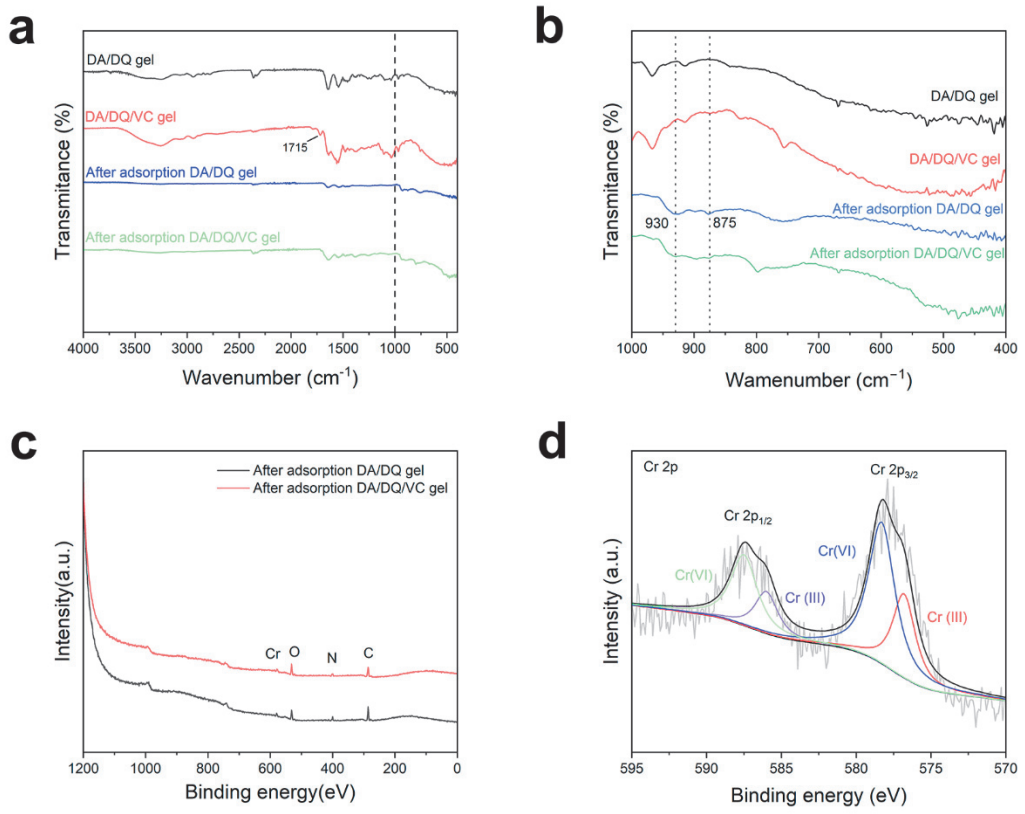

Fig. 3.6. FTIR spectrum of DA/DQ and DA/DQ/VC gels before and after adsorption at (a) 4000-400 cm^{-1} and (b) 1000-400cm^{-1}; (c) The XPS spectra of DA/DQ and DA/DQ/VC gels after Cr removal; (d) Cr 2p spectra of Cr element removed by DA/DQ

gel after removal.

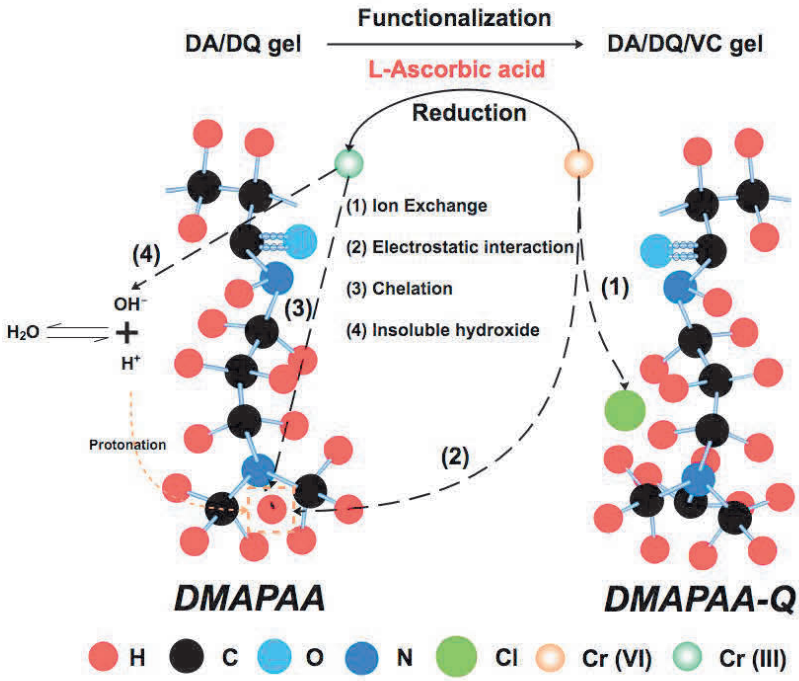

Scheme 3.2. Removal mechanism of Cr species by DA/DQ/VC gel.

3.4 Conclusion

In this study, a polymer gel adsorbent (DA/DQ) carrying a reductant (ascorbic acid) was successfully synthesized (DA/DQ/VC gel). The gel with abundant amino groups and a functionalized reductant adsorbed Cr (VI) via the ion exchange and electrostatic attraction method and subsequently removed the Cr (III) reduced by ascorbic acid via chelation and insoluble salt formation. Furthermore, the effect of aqueous physicochemical factors on Cr (VI) removal by the gel was investigated. The diversified adsorption methods in the gel exhibited remarkable chemical stability in acidic environments. Although both DA/DQ and DA/DQ/VC gels were not as effective in removing Cr (VI) at pH ≥ 11, the gels could still effectively maintain a high Cr

removal rate within the pH range of 3 to 6. Moreover, the DA/DQ/VC gel exhibited a higher Cr removal efficiency than the DA/DQ gel. The enhanced removal performance is likely due to the diversified removal methods it employs, and it is not significantly affected by the co-existing anions.

3.5 References

(1) Dayan, A. D.; Paine, A. J. Mechanisms of chromium toxicity, carcinogenicity and allergenicity: Review of the literature from 1985 to 2000, *Hum. Exp. Toxicol.* **2001**, *20*, 439–451.

(2) Rui, Z.; Xiang, L.; Bolun, S.; Yanzi, L.;Yumei, L.; Rui, Y.; Ce, W. Branched polyethylenimine grafted electrospun polyacrylonitrile fiber membrane: a novel and effective adsorbent for Cr(VI) remediation in wastewater, *J. Mater. Chem. A.* **2017**, *5*, 1133–1144.

(3) Ting, L.; Ronggang, M.; Ke, K.; Dong, Z.; Dongming, Q.; Hongting, Z. Synthesis of gallic acid functionalized magnetic hydrogel beads for enhanced synergistic reduction and adsorption of aqueous chromium, *Chem. Eng. J.* **2021**, *408*, 127327.

(4) Zhenxiong, Y.; Xiangbiao, Y.;Lifeng, C.; Xinyi, H; Ziming, L.; Caocong, L.; Shunyan, N.; Xinpeng, W.; Yuezhou, W. An integrated process for removal and recovery of Cr(VI) from electroplating wastewater by ion exchange and reduction–precipitation based on a silica-supported pyridine resin, *J. Clean. Prod.* **2019**, *236*, 117631.

(5) Linzhou, Z.; Qihan, L.; Jiasheng, C.; Beibei, M.; Shuixia, C. Carbothermal preparation of porous carbon-encapsulated iron composite for the removal of trace hexavalent chromium, *Chem. Eng. J.* **2014**, *253*, 24–33.

(6) Xiaoshu, L.; Jiang, X.; Guangming, J.; Xinhua, X. Removal of chromium(VI) from wastewater by nanoscale zero-valent iron particles supported on multiwalled carbon nanotubes, *Chemosphere* **2011**, *85*, 1204–1209.

(7) Tao, L.; Tianlei, Y.; Zhenyu, Y.; Guoli, X.; Qiuyue, H.; Guangyao, L.; Jiao, D.; Yueping, G.; Chen, G. Trivalent chromium removal from tannery wastewater with low cost bare magnetic Fe_3O_4 nanoparticles, *Chem. Eng. Process.* **2021**, *169*, 108611.

(8) WeiZhao, Y.; Yongtao, L.; Jinhua, W.; Guocai, C.; Gangbiao, J.; Ping, L.; Jingjing, G.; Hao, L.; Chuansheng, L. Enhanced Cr(VI) removal from groundwater by FeO-H_2O system with bio-amended iron corrosion, *J. Hazard. Mater.* **2017**, *332*, 42–50.

(9) Zhiwei, W.; Yahuan, W.; Shuai, C.; Shaohua, L.; Zhimin, C.; Jiafu, C.; Yong, C.; Jianwei, F. Fabrication of core@shell structural Fe-Fe_2O_3@PHCP nanochains with high saturation magnetization and abundant amino groups for hexavalent chromium adsorption and reduction, *J. Hazard. Mater.* **2020**, *384*, 121483.

(10) Shuoxun, D.; Yili, W.; Junyi, L.; Daxin, Z.; Yanqin, Z.; Yao, T. Tuning the crosslink structure of cationic hydrogel for enhanced chromium(VI) removal: The covalent and electrostatic co-crosslinked effects and adsorption mechanism, *Chem. Eng. J.* **2020**, *394*, 124944.

(11) Huanping, C.; Yuchun, W.; Hai, N. T. Removal of hexavalent chromium from groundwater by Mg/Al-layered double hydroxides using characteristics of in-situ synthesis, *Environ. Pollut.* **2018**, *243*, 620–629.

(12) Wenjing, Z.; Qifeng, D.; Chengsheng, L.; Dejun, Y.; Guozhu, C.; Xiaoying, P.; Qiongqiong, W.; Hantian, S.; Bonian, Z.; Dongsu, C. Cr(VI) and Pb(II) capture on pH-responsive polyethyleneimine and chloroacetic acid functionalized chitosan microspheres, *Carbohyd. Polym.* **2019**, *219*, 353–367.

(13) Ran, L.; Qingda, A.; Zuoyi, X.; Bin, Z.; Shangru, Z.; Zhan, S. Preparation of PEI/CS aerogel beads with a high density of reactive sites for efficient Cr(VI) sorption: batch and column studies, *RSC Adv.* **2017**, *7*, 40227–40236.

(14) Yu, S.; Takehiko, G.; Satoshi, N., Synthesis of Oxidant Functionalised Cationic Polymer Hydrogel for Enhanced Removal of Arsenic (III), *Gels* **2021**, *7*, 197.
(15) Ryoichi, K.; Aika, S.; Hideaki, T. Preparation of dual temperature/pH-sensitive polyampholyte gels and investigation of their protein adsorption behaviors, *Sep. Purif. Technol.* **2012**, *96*, 26–32.
(16) Toni, S.; Takehiko, G.; Satoshi, N. Simultaneous Adsorption of Cation and Anion by Thermosensitive Hydrogels, *MATEC Web Conf.* **2021**, *333*, 11007.
(17) Kairuo, Z.; Changlun, C.; Huan, X.; Yang, G.; Xiaoli, T.; Ahmed, A.; Tasawar, H. Cr(VI) Reduction and Immobilization by Core-Double-Shell Structured Magnetic Polydopamine@Zeolitic Idazolate Frameworks-8 Microspheres, *ACS Sustain. Chem. Eng.* **2017**, *5*, 6795–6802.
(18) Chaofan, Z.; Huaili, Z.; Yongjun, S.; Bincheng, X.; Yili, W.; Xinyu, Z.; Yongjuan, W. Simultaneous adsorption and reduction of hexavalent chromium on the poly(4-vinyl pyridine) decorated magnetic chitosan biopolymer in aqueous solution, *Bioresource Technol.* **2019**, *293*, 122038.
(19) Zhaohui, W.; Richard, T. B.; Leigh, A. S.; Jianshe, L. Simultaneous Redox Conversion of Chromium(VI) and Arsenic(III) under Acidic Conditions, *Environ. Sci. Technol.* **2013**, *47*, 6486–6492.
(20) Francois, B. Toxic effects of chromium and its compounds, *Biol. Trace Elem. Res.* **1992**, *32*, 145–153.
(21) Yongzhu, Y.; Qingda, A.; Zuoyi, X.; Shangru, Z.; Bin, Z.; Zhan, S. Interior multi-cavity/surface engineering of alginate hydrogels with polyethylenimine for highly efficient chromium removal in batch and continuous aqueous systems, *J. Mater. Chem. A.* **2017**, *5*, 17073–17087.
(22) Yuwei, C.; Jianlong, W. Preparation and characterization of magnetic chitosan nanoparticles and its application for Cu(II) removal, *Chem. Eng. J.* **2011**, *168*, 286–292.
(23) Yong, R.; Hayder, A. A.; Fengbo, H.; Hong, P.; Kaixun, H. Magnetic EDTA-modified chitosan/SiO_2/Fe_3O_4 adsorbent: Preparation, characterization, and application in heavy metal adsorption, *Chem. Eng. J.* **2013**, *226*, 300–311.
(24) YuhShan, H.; Gordon, M.; Wase, D. A. J.; Forster, C. F. Study of the Sorption of Divalent Metal Ions on to Peat, *Adsorp. Sci. Technol.* **2000**, *18*, 639–650.
(25) Liang, P.; Pufeng, Q.; Ming, L.; Qingru, Z.; Huijuan, S.; Jiao, Y.; Jihai, S.; Bohan, L.; Jidong, G. Modifying Fe_3O_4 nanoparticles with humic acid for removal of Rhodamine B in water, *J. Hazard. Mater.* **2012**, *209–210*, 193–198.
(26) Jian, W.; Yu, L.; Qingqing, J.; Jing, H.; Bei, L.; Xin, L.; Wanying, C.; Tasawar, H.; Ahmed, A.; Xiangke, W. Simultaneous Removal of Graphene Oxide and Chromium(VI) on the Rare Earth Doped Titanium Dioxide Coated Carbon Sphere Composites, *ACS Sustain. Chem. Eng.* **2017**, *5*, 5550–5561.
(27) Xitong, S.; Liangrong, Y.; Qian, L.; Junmei, Z.; Xiaopei, L.; Xiaoqin, W.; Huizhou, L. Amino-functionalized magnetic cellulose nanocomposite as adsorbent for removal of Cr(VI): Synthesis and adsorption studies, *Chem. Eng. J.* **2014**, *241*, 175–183.
(28) Weikang, L.; Liang, Y.; Shihao, X.; Yao, C.; Bianhua, L.; Zhong, L.; Changlong, J. Efficient removal of hexavalent chromium from water by an adsorption–reduction mechanism with sandwiched nanocomposites, *RSC Adv.* **2018**, *8*, 15087–15093.
(29) Jia, W.; Xiaohong, H.Metal selectivity and effects of co-existing ions on the removal of Cd, Cu, Ni, and Cr by ZIF-8-EGCG nanoparticles, *J. Colloid Interf. Sci.* **2021**, *589*, 578–586.
(30) Liying, D.; Jinsong, L.; Yue, L; Siqi, H.; Yingnan, W.; Xin, B.; Zonghui, J.; Meng, Z.; Juanjuan, Q. Effect of coexisting ions on Cr(VI) adsorption onto surfactant modified Auricularia auricula spent substrate in aqueous solution, *Ecotoxicol. Environ. Saf.* **2018**, *166*, 390–400.

(31) Aranda-García, E.; Chávez-Camarillo, G. M.; Cristiani-Urbina, E. Effect of Ionic Strength and Co-existing Ions on the Biosorption of Divalent Nickel by the Acorn Shell of the Oak Quercus crassipes Humb. & Bonpl., *Processes* **2020**, *8*, 1229.
(32) Minzi, L.; Xiaobing, W.; Shiyu, C.; Meiqi, L.; Xing, P.; Lizhi, Z. Oxalate Modification Dramatically Promoted Cr(VI) Removal with Zero-Valent Iron, *ACS ES&T Water* **2021**, *1*, 2109–2118.

Chapter 4: Simultaneous Removal of As (V) and Cr (III)

4.1 Introduction

Harmful cations and anions, such as arsenic (As) and chromium (Cr) ions, predominantly originate from manufacturing, mining, industrial processes, and chemical production.[1,2] These elements pose significant risks to human health and the environment, especially when they occur as complex mixtures in environments with high concentrations.[3,4] Copper smelting wastewater and effluents from the chrome-plating industry are prime examples of such hazardous waste, containing high levels of arsenic and chromium, thereby posing a serious threat to both human health and ecological safety.[5,6] Consequently, the World Health Organization recommends a maximum permissible limit of 10 μg L^{-1} for arsenic and 0.05 mg L^{-1} for chromium (0.02 mg L^{-1} in Japan) in drinking water.[7-10] Arsenic and chromium can exist as co-containment in the environment and the coexistence of hexavalent chromium and trivalent arsenic can lead to a coupled reaction of Cr reduction and As oxidation in the cold periods, so that the resulting less toxic trivalent chromium and pentavalent arsenic widely exist in the industrial environment.[11]

Various methods have been proposed to address this, including chemical precipitation, ion exchange, oxidation-reduction, and adsorption, etc..[12-17] For example, Boo et al. proposed a new method, namely thermomorphic hydrophilicity base-induced precipitation (THBIP), for the effective removal of hardness ions (Mg^{2+}, Ca^{2+},) from hypersaline, which uses thermoresponsive amine bases to trigger the phase separation of amine.[18] Geng et al. recovered Mg^{2+} from saline wastewater collected from a coal-fired power plant through thermomorphic hydrophilicity amines.[19] Among these methods, adsorption has been widely used and studied by

scientists owing to its simplicity, ease of design, and flexibility.[20-22] However, the strength of the adsorption effect relies heavily on the presence of some functional groups in the adsorbent materials. Consequently, numerous researchers have modified existing adsorbent materials through grafting, modification, functionalization, and other methods to enhance their adsorption capacities for heavy metal ions. For example, Xu et al. proposed using sulfonated PVC-derived hydrochar (HS-PVC) from PVC waste, synthesized via two-stage hydrothermal treatment (HT) and sulfonation, to efficiently adsorb Cu (II) and Cr (VI) through the electrostatic adsorption and complexation method; maximum adsorptions of Cu (II) and Cr (VI) of 48.9 and 20.2 mg g^{-1} , respectively, could be achieved.[23] Liu et al. proposed a novel nanostructured calcined MgZnFe-CO_3 layered double hydroxide (CMZF) for removal of As (III) and Cd (II) simultaneously by photooxidation, formation of ternary As-Cd surface complexes, and enhanced hydrogen bonding.[24] Zhou et al. synthesised sulphur-intercalated hydrotalcite LDH [$Mg_4Al_2(OH)_{12}CO_3 \cdot mH_2O$] with S^{2-} anions to capture cationic heavy metals and oxyanion pollutants.[25]

Researchers have exploited the properties of hazardous ions and combined various other adsorption methods to efficiently adsorb anions and cations simultaneously.[26, 27] For example, materials functionalized with oxidising functional groups can facilitate the adsorption of As (III) into the more readily adsorbable As (V) (under acidic conditions, As (III) is less ionizable than As (V), which exists in an ionic state under both acidic and alkaline conditions).[28] In addition, Cr (VI) can be reduced to the less toxic Cr (III), which can be readily fixed on the material surface.[29, 30] They can also be adsorbed in large quantities via surface complexation with amino groups on the material surface.[1]

Several materials can be used to remove harmful ions, such as activated carbon,[31] manganese nanomaterials,[32] zero-valent iron,[33] and polymers. Among these, polymers have received widespread attention owing to their low cost and chemical modification properties.[34-36] Hydrogels are polymeric materials with various hydrophilic functional

group types that can provide adsorption sites to remove harmful ions.[37,38] Hydrogels can introduce the required functional groups through ion exchange or electrostatic attraction to efficiently remove hazardous ions.[39] For example, *N*-[3-(Dimethylamino) propyl] acrylamide methyl chloride quaternary (DMAPAAQ), whose monomer contains a positively charged quaternary ammonium group and a chlorine ion that maintains the charge balance, can remove hazardous anions through ion exchange with anions or introduce functional anions.[40] Similarly, 2-acrylamido-2-methyl-1-propanesulfonic acid sodium salt solution (50 wt% in H_2O) (AMPS(Na)), whose monomer contains a negatively charged sulfonic acid group and a sodium ion, can remove heavy metal cations via ion exchange adsorption.[41] From numerous studies on simultaneous adsorption, it can be inferred that the modification of the adsorbent material structure (such as the introduction of required functional groups) represents the main way to enhance its adsorption performance. The development of various new adsorbents has also been based on this foundation. However, this method results in increased complexity.

Dong et al. proposed that chromium and arsenic can exist as co-contaminants in the environment the opinion where the coexistence of hexavalent chromium and trivalent arsenic can lead to a coupled reaction of Cr reduction and As oxidation in the cold period.[11] Although the toxicity of arsenic (V) and chromium (III) is significantly lower compared to arsenic (III) and chromium (VI), the hazards posed by high concentrations of coexisting arsenic (V) and chromium (III) should not be overlooked. However, many researchers did not indicate how the resulting less toxic trivalent chromium and pentavalent arsenic could be removed simultaneously. Currently, there is no report about studies related to the simultaneous adsorption of trivalent chromium and pentavalent arsenic. Therefore, in this study, a removal method is proposed by adsorption on to ionic hydrogel. The adsorption capacity of the hydrogel was increased by converting multiple ions [As (V) and Cr (III)] into single complexes, rather than modifying the surface structure of the material. This method primarily utilises As (V)

and Cr (III) to form positively charged complexes under specific environmental conditions, which can be adsorbed in substantial quantities by anionic gels through ion exchange, which differs from surface complexation reactions. Moreover, the effects of various physicochemical factors on the adsorption capacity of the gel were investigated to elucidate the adsorption mechanism and form of the arsenic-chromium complex system.

4.2 Materials and methods

4.2.1 Materials

N, N-dimethylamino propylacrylamide (DMAPAA) and N,N-dimethylamino propylacrylamide, methyl chloride quaternary (DMAPAAQ) monomers were supplied by KJ Chemicals Co. (Tokyo, Japan). N, N, N', N'- tetrathylethylenediamine (TEMED), 1 mol L^{-1}-nitric acid (HNO_3), chromium nitrate [$Cr(NO_3)_3 \cdot 9H_2O$], disodium hydrogenarsenate heptahydrate ($Na_2HAsO_4 \cdot 7H_2O$), sodium nitrate ($NaNO_3$), sodium chloride (NaCl), 1 mol L^{-1}-sodium hydroxide solution (NaOH), sodium sulphate (Na_2SO_4), and sodium phosphate dodecahydrate ($Na_3PO_4 \cdot 12H_2O$) were obtained from Nacalai Tesque, Inc. (Kyoto, Japan), and N, N'-methylenebisacrylamide (MBAA), ammonium peroxodisulfate (APS), 2-acrylamido-2-methyl-1-propanesulfonic acid sodium salt solution (50 wt% in H_2O) [AMPS(Na)], were obtained from Sigma Aldrich Co., (St. Louis, MO, USA). Iron (III) chloride, anhydrous ($FeCl_3$), and copper (II) chloride dihydrate ($CuCl_2 \cdot 2H_2O$) were obtained from Kanto Chemical Co., Inc. (Tokyo, Japan). Ion exchange resins, including PK 208, WK 20, WK 40L, and CR 11, were supplied by Mitsubishi Chemical Corp. (Tokyo, Japan). Hydrochloric acid (HCl; 1 mol L^{-1}) was obtained from Kishida Chemical Co., Ltd. (Osaka, Japan). All reagents were of analytical grade and were used as received. Aqueous solutions were prepared using distilled water (DW).

4.2.2 Gel fabrication

4.2.2.1 Synthesis of AMPS(Na) and DMAPAAQ gels

The hydrogel synthesis process is illustrated in **Scheme 4.1**. AMPS(Na) or DMAPAAQ (25 mmol, monomer), MBAA (1.25 mmol, cross-linking agent), and TEMED (1.25 mmol, accelerator) were mixed with DW in a 25-mL beaker while magnetically stirring for 15 min. Subsequently, the volume of the mixed solution, representing the monomer solution, was increased to 20 mL with DW in a volumetric flask. Subsequently, an initiator solution containing 0.5 mmol of APS (the initiator) was dissolved with DW in a 5-mL volumetric flask. To prevent the inhibition of radical polymerisation originating from O_2 in air, the monomer and initiator solutions prepared as above were infused with pure N_2 for 45 min. The initiator solution was then added to the monomer solution and stirred for 20 s, after which the mixture was injected into some column tubes (Diameter: 7 mm × 9 mm). The monomers [AMPS(Na)] and linker (MBAA) were polymerised at 25 °C for 24 h, after which the gel was extracted from the tubes. A Soxhlet extractor (Asahi Glassplant Inc., Arao City, Japan) was used to wash the gels with methanol to remove the unreacted components and eliminate the possibility of other substances affecting the adsorption results. After washing, the gel was air-dried at 25 °C for 2 days and subsequently dried in an oven at 50 °C for 24 h. Finally, the gels were crushed into a powder using Wonder Crusher WC-3 (Osaka Chemical Co., Ltd., Osaka City, Japan).

AMPS (Na) and DMAPAAQ gels are anionic and cationic polymer hydrogels, and contain a sulfonic acid group ($-SO_3^-Na^+$) and a quaternary amino group [$-N^+(CH_3)_3Cl^-$], respectively (as shown in **Scheme 4.1**). Their adsorption performances in aqueous environment (binary and single system) can be used to demonstrate the presence of the As-Cr positively charged complexes.

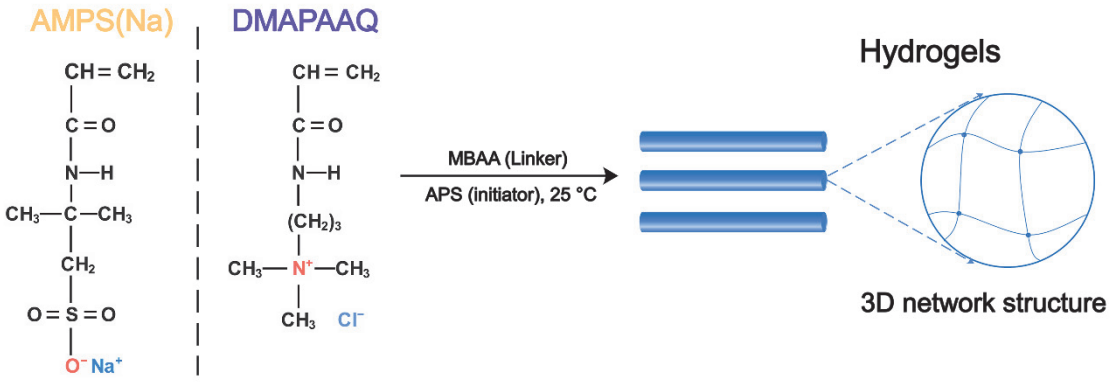

Scheme 4.1. Flowchart of the hydrogel preparation process.

4.2.2.2 Synthesis of other gels

Other gels were synthesised using the same method used for the AMPS(Na) gel.

The synthesis of gels such as DMAPAA is the same as that for the AMPS(Na) gel, for the synthesis of which the amounts of reagents used are shown in **Tables 4.1–4.4**.

Table 4.1. Preparation of AMPS(Na)-DMAPAAQ (A-D) gel.

Component	Function	Molecular Weight (g mol^{-1})	Concentration (mol m^{-3})	Mass (g)
DMAPAAQ	Monomer	206.71	500	2.5839
AMPS(Na) (50 wt %)	Monomer	229.23	500	2.8654 (5.7308)
MBAA	Linker	154.17	50	0.1927
TEMED	Accelerator	126.04	20	0.0581
APS	Initiator	228.19	20	0.1141

$-N^+Cl^-$ adsorption site (As anionic species adsorbed via ion-exchange): 2.15 mmol g^{-1}

$-SO_3^- Na^+$ adsorption site (Cr^{3+} adsorbed via ion-exchange): 2.15 mmol g^{-1}

Table 4.2. Preparation of AMPS(Na) gel.

Component	Function	Molecular Weight (g mol^{-1})	Concentration (mol m^{-3})	Mass (g)
AMPS(Na) (50 wt %)	Monomer	229.23	1000	5.7308(11.4615)
MBAA	Linker	154.17	50	0.1927
TEMED	Accelerator	126.04	20	0.0581
APS	Initiator	228.19	20	0.1141

$-SO_3^-\,Na^+$ adsorption site (Cr^{3+} adsorbed via ion-exchange): 4.1 mmol g^{-1}

Table 4.3. Preparation of DMAPAAQ gel.

Component	Function	Molecular Weight (g mol^{-1})	Concentration (mol m^{-3})	Mass (g)
DMAPAAQ	Monomer	206.71	1000	5.1678
MBAA	Linker	154.17	50	0.1927
TEMED	Accelerator	126.04	20	0.0581
APS	Initiator	228.19	20	0.1141

$-N^+Cl^-$ adsorption site (As anionic species adsorbed via ion-exchange): 4.5 mmol g^{-1}

Table 4.4. Preparation of DMAPAA gel.

Component	Function	Molecular Weight (g mol^{-1})	Concentration (mol m^{-3})	Mass (g)
DMAPAA	Monomer	156.22	1000	3.9055
MBAA	Linker	154.17	50	0.1927
TEMED	Accelerator	126.04	20	0.0581
APS	Initiator	228.19	20	0.1141

$-NH^{+}$ adsorption site (As anionic species are adsorbed via electrostatic interaction and Cr cationic species are adsorbed via chelation): 5.9 mmol g^{-1}

(the DMAPAA gel does not have the ability to adsorb any ions if it has not undergone protonation)

4.2.3 Preparation of As-Cr adsorbate solution in a binary and single system

Binary system: First, 10 mmol of Na_2HAsO_4 and 10 mmol of Cr $(NO_3)_3$ were added to a 500 mL volumetric flask, where 5 mL of 1 mol L^{-1} of HNO_3 was added simultaneously to adjust the solution pH to 2. Distilled water was then added to increase the volume to 500 mL. Gradually, the As-Cr adsorbate solution turned green. The prepared adsorbate solution could be used as a stock solution to prepare As-Cr adsorbate solutions of various initial concentrations, and the pH could be adjusted by adding HNO_3 and NaOH. In the subsequent discussion, unless stated otherwise, the solution concentration refers to the As or Cr concentration rather than the total concentration.

Single system: 10 mmol of Na_2HAsO_4 or 10 mmol of Cr $(NO_3)_3$ in 500 mL. (pH adjusted to 2 using HNO_3).

4.2.4. Adsorption Experiments

Batch adsorption experiments were performed in 40 mL plastic vials with 0.5 g L^{-1} of gel adsorbent (20 mg) to investigate the effects of physicochemical factors, such as pH, time, and co-existing ions, on As and Cr removal in the As-Cr adsorbate solution by the AMPS(Na) gel and analyse the adsorption mechanism to determine why the anionic polymer gel adsorbent could adsorb anionic and cationic species simultaneously. Firstly, to confirm the existence of a positively charged As-Cr complex, the AMPS(Na) and DMAPAAQ gels were added into the As-Cr adsorbate solution at a different mass ratio (10:0; 9:1; 8:2; 7:3; 6:4; 5:5; 4:6; 3:7; 2:8; 1:9; and 0:10) at 25 °C for 48 h in a single and binary system, respectively. The initial adsorbate solution concentration was 2 mM, and the solution pH was adjusted to 2 using 1 M of HNO_3 and NaOH. The As-Cr adsorbate solution concentrations were determined using inductively coupled plasma atomic emission spectroscopy (ICP-AES). The desorption capacity (Q_e) was calculated as follows:[1]

$$Q_e(Desorption) = \frac{(C_0 - C_e)V}{m} \quad (4.1)$$

where C_0 (mg L^{-1}) and C_e (mg L^{-1}) are the initial and equilibrium concentrations; V (L) is the solution volume; and m (g) is the gel mass.

Adsorption models, such as the Langmuir, Freundlich models, Dubinin-Radushkevich, and Temkin models,[2, 3] were used to study the adsorption isotherms and further elucidate the mechanism underlying As and Cr adsorption by the gels.

To further understand the adsorption mechanism of the complex adsorption of AMPS(Na) gel towards As and Cr species, various concentrations (0, 0.5, 2, 5 mM) of co-existing anions (Cl^-, NO_3^-, SO_4^{2-}, and PO_4^{3-}) and cations (Fe^{3+}, Ni^{2+}, Cu^{2+}, and Pb^{2+}) were added. Subsequently, the dosage effect of AMPS(Na) gel was investigated

with 0.25–5 g L^{-1}. Finally, the adsorption capacities of the AMPS(Na) and DMAPAA gels synthesized in the laboratory were compared with those of other ion-exchange resins.

4.2.5 Stability and regeneration (Desorption experiment)

4.2.5.1 Stability

Stability: After the adsorption experiment, the AMPS (Na) gel containing adsorbates was separated from the supernatant and washed three times with deionized water. Desorption experiment was then performed using HCl (0.1 mol L^{-1}) at different doses (0.1, 0.2, 0.3, 0.4, 0.5, 0.6, 0.7, 0.8, 0.9, 1.0 L g^{-1}/2, 4, 6, 8, 10, 12, 14, 16, 18, 20 mL-HCl) to evaluate the elution performance and stability of the AMPS(Na) gel.

4.2.5.2 Regeneration

In the regeneration experiment, the spent adsorbent was eluted with 2 M Na_2SO_4, Na_2SO_4 (pH:2), and NaCl (pH:2) solution, and the adsorption-desorption experiments were cycled three times. To confirm the effect of time on the desorption of spent AMPS(Na) hydrogel, the time-dependent desorption experiment was performed. The desorption ratio (R) was calculated as follows:

$$R = \frac{Q_e(Desorption)}{Q_e(Adsorption)} \tag{4.2}$$

4.2.6 Characterizations

ICP-AES (SPS-3500, Shimadzu Corp., Japan) was used to measure the concentrations. After adsorption, all Cr solutions were filtered using a 0.22-μm

membrane to prevent the gels from affecting the measurement results of the equilibrium concentration, and all data were obtained by calculating the average of three measurements. X-ray photoelectron spectroscopy (ESCA-3400, Shimadzu Corp., Japan) was used to record the surface element information. The structural information of gels was detected using Fourier transform infrared spectroscopy (FTIR; IRTracer-100, Shimadzu Corp., Japan) at a wavelength of 4000–400 cm^{-1}.

4.3 Results and discussion

4.3.1 Positive-charged complex adsorption in the arsenic and chromium aqueous mixture

The colours of the As and Cr solutions in the As–Cr single system were transparent and blue, respectively, whereas the binary As–Cr system turned green, and its colour changed more deeply as the initial As-Cr adsorbate solution concentration increased (**Fig. 4.1**). This indicates that the binary system underwent a reaction in which As (V) and Cr (III) formed a new compound different from the anionic As (V) and cationic Cr (III) species. Therefore, the effect of changes in the mass ratio of AMPS(Na) and DMAPAAQ gels (A+D gels) was investigated to clarify this phenomenon, and the results are shown in **Fig. 4.2**.

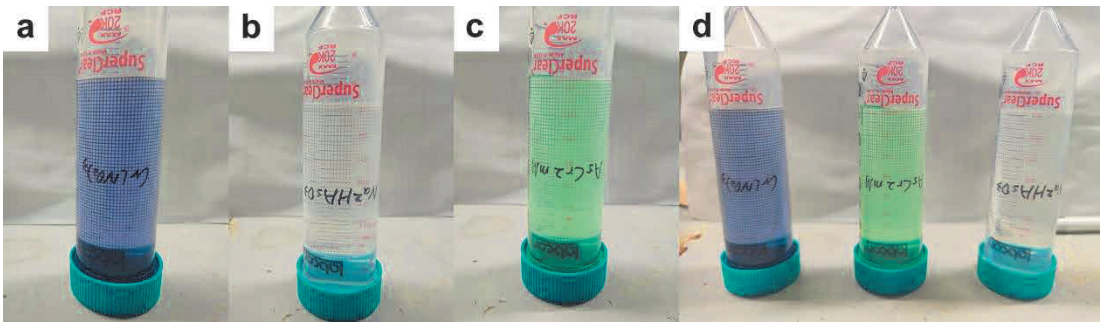

Fig. 4.1. Photographs of (a) Cr $(NO_3)_3$, (b) Na_2HAsO_3, (c) As-Cr positively charged complex ions solution, and (d) total comparison.

In the single system, the AMPS(Na) gel only adsorbed the Cr^{3+} cation, while the DMAPAAQ gel only adsorbed the $HAsO_4^{2-}$ anion. However, in the binary system, the AMPS(Na) gel not only adsorbed cations but also adsorbed a substantial amount of As in anions, and its adsorption capacity is substantially higher than that in a single system. Correspondingly, DMAPAAQ could not adsorb Cr, and As adsorption was substantially affected. This information shows that As and Cr form a stable positively charged group, which allows the group to be adsorbed by AMPS(Na) in large quantities but cannot be adsorbed by DMAPAAQ. To further confirm the presence of the positively charged As-Cr complex, AMPS(Na)-co-DMAPAAQ copolymer hydrogels with different molar ratios (1000:0−0:1000) were synthesised (**Fig. 4.3**), and the effect of time on the adsorption of AMPS(Na) and DMAPAAQ gels in single and binary systems was investigated (**Fig. 4.4**). **Fig. 4.4**a and **4.4**b show that AMPS(Na) gel could rapidly achieve the adsorption equilibrium for the adsorption of Cr in a binary system than in a single system. This is because the volume of Cr is much lower than that of As–Cr positively charged complex ions and is adsorbed more easily by the gel, resulting in less time to achieve the adsorption equilibrium.

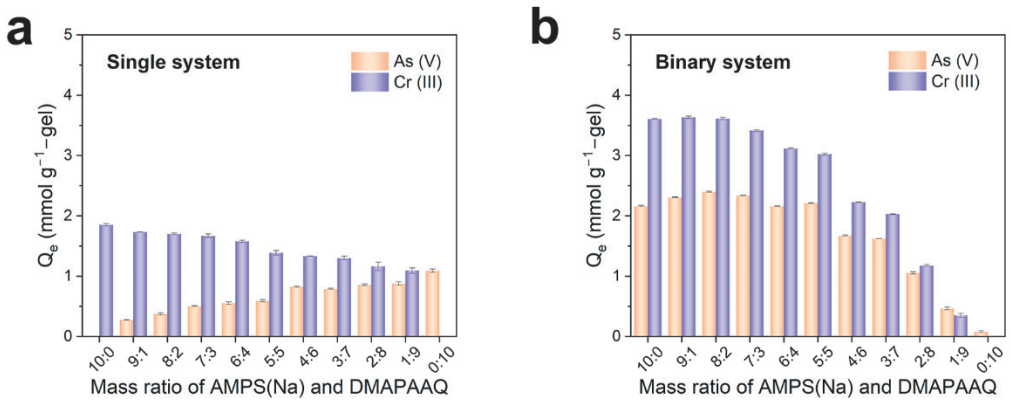

Fig. 4.2. (a) Effect of mass ratio of AMPS(Na) and DMAPAAQ on removal of As (V) or Cr (III) in a single system by A+D gels; (b) Effect of mass ratio of AMPS(Na) and DMAPAAQ on simultaneous removal of As (V) and Cr (III) in the binary system by A+D gels.

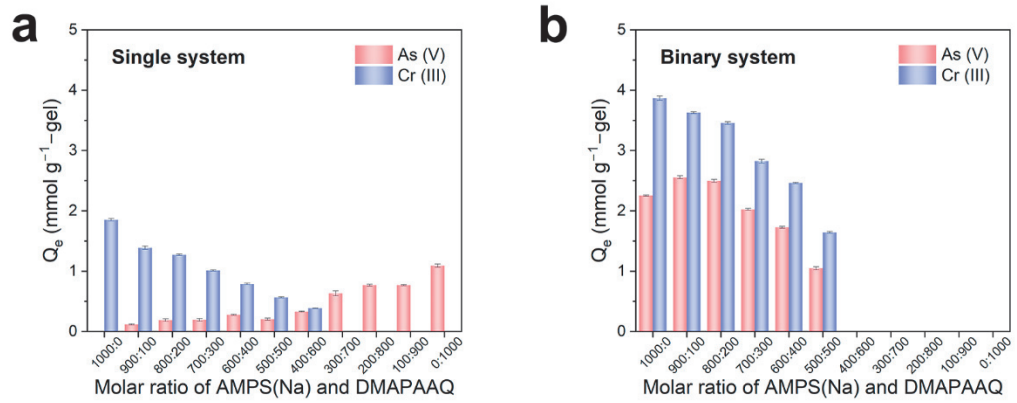

Fig. 4.3. (a) Effect of mass ratio of AMPS(Na) and DMAPAAQ on removal of As (V) or Cr (III) in a single system by A-D gels; (b) Effect of mass ratio of AMPS(Na) and DMAPAAQ on simultaneous removal of As (V) and Cr (III) in the binary system by A-D gels.

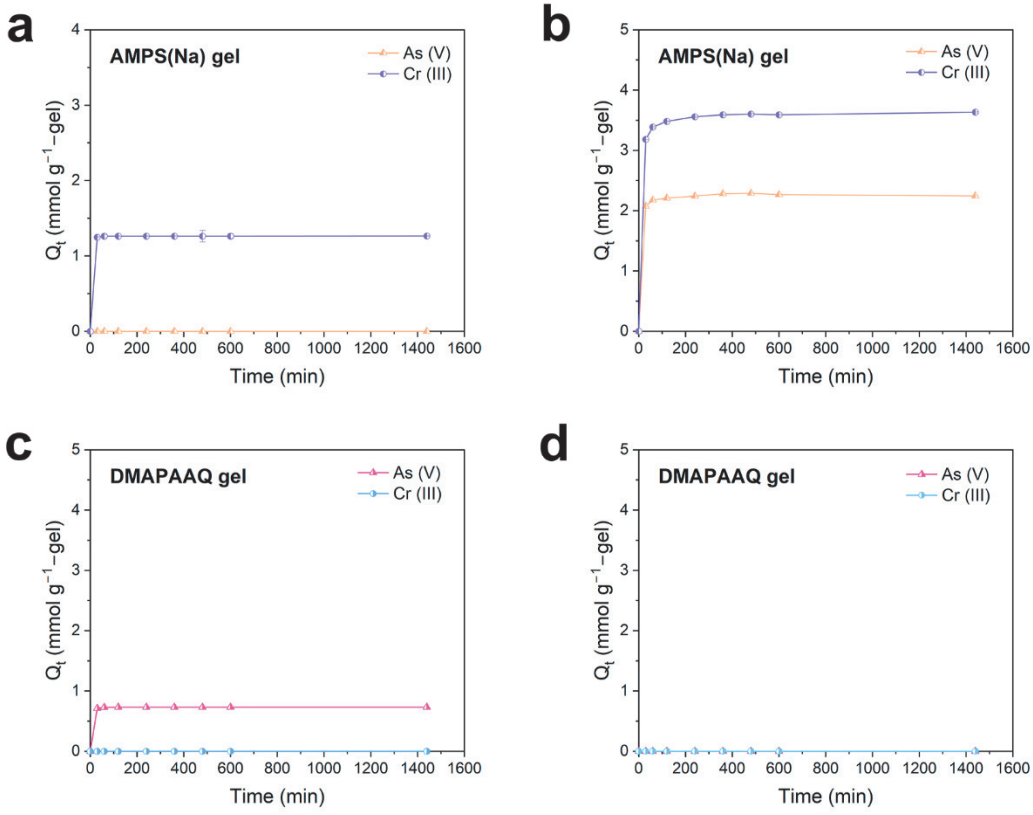

Fig. 4.4. Effect of time on As (V) and Cr (III) adsorption by the AMPS(Na) gel in a

(a) single system and (b) binary system; Effect of time on As (V) and Cr (III) adsorption by the DMAPAAQ gel in a (c) single system and (d) binary system

4.3.2 Effect of solution pH on the simultaneous removal of As (V) and Cr (III) by AMPS(Na) gel

The existing state of the As-Cr complex in various environments at a pH range of 2–12 was transformed with changes in solution pH. Therefore, the effect of solution pH on the adsorption of As and Cr by the AMPS(Na) gel was investigated, and the solution pH before and after adsorption was investigated (**Fig. 4.5**). **Fig. 4.5** shows that the adsorption capacity of the gel was exceedingly high under acidic and neutral conditions, with the adsorption capacity of Cr remaining constant as the As content increased. Concurrently, solution pH after adsorption above a pH of 3 was observed to decrease compared with that before adsorption. As-Cr complex ions are primarily found in forms like $[Cr(H_2O)_2(H_2AsO_4)]^{2+}$ and $[Cr(H_2O)_2(H_2AsO_4)_2]^{+}$. Therefore, when these complex ions undergo significant adsorption, the chemical equilibrium shifts towards the generation of more complex ions. This shift leads to the consumption of $H_2AsO_4^{-}$, facilitating the additional dissociation of arsenic acid molecules (H_3AsO_4), which in turn results in a reduction of the pH value. When the gel was transformed to an alkaline state, a significant decrease in the adsorption capacity of the AMPS(Na) gel was observed for both As and Cr adsorbates. This was because the As-Cr complex ions formed under acidic conditions decomposed, and new anionic complex ions were reformed under alkaline conditions. To verify this phenomenon, photographs of the adsorbate solution before and after adsorption on the AMPS(Na) gel at pH 2, 7, and 12 are shown in **Fig. 4.6**. The gel had a rapid adsorption rate and significant effectiveness at pH 2; A green flocculent precipitate appeared in the adsorbate solution, and a substantial amount of green solid particles were suspended in the solution at a pH of 7; The solution exhibited a light blue colour, indicating that the complex ions were

decomposed and transformed into an anionic complex ion $[Cr(OH)_4]^-$ at a pH of 12.

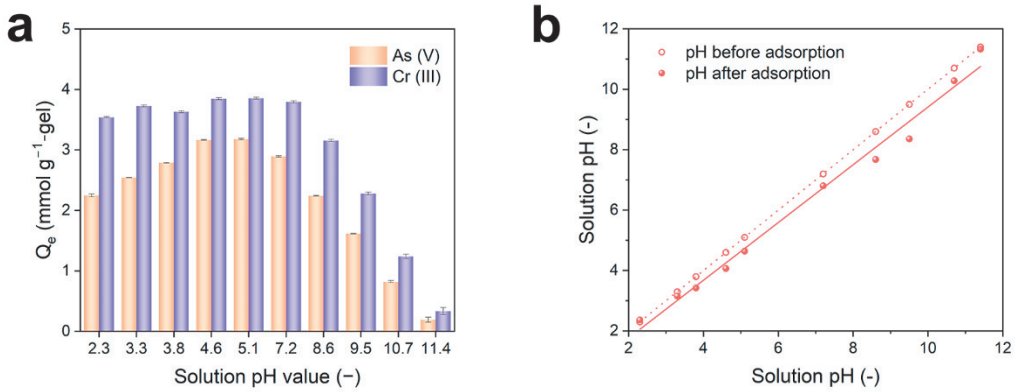

Fig. 4.5. (a) Effect of solution pH on As (V) or Cr (III) removal by AMPS(Na) gel; (b) Solution pH trends before and after adsorption and fitted with linear regression.

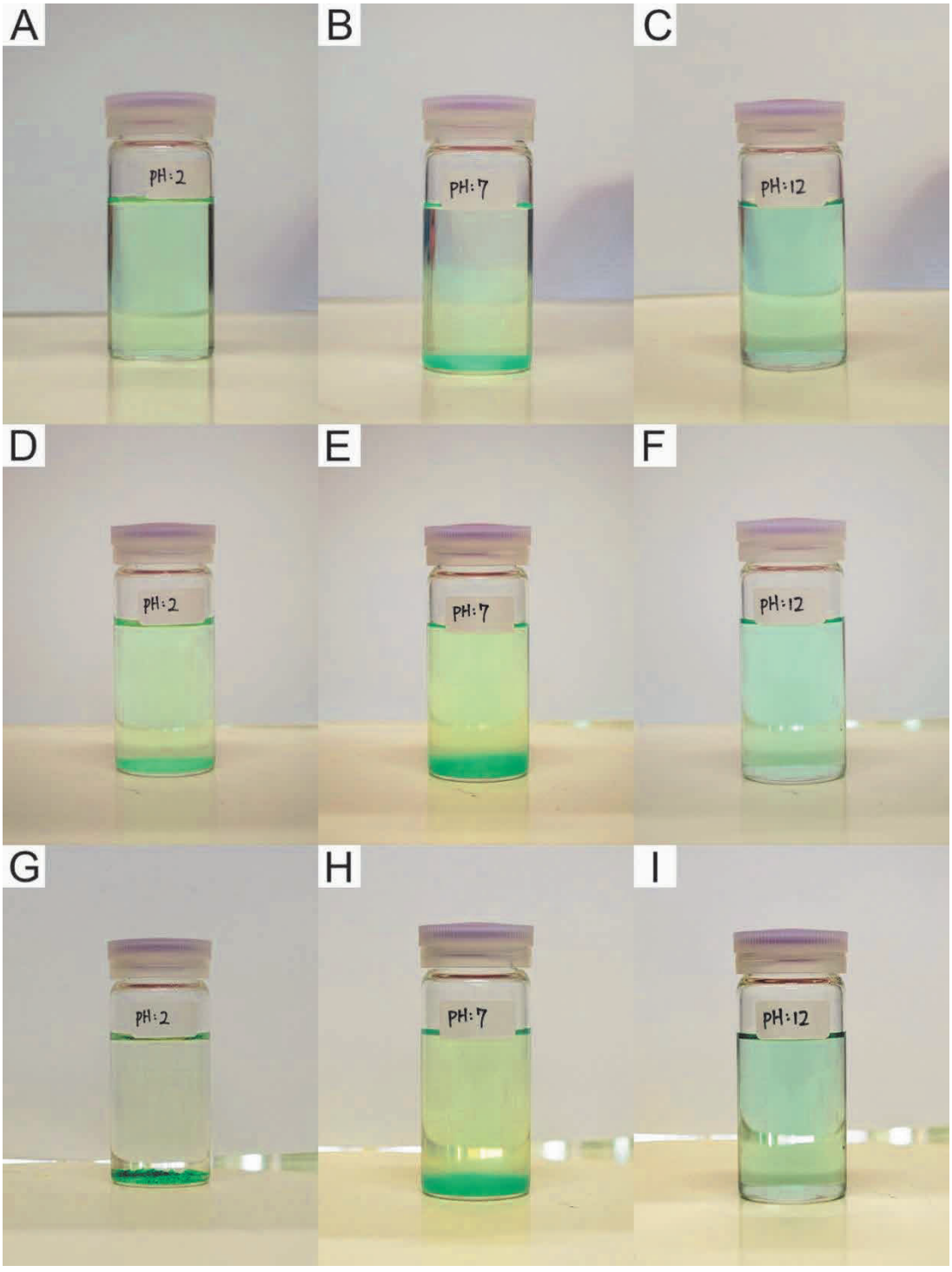

Fig. 4.6. Photographs of As and Cr aqueous mixtures at (A) a pH of 2, (B) pH of 7, and (C) pH of 12; Photographs of As and Cr aqueous mixtures at (D) a pH of 2, (E) pH of 7, and (F) pH of 12 after 10 min of adsorption; Photographs of As and Cr aqueous mixtures at (G) a pH of 2, (H) pH of 7, and (I) pH of 12 after 24h of adsorption.

4.3.3 Effect of initial concentration on the simultaneous removal of AMPS(Na) gel

Adsorption experiments were conducted to investigate the influence of physical and chemical conditions and understand the adsorption mechanism of the AMPS(Na) gel. First, the effect of initial adsorbate concentration on the adsorption capacity of the gel in the binary system was studied, as shown in **Fig. 4.7**.

Fig. 4.7 shows that the adsorption of As and Cr was highly correlated with the Freundlich adsorption isotherm model than that of the Langmuir model (as shown in **Table 4.5**). This suggests that multiple As (V) anions are adsorbed on a single adsorption site, whereas multiple Cr (III) atoms are adsorbed on the same site. Presently, there are two potential adsorbate states: one is that it exists in the form of a single-Cr, multiple-As complex ion, with each adsorption site of the gel adsorbing several complex ions; the other is that the gel adsorbs not only the complex ion containing As and Cr, but also Cr (III) adsorbed at the same site. The adsorption capacities of As (V) and Cr (III) at initial concentrations of 7.5 mmol were 4.0 mmol g^{-1} (299.7 mg g^{-1}) and 5.7 mmol g^{-1} (296.7 mg g^{-1}), respectively. A comparison of adsorption capacities using other materials as adsorbents is shown in **Table 4.6**.

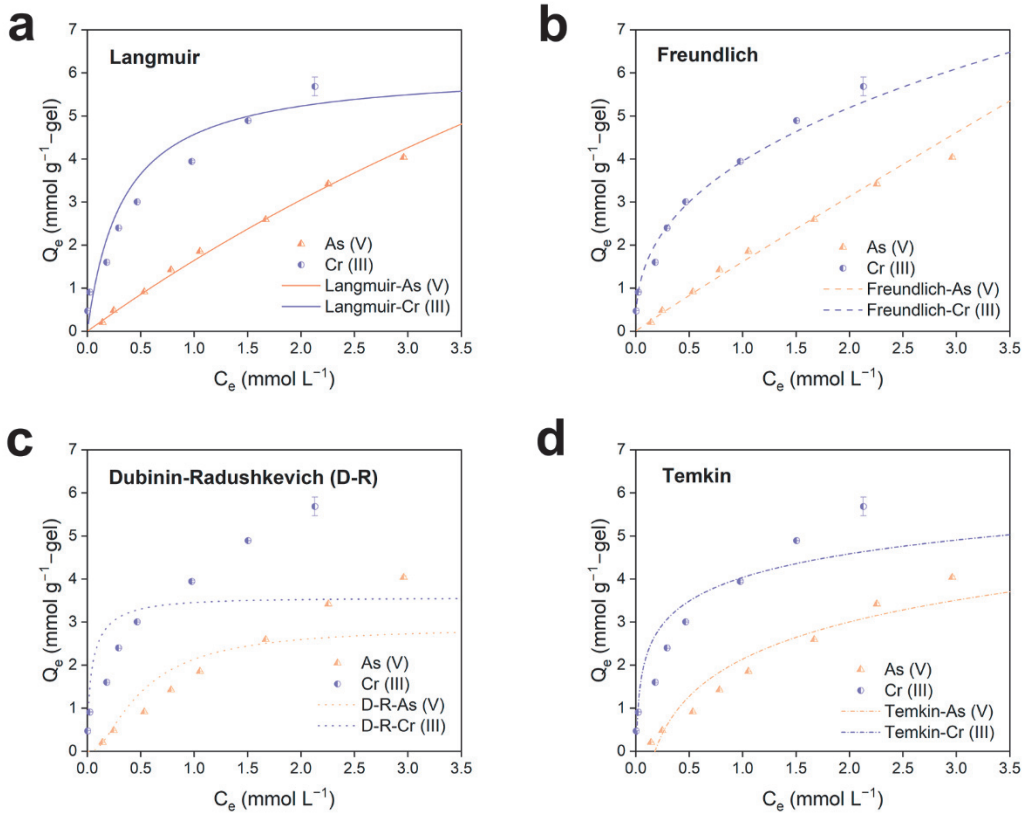

Fig. 4.7. Adsorption capacities of As (V) and Cr (III) by AMPS(Na) gel fitted for (a) Langmuir, (b) Freundlich, (c) Dubinin-Radushkevich, and (d) Temkin models.

Table 4.5. Parameters of adsorption isotherms fitted for adsorption capacities of As (V) and Cr (III) by AMPS(Na) gel at an initial concentration of 2 mM.

Isotherms	Parameters	Adsorbate	
		As (V)	Cr (III)
Langmuir	Q_m (mmol g^{-1})	21	6.1
	K_L (L $mmol^{-1}$)	0.086	3.0
	R^2	0.3952	0.9413
Freundlich	1/n	0.96	0.40
	K_F (mmol g^{-1} (L $mmol^{-1})^{1/n}$)	1.6	3.9
	R^2	0.9873	0.9875
D-R	Q_m (mmol g^{-1})	2.9	3.6
	E (kJ mol^{-1})	2.2	6.5
	R^2	0.8313	0.9278
Temkin	A (L $mmol^{-1}$)	5.6	164.6
	b (J mol^{-1})	1989	3134
	R^2	0.9155	0.8410

Table 4.6. Adsorption capacities (Q_e) of different adsorbents used for simultaneous adsorption of anionic and cationic species.

Adsorbents	Adsorbate species	Q_e (mg g^{-1})	References
AMPS(Na) hydrogel	As (V) / Cr (III)	299.7/296.4	This work
Graphene-like biochar supported nZero-valent iron	As (III) / Cd (II)	181.5/169.5	45
Flower-like Fe_3S_4 micro-crystal	Cr (VI) / U (VI)	274.1/505.4	46
S^{2-} intercalated layered double hydroxide	Co (II) / Ni (II) / Cr (VI)	88.6/76.2/34.7	25
Zwitterionic plastic-hydrogel	Pb (II) / Cd (II) /Ba (II) /Cr (VI)	132.1/85.6/69.9/85.2	47
TiO_2-modified ultrasonic biochar	Cd (II) / As (V)	72.6/118.1	48
Cetyltrimethylammonium bromide-modified zeolites	Cs (I) / Cr (VI)	94.8/63.2	49
Mg-Al-Cl-layered double hydroxide	Cu (II) / Cr (VI)	143.9/112.7	50
NH_2/MCM-41/NTAA	Pb (II) / Mn (VII)	147.5/164.5	51

4.3.4 Effect of contact time of adsorption in AMPS(Na) gel

Fig. 4.8 shows adsorbate concentration trends of As (V) and Cr (III) over time in AMPS(Na) gel based on initial concentrations of 1 mM, 2 mM, and 3 mM. In addition, their adsorption capacity trends over time are shown in **Fig. 4.9** as supporting information. As shown in **Fig. 4.8**a and **4.8**b, As (V) concentration reached the minimum value within 40 min, and then increased over time (i.e., the adsorbate

absorbed by the gel was discharged out of the gel into the solution); higher As amounts were discharged when compared with Cr. This was because the As-Cr complex formed at low concentrations was unstable and decomposed gradually, whereas the decomposed Cr^{3+} was still adsorbed by the gel through the ion exchange adsorption method. AMPS(Na) gel shows a high correlation with the pseudo-second-order model at higher initial concentrations of As (V) and Cr (III), indicating that the adsorption is chemical (**Tables 4.7** and **4.8**). Moreover, Cr required a longer time to reach adsorption equilibrium than As at both 2 and 3 mM, indicating that a second stage of Cr ion adsorption exists, excluding As-Cr complex adsorption; that is, the proportion of the As-Cr complex would decrease at high concentrations. In summary, changes in adsorbate concentration affect As-Cr complex formation, which, in turn, affect the gel adsorption rate and other gel characteristics.

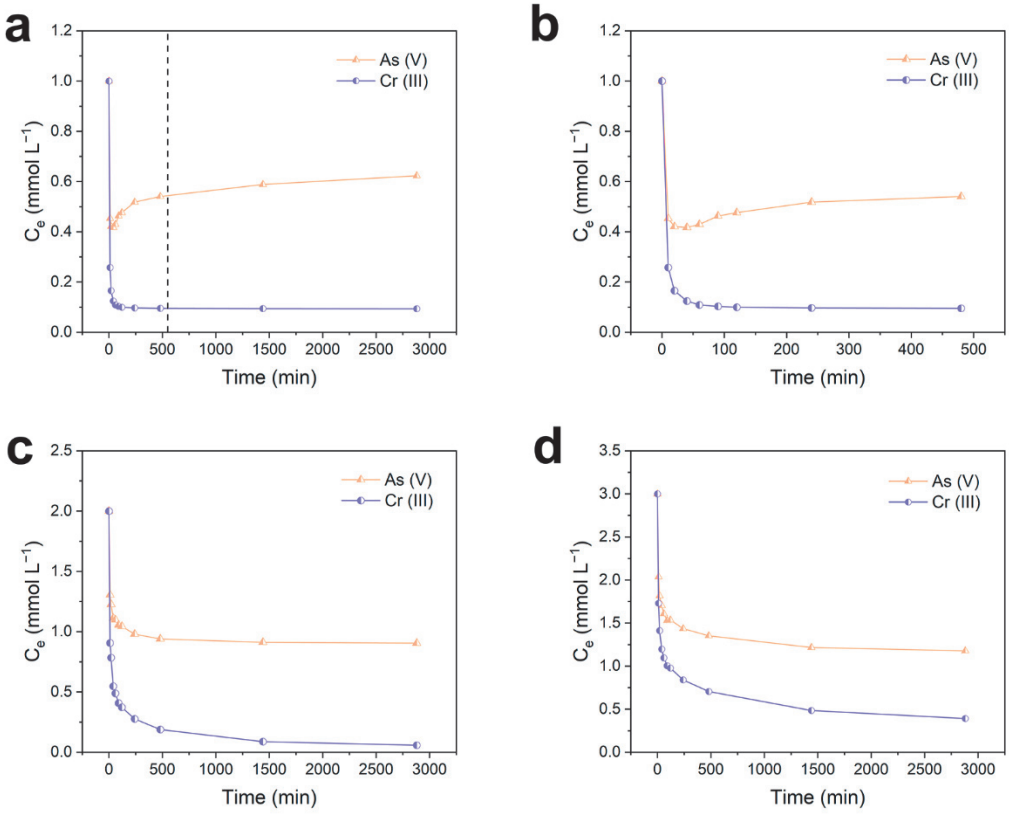

Fig. 4.8. Adsorbate concentrations of As (V) and Cr (III) over time based on AMPS(Na) gel at initial concentrations of (a)(b) 1 mM, (c) 2 mM, and (d) 3 mM.

(Time: (a)(c)(d) 0–2880 min, (b): 0–480 min)

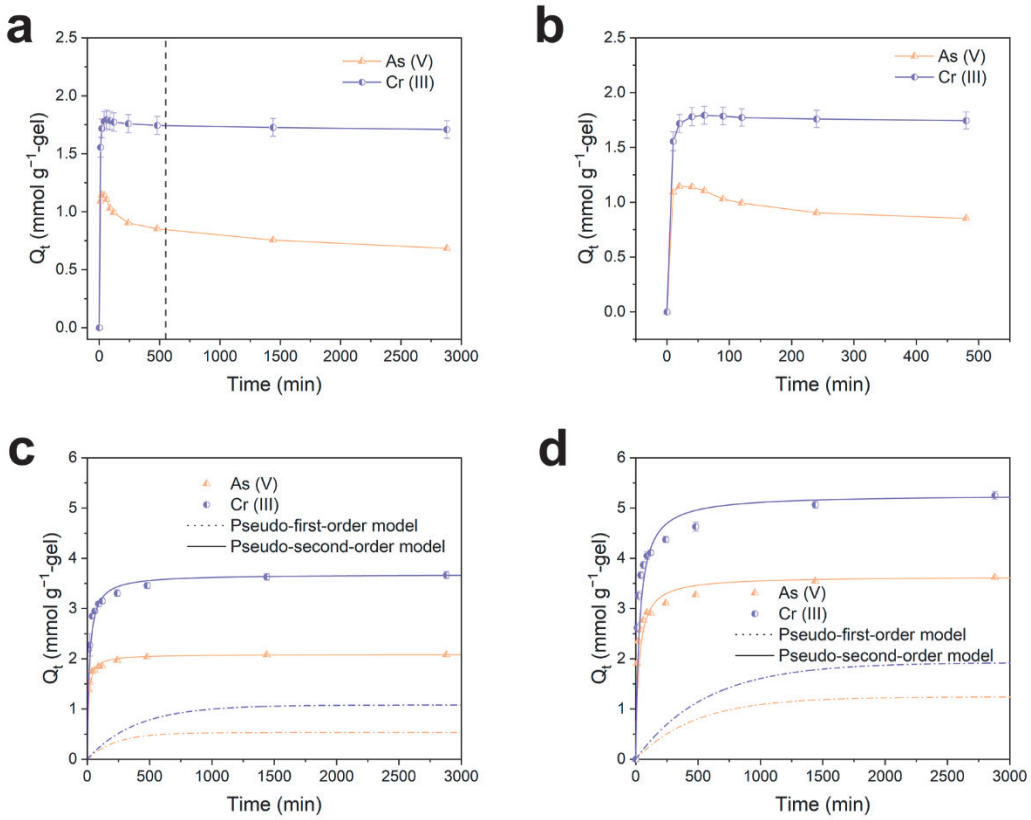

Fig. 4.9. Adsorption capacities of As (V) and Cr (III) with time by AMPS(Na) fitted for pseudo-first and second-order models at initial concentration of (a)(b) 1 mM, (c) 2 mM, and (d) 3 mM. (Time: (a)(c)(d) 0–2880 min, (b): 0–480 min)

Table 4.7. Parameters of pseudo-first-order and pseudo-second-order models at an initial concentration of 2 mM.

Isotherms	Parameters	Adsorbate	
		As (V)	Cr (III)
Pseudo-first-order	Q_e (mmol g^{-1})	0.53	1.1
	k_1 (min^{-1})	0.0045	0.0026
	R^2	0.9285	0.8174
Pseudo-second-order	Q_e (mmol g^{-1})	2.1	3.7
	k_2 (g $mmol^{-1}$ min^{-1})	0.047	0.016
	R^2	0.9999	0.9999

Table 4.8. Parameters of pseudo-first-order and pseudo-second-order models at an initial concentration of 3 mM.

Isotherms	Parameters	Adsorbate	
		As (V)	Cr (III)
Pseudo-first-order	Q_e (mmol g^{-1})	1.2	1.9
	k_1 (min^{-1})	0.0021	0.0018
	R^2	0.8007	0.7728
Pseudo-second-order	Q_e (mmol g^{-1})	3.6	5.3
	k_2 (g $mmol^{-1}$ min^{-1})	0.011	0.0062
	R^2	0.9997	0.9995

4.3.5 Effect of gel dosage on the adsorption of AMPS(Na) gel

Fig. 4.10a and **4.10**b show the effect of the AMPS(Na) gel dosage on the adsorption capacity and change in solution pH, respectively. As shown in **Fig. 4.10**a, AMPS(Na) gel adsorption amount decreased with an increase in the gel dosage, indicating that the gel could reach a fully adsorbed state with a small dosage. The molar

ratio of adsorbed Cr to As also increased with an increase in dosage (1.5, 1.7, 2.0, 2.2, and 2.6), which showed that an increase in the gel significantly changed the existing state of As-Cr in the solution. Therefore, to understand the reasons for such changes in Cr and As, pH changes in the adsorbate solution under different gel dosages were investigated, as shown in **Fig. 4.10**b. The pH increased with increasing gel dosage but never exceeded a pH of 4. This shows that the adsorption process of Cr^{3+} was dominant compared to that of the positively charged As-Cr complex.

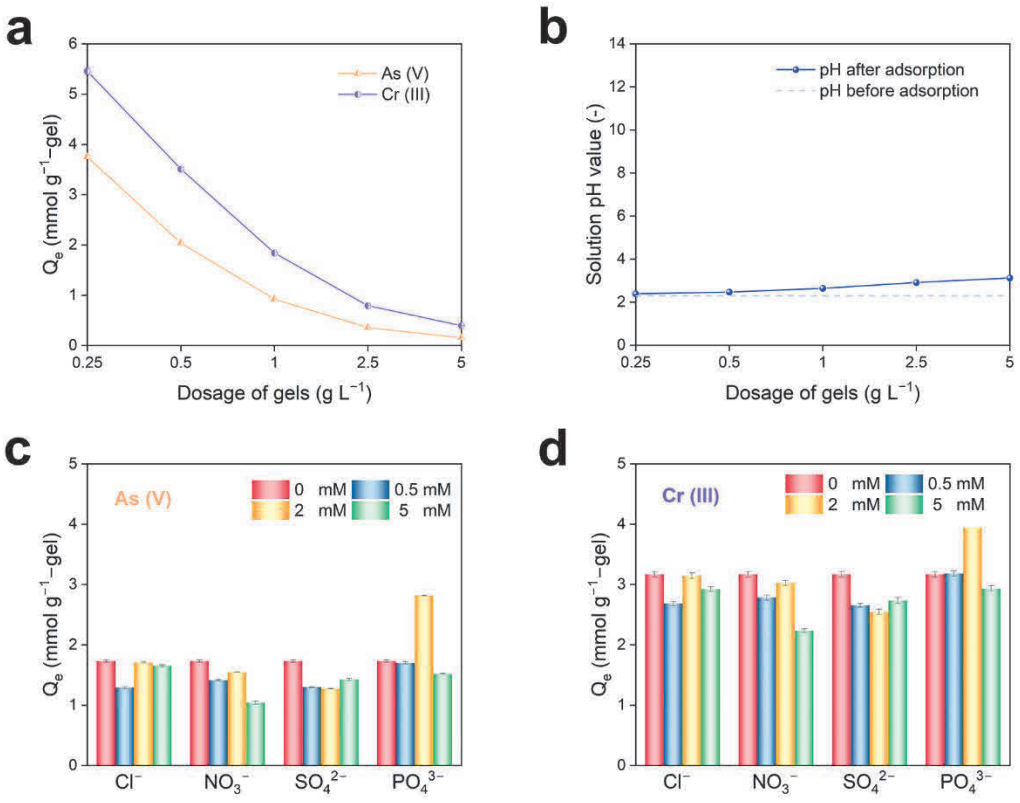

Fig. 4.10. (a) Adsorption capacities of As (V) and Cr (III) with change in gel dosage; (b) Solution pH before and after adsorption; effect of co-existing anions on adsorption capacity of (c) As (V) and (d) Cr (III) by AMPS(Na) gels in the binary system.

4.3.6 Effect of co-existing anions on adsorption

Fig. 4.10c and **4.10**d show the change in the amounts of As and Cr adsorbed by the AMPS(Na) gel in the presence of co-existing anions. The trends in the adsorption of As and Cr were similar, indicating that the co-existing ions indirectly affected the adsorption of cationic Cr by influencing the formation of complex ions. The gel adsorption was most affected when the concentration of co-existing ions was less or greater than that of As or Cr ions. In addition, the higher the valence of the co-existing ions, the greater their impact on gel adsorption. Regarding PO_4^{3-}, its hydrolysis reaction causes the surrounding environment to become neutral or slightly alkaline, resulting in a significant increase or slight decrease in the adsorption capacity of the gel.

4.3.7 Ion strength

Variations in the adsorption of As and Cr in the presence of Ni^{2+} or Cu^{2+}, as shown in **Fig. 4.11**a and **Fig. 4.11**b exhibit a similar trend, indicating that Ni or Cu ions indirectly affect Cr and As adsorption by influencing the formation of their complex ions rather than by competing with the central ion (Cr^{3+}) of the complex ion. However, in the presence of Fe^{3+}, the adsorption of Cr decreased significantly with an increase in the concentration of co-existing ions, whereas the adsorption of Fe increased continually (as shown in **Fig. 4.11**c). In this case, the adsorption of As showed an initial decreasing trend, followed by an increasing trend, indicating a transition from competing between metal ions to competing between complex ions with an increase in Fe concentration. In the presence of Pb^{2+}, Pb^{2+} directly competes with the central ion of the complex, increasing and decreasing the adsorption of As and Cr, respectively.

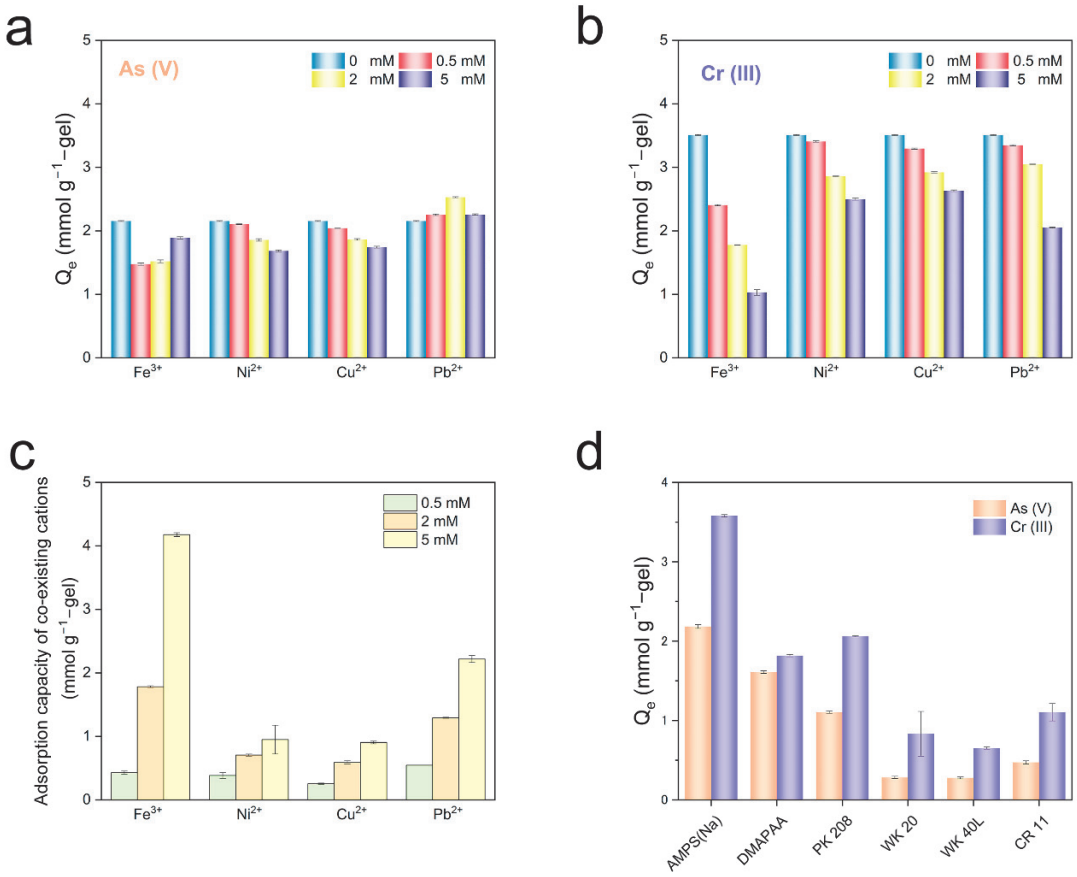

Fig. 4.11. Effect of co-existing anions on the Q_e of (a) As and (b) Cr by AMPS(Na) gels; (c) adsorption capacities of co-existing metal cations by AMPS(Na) gels at different initial concentrations of co-existing cations; (d) comparison of As and Cr adsorption by AMPS(Na) and DMAPAA gels with other ion exchange resins. (The initial concentrations of Cr and As are both 2 mM).

4.3.8 Comparison of adsorption capacities by AMPS(Na) gel with other ion exchange resins

The adsorption capacities of AMPS(Na) and DMAPAA were also compared with those of the other ion-exchange resins (**Fig. 4.11**d). At an initial concentration of 2 mM, the adsorption capacity of the AMPS(Na) gel for As and Cr was the highest. By comparing the molar ratios of Cr and As adsorbed by each adsorbent (1.6, 1.1, 1.9, 3.0, 2.4, and 2.3), it was discovered that the Cr-As ratios of these ion exchange resins were

substantially larger than those of AMPS(Na), which showed that the proportion of Cr-As complexes was smaller than that of Cr^{3+} in the ion exchange resins. This makes it difficult for ion-exchange resins to adsorb complexes of Cr and As and to achieve the goal of adsorbing several anions and cations simultaneously.

4.3.9 Gel stability and regeneration

Figs. 4.12a–d illustrates the effect of the eluent-to-adsorbent ratio (L g^{-1}) (HCl and NaOH) on the desorption capacities and desorption rate of As and Cr in the binary system. Based on the figures, as the ratio increases, the desorption ratio increases initially to a maximum value and then fluctuates around a certain constant value. However, due to the strong stability of complex ions, even under a strong acid environment, complete desorption does not occur, and the desorption ratios of As and Cr with the eluent HCl solution remain at around 31% and 20%, respectively. Furthermore, comparing the desorption amounts of As and Cr, their molar ratios are approximately equal. The result indicates that As and Cr are released from the gel into the solution in the form of complex ions. Consequently, ions adsorbed in the form of complex ions through ion exchange can stably exist within the adsorbent's interior and surface, maintaining relatively low desorption ratios even under extreme conditions. **Figs. 4.12**e–g shows the regeneration performance and reusability of the AMPS(Na) gel after three cycles using desorbing agents Na_2SO_4, Na_2SO_4 (pH 2), NaCl (pH 2). The decrease in adsorption capacity can be ascribed to incomplete desorption. During the third cycle, the adsorption capacity of AMPS (Na) gel for As and Cr decreased by 11% and 9.2%, 6.4% and 8.0%, 29% and 16%, respectively, when compared to the first adsorption using Na_2SO_4, Na_2SO_4 (pH 2), NaCl (pH 2) desorbing agents, respectively. The results indicate that the gel exhibits good regeneration performance using Na_2SO_4 (pH 2). The efficiency of using Na_2SO_4 as a desorbing agent is much greater than that of NaCl. **Fig. 4.12**h illustrates the desorption capacity and desorption

rate trends of AMPS (Na) gel over time. The desorption capacities of AMPS(Na) gel decrease rapidly after reaching its maximum desorption rate within the first 10 min. This indicates that the gel can achieve rapid desorption within 10 min. This is because the presence of a large amount of Na^+ allows the adsorbed As-Cr complex ions inside and on the surface of the gel to discharge out of the gel and enter the solution through ion exchange. However, due to the strong adsorption affinity of the complex ions, the gel re-enters the adsorption state after desorption for 10 min.

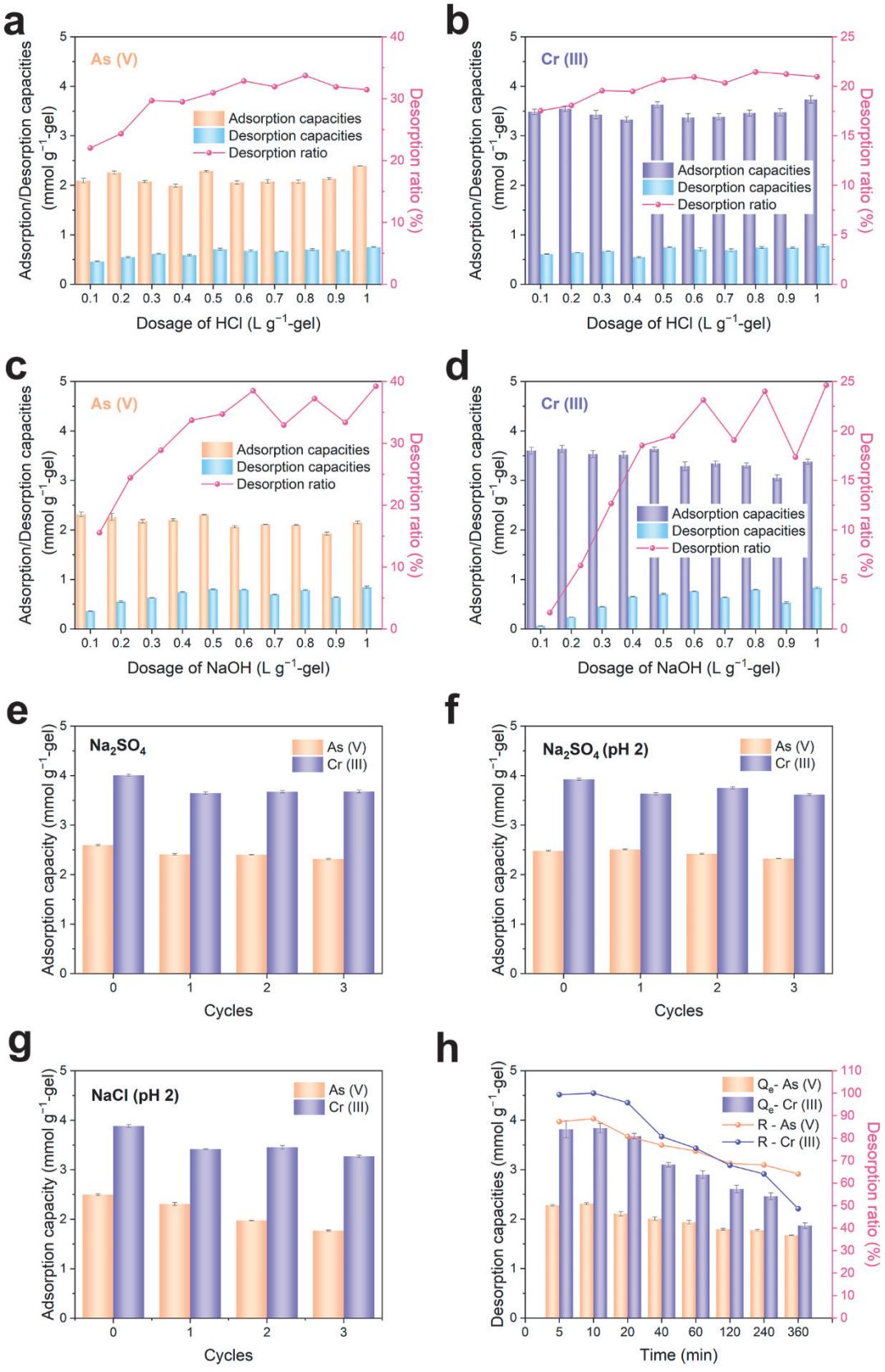

Fig. 4.12. Effect of dosage of desorbing agent (HCl) on the desorption of (a) As and

(b) Cr using AMPS(Na) gel; Effect of dosage of desorbing agent (NaOH) on the desorption of (a) As and (b) Cr using AMPS(Na) gel; Regeneration performance of the AMPS(Na) gel with desorbing agent (c) Na_2SO_4, (d) Na_2SO_4 (pH 2), and (e) NaCl (pH 2); (f) Desorption capacities and ratios over time based on AMPS(Na) gel when using Na_2SO_4 (pH 2) as a desorbing agent.

4.3.10 Adsorption mechanism

To analyse the mechanism of As (V) and Cr (III) adsorption onto the AMPS(Na) gel, FTIR spectra were recorded before and after adsorption (**Fig. 4.13**a). The absorption bands at 1175, 1040, and 620 cm^{-1} were observed and attributed to the sulfonyl hydroxide group in the AMPS(Na) gel spectra before and after adsorption.[27] The apparent intensity appearance of a wide peak at 3678–2542 cm^{-1} could be explained by an increase of arsenate hydroxyl after adsorption.[52] In addition, a peak at 810 cm^{-1} appeared after adsorption, which could be attributed to the metal-O-metal binding As-O-Cr,[53] indicating the successful removal of As (V) and Cr (III).

Fig. 4.13b shows the wide spectra of As (V) and Cr (III) adsorbed on the AMPS(Na) gel. One peak at 45.6 eV was attributed to As (V),[18] and two peaks at 577.8 and 587.3 eV were attributed to Cr $2p_{3/2}$ and Cr $2p_{1/2}$ of Cr (III), respectively (as shown in **Figs. 4.13**c-d). Compared to the original electronic binding energy of Cr (III) (at 576.2 and 585.7 eV) according to a previous study,[54] the peak of Cr (III) after adsorption by the AMPS(Na) gel showed a horizontal shift. This is because the appearance of coordination bonds caused by the interaction of newly formed complex ions between As (V) and Cr (III) enhanced the electron binding ability of Cr (III), thereby increasing its electronic binding energy. The above results suggest that As (V) and Cr (III) were adsorbed successfully on the surface of the AMPS(Na) gel without any oxidation–reduction reactions.

Based on the above results, it can be concluded that the adsorption of the

AMPS(Na) gel is a highly efficient simultaneous adsorption process via an ion-exchange method with positively charged complex ions consisting of As and Cr. Complex ions undergo different chemical changes under different physicochemical conditions, thereby affecting the gel adsorption capacity. Meanwhile, the adsorption mechanism of the AMPS(Na) gel was analysed using various adsorption models, such as adsorption isotherms and kinetic models. The results obtained were as follows:

Formation of complex ions: As (V) and Cr (III) formed positively charged complex ions under strongly acidic conditions, which were affected by the solution pH and could exist in different states with changes in pH, as shown in equations (4.3)-(4.11).

$$H_2AsO_4^- + [Cr(H_2O)_3]^{3+} \rightleftharpoons [Cr(H_2O)_2(H_2AsO_4)]^{2+} + H_2O \quad (4.3)$$

$$2H_2AsO_4^- + [Cr(H_2O)_3]^{3+} \rightleftharpoons [Cr(H_2O)(H_2AsO_4)_2]^{+} + 2H_2O \quad (4.4)$$

$$HAsO_4^{2-} + [Cr(H_2O)_3]^{3+} \rightleftharpoons [Cr(H_2O)_2(HAsO_4)]^{+} + 2H_2O \quad (4.5)$$

$$OH^- + [Cr(H_2O)_3]^{3+} \rightleftharpoons [Cr(H_2O)_2(OH)]^{2+} + H_2O \quad (4.6)$$

$$2OH^- + [Cr(H_2O)_3]^{3+} \rightleftharpoons [Cr(H_2O)(OH)_2]^{+} + 2H_2O \quad (4.7)$$

$$3OH^- + [Cr(H_2O)_3]^{3+} \rightleftharpoons Cr(OH)_3 \quad (4.8)$$

$$2H_2AsO_4^- + [Cr(H_2O)_2(OH)]^{2+} \rightleftharpoons Cr(H_2AsO_4)(HAsO_4) + 3H_2O \quad (4.9)$$

$$HAsO_4^- + [Cr(H_2O)_2(OH)]^{2+} \rightleftharpoons CrAsO_4 + 3H_2O \quad (4.10)$$

$$Cr^{3+} + 4OH^- = [Cr(OH)_4]^- \quad (4.11)$$

Complex ions consisting of As (V) and Cr (III) were adsorbed in substantial quantities by exchange with the sodium ions inside the gel. Thus, both As and Cr were adsorbed onto the gel surface. Because the two adsorbates adsorbed by the AMPS(Na) gel had different adsorption rates, the adsorption process of the gel could be divided into two stages: the adsorption of complex ions and the adsorption of Cr (III) ions.

The gel has a high simultaneous adsorption efficiency for As and Cr because it can form complex ions, and the adsorption efficiency of complex ions is substantially higher than that of single ions. In addition, several metal cations other than Cr can form complex structures with As, allowing the gel to efficiently adsorb various heavy metal ions.

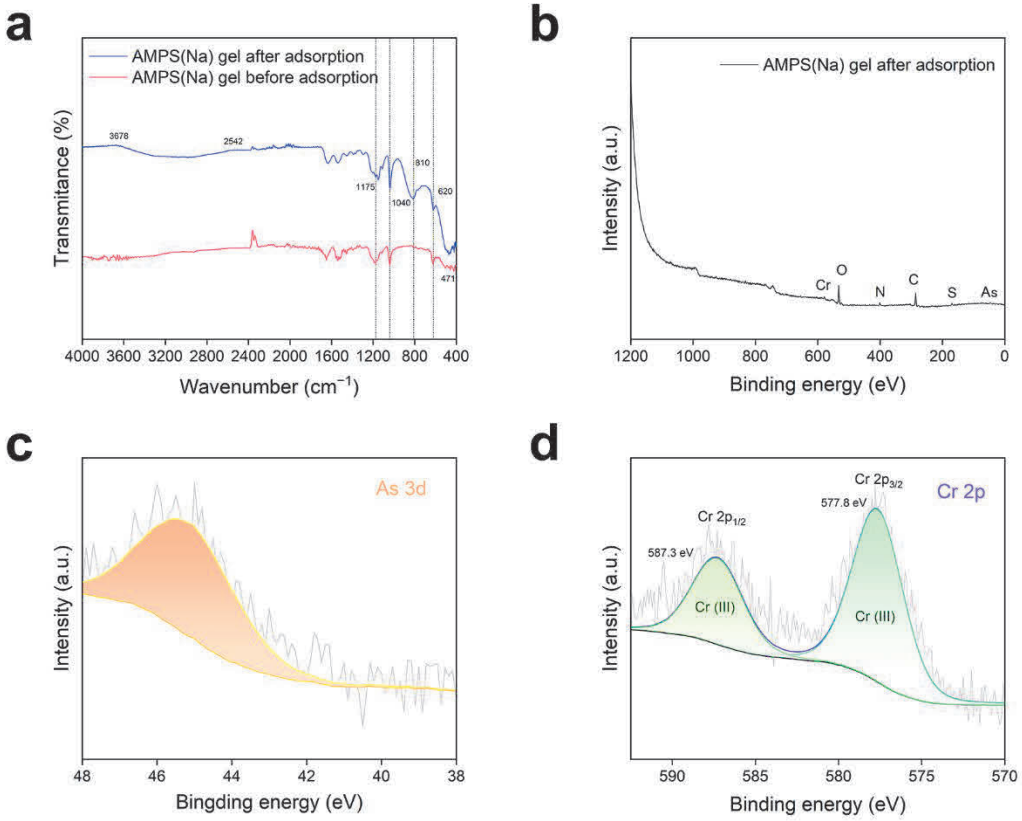

Fig. 4.13. (a) Fourier Transform Infrared spectra of AMPS(Na) gel before and after adsorption; (b) X-ray Photoelectron Spectroscopy wide spectra of AMPS(Na) gel after

adsorption; High-resolution (c) As 3d and (d) Cr 2p spectra of AMPS(Na) gel after adsorption.

4.4 Conclusion

In the present study, the existence of an As-Cr adsorbate positively charged complex was successfully demonstrated. The AMPS(NA) gel with excess sulfonyl hydroxide groups adsorbed As (V) and Cr (III) via the ion exchange method, in which a positively charged complex consisting of As (V) and Cr (III) was formed in a strongly acidic environment and exchanged with sodium ions on the AMPS(Na) gel surface. Furthermore, the effects of various physicochemical factors on the simultaneous adsorption of the gel were investigated. The AMPS(Na) gel, an anionic hydrogel that only adsorbs cations via ion exchange adsorption, can not only adsorb the cationic species, Cr (III), but also remove the anionic species, As (V). The adsorption capacities of the binary systems were substantially higher than those of the single systems. Although the As-Cr complex is moderately stable, its existing state changes under different pH environments, which affects the adsorption capacity of the gel. In addition, when co-existing with other heavy metal cations, the As–Cr adsorbate complex decreased because metal ions, such as Fe^{3+}, could also form complexes with As at higher concentrations and be adsorbed in large amounts, indicating that not only Cr but also several other metal ions could be adsorbed by combining into the complexes. The AMPS(Na) gel could maintain relatively good regeneration performance using Na_2SO_4 (pH 2).

4.5 References

(1) Hao, Y.; Ma, H.; Wang, Q.; Zhu, C.; He, A. Complexation behaviour and removal of organic-Cr(III) complexes from the environment: A review. *Ecotoxicol. Environ. Saf.* **2022**, *240*, 113676.

(2) Li, S.; Xu, H.; Wang, L.; Ji, L.; Li, X.; Qu, Z.; Yan, N. Dual-functional Sites for Selective Adsorption of Mercury and Arsenic ions in $[SnS_4]^{4-}$/MgFe-LDH from Wastewater. *J. Hazard. Mater.* **2021**, *403*, 123940.

(3) Song, L.; Feng, Y.; Zhu, C.; Liu, F.; Li, A. Enhanced synergistic removal of Cr(VI) and Cd(II) with bi-functional biomass-based composites. *J. Hazard. Mater.* **2020**, *388*, 121776.

(4) Li, Z.; Wang, L.; Meng, J.; Liu, X.; Xu, J.; Wang, F.; Brookes, P. Zeolite-supported nanoscale zero-valent iron: New findings on simultaneous adsorption of Cd(II), Pb(II), and As(III) in aqueous solution and soil. *J. Hazard. Mater.* **2018**, *344*, 1-11.

(5) Li, Y.; Qi, X.; Li, G.; Wang, H. Efficient removal of arsenic from copper smelting wastewater via a synergy of steel-making slag and $KMnO_4$. *J. Clean. Prod.* **2021**, *287*.

(6) Silva, R. d. A.; Secco, M. P.; Menezes, J. C. S. d. S.; Schneider, I. A. H.; Lermen, R. T. Reduction of High-Chromium-Containing Wastewater in the Leaching of Pyritic Waste Rocks from Coal Mines. *Sustainability* **2022**, *14* (19), 11814.

(7) Ministry of the Environment Government of Japan (JCN1000012110001) Website; https://www.env.go.jp/press/110052.html.

(8) Liu, G.; Zhang, X.; Talley, J. W.; Neal, C. R.; Wang, H. Effect of NOM on arsenic adsorption by TiO_2 in simulated As(III)-contaminated raw waters. *Water Res.* **2008**, *42* (8-9), 2309-2319.

(9) Tang, W. W.; Zeng, G. M.; Gong, J. L.; Liang, J.; Xu, P.; Zhang, C.; Huang, B. B. Impact of humic/fulvic acid on the removal of heavy metals from aqueous solutions using nanomaterials: a review. *Sci. Total Environ.* **2014**, *468-469*, 1014-1027.

(10) Wang, X. S.; Chen, L. F.; Li, F. Y.; Chen, K. L.; Wan, W. Y.; Tang, Y. J. Removal of Cr (VI) with wheat-residue derived black carbon: reaction mechanism and adsorption performance. *J Hazard. Mater.* **2010**, *175* (1-3), 816-822.

(11) Dong, X.; Ma, L. Q.; Gress, J.; Harris, W.; Li, Y. Enhanced Cr(VI) reduction and As(III) oxidation in ice phase: important role of dissolved organic matter from biochar. *J. Hazard. Mater.* **2014**, *267*, 62-70.

(12) Deng, Y.; Tang, L.; Zeng, G.; Zhu, Z.; Yan, M.; Zhou, Y.; Wang, J.; Liu, Y.; Wang, J. Insight into highly efficient simultaneous photocatalytic removal of Cr(VI) and 2,4-diclorophenol under visible light irradiation by phosphorus doped porous ultrathin g-C_3N_4 nanosheets from aqueous media: Performance and reaction mechanism. *Appl. Catal. B: Environ.* **2017**, *203*, 343-354.

(13) Li, C.; Chen, G.; Sun, J.; Rao, J.; Han, Z.; Hu, Y.; Xing, W.; Zhang, C. Doping effect of phosphate in Bi_2WO_6 and universal improved photocatalytic activity for removing various pollutants in water. *Appl. Catal. B: Environ.* **2016**, *188*, 39-47.

(14) Luo, S.; Qin, F.; Ming, Y.; Zhao, H.; Liu, Y.; Chen, R. Fabrication uniform hollow Bi_2S_3 nanospheres via Kirkendall effect for photocatalytic reduction of Cr(VI) in electroplating industry wastewater. *J. Hazard. Mater.* **2017**, *340*, 253-262.

(15) Tan, P.; Sun, J.; Hu, Y.; Fang, Z.; Bi, Q.; Chen, Y.; Cheng, J. Adsorption of Cu^{2+}, Cd^{2+} and Ni^{2+} from aqueous single metal solutions on graphene oxide membranes. *J. Hazard. Mater.* **2015**, *297*, 251-

260.
(16) Wang, T.; Zhang, L.; Li, C.; Yang, W.; Song, T.; Tang, C.; Meng, Y.; Dai, S.; Wang, H.; Chai, L.; et al. Synthesis of Core-Shell Magnetic Fe_3O_4@poly(m-Phenylenediamine) Particles for Chromium Reduction and Adsorption. *Environ. Sci. Technol.* **2015**, *49* (9), 5654-5662.
(17) Ying, Y.; Liu, Y.; Wang, X.; Mao, Y.; Cao, W.; Hu, P.; Peng, X. Two-dimensional titanium carbide for efficiently reductive removal of highly toxic chromium(VI) from water. *ACS Appl. Mater. Interfaces* **2015**, *7* (3), 1795-1803.
(1) Sherlala, A. I. A.; Raman, A. A. A.; Bello, M. M.; Buthiyappan, A. Adsorption of arsenic using chitosan magnetic graphene oxide nanocomposite. *J. Environ. Manage.* **2019**, *246*, 547-556. DOI: 10.1016/j.jenvman.2019.05.117 From NLM Medline.
(2) Mozaffari Majd, M.; Kordzadeh-Kermani, V.; Ghalandari, V.; Askari, A.; Sillanpaa, M. Adsorption isotherm models: A comprehensive and systematic review (2010-2020). *Sci. Total Environ.* **2022**, *812*, 151334. DOI: 10.1016/j.scitotenv.2021.151334 From NLM Medline.
(3) Simonin, J.-P. On the comparison of pseudo-first order and pseudo-second order rate laws in the modeling of adsorption kinetics. *Chem. Eng. J.* **2016**, *300*, 254-263. DOI: 10.1016/j.cej.2016.04.079.
(20) Uddin, M. K. A review on the adsorption of heavy metals by clay minerals, with special focus on the past decade. *Chem. Eng. J.* **2017**, *308*, 438-462.
(21) Liu, J.; Ge, X.; Ye, X.; Wang, G.; Zhang, H.; Zhou, H.; Zhang, Y.; Zhao, H. 3D graphene/δ-MnO_2 aerogels for highly efficient and reversible removal of heavy metal ions. *J. Mater. Chem. A* **2016**, *4* (5), 1970-1979.
(22) Huang, R.; He, L.; Zhang, T.; Li, D.; Tang, P.; Feng, Y. Novel Carbon Paper@Magnesium Silicate Composite Porous Films: Design, Fabrication, and Adsorption Behavior for Heavy Metal Ions in Aqueous Solution. *ACS Appl. Mater. Interfaces* **2018**, *10* (26), 22776-22785.
(23) Xu, X.; Zhu, D.; Wang, X.; Deng, L.; Fan, X.; Ding, Z.; Zhang, A.; Xue, G.; Liu, Y.; Xuan, W.; et al. Transformation of polyvinyl chloride (PVC) into a versatile and efficient adsorbent of Cu(II) cations and Cr(VI) anions through hydrothermal treatment and sulfonation. *J. Hazard. Mater.* **2022**, *423* (Pt A), 126973.
(24) Liu, J.; Wu, P.; Li, S.; Chen, M.; Cai, W.; Zou, D.; Zhu, N.; Dang, Z. Synergistic deep removal of As(III) and Cd(II) by a calcined multifunctional MgZnFe-CO_3 layered double hydroxide: Photooxidation, precipitation and adsorption. *Chemosphere* **2019**, *225*, 115-125.
(25) Zhou, Y.; Liu, Z.; Bo, A.; Tana, T.; Liu, X.; Zhao, F.; Sarina, S.; Jia, M.; Yang, C.; Gu, Y.; et al. Simultaneous removal of cationic and anionic heavy metal contaminants from electroplating effluent by hydrotalcite adsorbent with disulfide (S^{2-}) intercalation. *J. Hazard. Mater.* **2020**, *382*, 121111.
(26) Lin, S.-T.; Tran, H. N.; Chao, H.-P.; Lee, J.-F. Layered double hydroxides intercalated with sulfur-containing organic solutes for efficient removal of cationic and oxyanionic metal ions. *Appl. Clay Sci.* **2018**, *162*, 443-453.
(27) Badsha, M. A. H.; Lo, I. M. C. An innovative pH-independent magnetically separable hydrogel for the removal of Cu(II) and Ni(II) ions from electroplating wastewater. *J. Hazard. Mater.* **2020**, *381*, 121000.
(28) Ding, W.; Wan, X.; Zheng, H.; Wu, Y.; Muhammad, S. Sulfite-assisted oxidation/adsorption coupled with a TiO_2 supported CuO composite for rapid arsenic removal: Performance and mechanistic studies. *J. Hazard. Mater.* **2021**, *413*, 125449.
(29) Zhao, Z.; An, H.; Lin, J.; Feng, M.; Murugadoss, V.; Ding, T.; Liu, H.; Shao, Q.; Mai, X.; Wang,

N.; et al. Progress on the Photocatalytic Reduction Removal of Chromium Contamination. *Chem. Rec.* **2019**, *19* (5), 873-882.
(30) Peng, H.; Guo, J. Removal of chromium from wastewater by membrane filtration, chemical precipitation, ion exchange, adsorption electrocoagulation, electrochemical reduction, electrodialysis, electrodeionization, photocatalysis and nanotechnology: a review. *Environ. Chem. Lett.* **2020**, *18* (6), 2055-2068.
(31) Chen, Y.; Qian, Y.; Ma, J.; Mao, M.; Qian, L.; An, D. New insights into the cooperative adsorption behavior of Cr(VI) and humic acid in water by powdered activated carbon. *Sci. Total Environ.* **2022**, *817*, 153081.
(32) Li, M.; Kuang, S.; Kang, Y.; Ma, H.; Dong, J.; Guo, Z. Recent advances in application of iron-manganese oxide nanomaterials for removal of heavy metals in the aquatic environment. *Sci. Total Environ.* **2022**, *819*, 153157.
(33) Zhang, S.-H.; Wu, M.-F.; Tang, T.-T.; Xing, Q.-J.; Peng, C.-Q.; Li, F.; Liu, H.; Luo, X.-B.; Zou, J.-P.; Min, X.-B.; et al. Mechanism investigation of anoxic Cr(VI) removal by nano zero-valent iron based on XPS analysis in time scale. *Chem. Eng. J.* **2018**, *335*, 945-953.
(34) Zare, E. N.; Motahari, A.; Sillanpaa, M. Nanoadsorbents based on conducting polymer nanocomposites with main focus on polyaniline and its derivatives for removal of heavy metal ions/dyes: A review. *Environ. Res.* **2018**, *162*, 173-195.
(35) Sadeghi, M. M.; Rad, A. S.; Ardjmand, M.; Mirabi, A. Preparation of magnetic nanocomposite based on polyaniline/Fe_3O_4 towards removal of lead (II) ions from real samples. *Synth. Met.* **2018**, *245*, 1-9.
(36) Kumar, R.; Barakat, M. A.; Taleb, M. A.; Seliem, M. K. A recyclable multifunctional graphene oxide/SiO_2@polyaniline microspheres composite for Cu(II) and Cr(VI) decontamination from wastewater. *J. Clean. Prod.* **2020**, *268*.
(37) Thakur, S.; Sharma, B.; Verma, A.; Chaudhary, J.; Tamulevicius, S.; Thakur, V. K. Recent progress in sodium alginate based sustainable hydrogels for environmental applications. *J. Clean. Prod.* **2018**, *198*, 143-159.
(38) Ren, H.; Gao, Z.; Wu, D.; Jiang, J.; Sun, Y.; Luo, C. Efficient Pb(II) removal using sodium alginate-carboxymethyl cellulose gel beads: Preparation, characterization, and adsorption mechanism. *Carbohydr. Polym.* **2016**, *137*, 402-409.
(39) Song, Y.; Gotoh, T.; Nakai, S. Hexavalent Chromium Removal by an Ascorbic Acid Functionalized Polymer Hydrogel Adsorbent: the Effect of Physicochemical Factors. *ACS Appl. Polym. Mater.* **2023**, *5* (3), 2105-2112.
(40) Song, Y.; Gotoh, T.; Nakai, S. Synthesis of Oxidant Functionalised Cationic Polymer Hydrogel for Enhanced Removal of Arsenic (III). *Gels* **2021**, *7* (4), 197.
(41) Wan, J.; Chen, L.; Li, Q.; Ye, Y.; Feng, X.; Zhou, A.; Long, X.; Xia, D.; Zhang, T. C. A novel hydrogel for highly efficient adsorption of Cu(II): synthesis, characterization, and mechanisms. *Environ. Sci. Pollut. Res.* **2020**, *27* (21), 26621-26630.
(42) Sherlala, A. I. A.; Raman, A. A. A.; Bello, M. M.; Buthiyappan, A. Adsorption of arsenic using chitosan magnetic graphene oxide nanocomposite. *J. Environ. Manage.* **2019**, *246*, 547-556.
(43) Mozaffari Majd, M.; Kordzadeh-Kermani, V.; Ghalandari, V.; Askari, A.; Sillanpaa, M. Adsorption isotherm models: A comprehensive and systematic review (2010-2020). *Sci. Total Environ.* **2022**, *812*, 151334.

(44) Simonin, J.-P. On the comparison of pseudo-first order and pseudo-second order rate laws in the modeling of adsorption kinetics. *Chem. Eng. J.* **2016**, *300*, 254-263.
(45) Liu, K.; Li, F.; Cui, J.; Yang, S.; Fang, L. Simultaneous removal of Cd(II) and As(III) by graphene-like biochar-supported zero-valent iron from irrigation waters under aerobic conditions: Synergistic effects and mechanisms. *J. Hazard. Mater.* **2020**, *395*, 122623.
(46) Yang, S.; Li, Q.; Chen, L.; Chen, Z.; Hu, B.; Wang, H.; Wang, X. Synergistic removal and reduction of U(VI) and Cr(VI) by Fe_3S_4 micro-crystal. *Chem. Eng. J.* **2020**, *385*.
(47) Yue, X. H.; Zhang, F. S.; Zhang, C. C.; Qian, P. Upcycling of blending waste plastics as zwitterionic hydrogel for simultaneous removal of cationic and anionic heavy metals from aqueous system. *J. Hazard. Mater.* **2022**, *432*, 128746.
(48) Luo, M.; Lin, H.; He, Y.; Li, B.; Dong, Y.; Wang, L. Efficient simultaneous removal of cadmium and arsenic in aqueous solution by titanium-modified ultrasonic biochar. *Bioresour. Technol.* **2019**, *284*, 333-339.
(49) Hamoud, M. A.; Abo-Zahra, S. F.; Attia, M. A.; Someda, H. H.; Mahmoud, M. R. Efficient adsorption of cesium cations and chromate anions by one-step process using surfactant-modified zeolite. *Environ. Sci. Pollut. Res.* **2023**, *30* (18), 53140-53156.
(50) Yue, X.; Liu, W.; Chen, Z.; Lin, Z. Simultaneous removal of Cu(II) and Cr(VI) by Mg-Al-Cl layered double hydroxide and mechanism insight. *J. Environ. Sci.* **2017**, *53*, 16-26.
(51) Chen, F.; Hong, M.; You, W.; Li, C.; Yu, Y. Simultaneous efficient adsorption of Pb^{2+} and MnO_4^- ions by MCM-41 functionalized with amine and nitrilotriacetic acid anhydride. *Appl. Surf. Sci.* **2015**, *357*, 856-865.
(52) Li, C.; Yan, Y.; Zhang, Q.; Zhang, Z.; Huang, L.; Zhang, J.; Xiong, Y.; Tan, S. Adsorption of Cd^{2+} and Ni^{2+} from Aqueous Single-Metal Solutions on Graphene Oxide-Chitosan-Poly(vinyl alcohol) Hydrogels. *Langmuir* **2019**, *35* (13), 4481-4490.
(53) Pavithra, S.; Thandapani, G.; S, S.; P, N. S.; Alkhamis, H. H.; Alrefaei, A. F.; Almutairi, M. H. Batch adsorption studies on surface tailored chitosan/orange peel hydrogel composite for the removal of Cr(VI) and Cu(II) ions from synthetic wastewater. *Chemosphere* **2021**, *271*, 129415.
(54) Wang, Z.; Wang, Y.; Cao, S.; Liu, S.; Chen, Z.; Chen, J.; Chen, Y.; Fu, J. Fabrication of core@shell structural Fe-Fe_2O_3@PHCP nanochains with high saturation magnetization and abundant amino groups for hexavalent chromium adsorption and reduction. *J. Hazard. Mater.* **2020**, *384*, 121483.

Chapter 5: Summary

5.1 Introduction

This chapter summarizes conclusions and novelty of this work and outlook.

5.2 Conclusions

This thesis is dedicated to the efficient elimination and adsorption of heavy metal ions in aqueous solutions, with a focus on polymer hydrogels as the chosen adsorbent materials. A variety of functionalized polymer hydrogels, including DMAPAAQ hydrogel, DA/DQ copolymer hydrogel, DA/DQ/VC hydrogel, and AMPS(Na) hydrogel, were meticulously developed through chemical modification. Comprehensive studies were conducted to evaluate the structural and stability properties of these hydrogel materials, emphasizing their chemical composition and behavior in solutions. Targeting arsenic and chromium as the principal heavy metal ions, this research extensively examined the adsorptive performance of the hydrogels. The dynamic interactions between these materials and the heavy metal ions were thoroughly analyzed, incorporating findings from experiments on coexistent ion competition, the influence of solution pH, adsorption kinetics, isotherm studies, and thermodynamic aspects. These were complemented with detailed material characterizations using FTIR and XPS spectroscopy, both pre- and post-adsorption of heavy metal ions. The primary conclusions of this thesis are outlined as follows:

(1) **Efficient removal of As**: DMAPAAQ hydrogels, crafted through free radical polymerization, were further enhanced by oxidant-based modifications, resulting in the creation of D-Mn and D-Cr gels. Post-modification, the hydrogels saw about 73.7% of their adsorption sites imbued with oxidative functional groups. These D-Mn and D-Cr gels exhibit a robust, highly cross-linked network structure, showcasing superior

adsorption efficacy for As (III). At 298 K, the gels' theoretical maximum adsorption capacities for As (III) reach 163 mg g^{-1} for D-Mn and 263 mg g^{-1} for D-Cr. In both acidic and neutral water environments, the gels consistently achieve an As (III) removal efficiency exceeding 85%. The kinetics and isotherm data of As (III) adsorption onto these gels align precisely with the Pseudo-second Order and Langmuir models, respectively, signifying the occurrence of chemical interactions within the adsorption process.

(2) **Efficient removal of Cr**: The DA/DQ copolymer hydrogel, synthesized through free radical polymerization, was effectively functionalized using the reducing agent ascorbic acid, culminating in the formation of the DA/DQ/VC gel. This gel, rich in amino groups and enhanced with a functional reductant, successfully adsorbed Cr (VI) through ion exchange and electrostatic attraction, and then efficiently removed the resulting Cr (III), reduced by ascorbic acid, via chelation and formation of insoluble salts. The study further delved into the influence of various physicochemical factors in aqueous environments on the gel's capacity to remove Cr (VI). Exhibiting substantial chemical stability, particularly in acidic conditions, the gel's diverse adsorption mechanisms played a crucial role. While both DA/DQ and DA/DQ/VC gels demonstrated reduced effectiveness in removing Cr (VI) at pH levels equal to or greater than 11, they maintained a high rate of Cr removal within a pH range of 3 to 6. Notably, the DA/DQ/VC gel outperformed the DA/DQ gel in terms of Cr removal efficiency, a testament to its varied and effective removal methods. Additionally, the presence of co-existing anions did not significantly impede its enhanced removal capabilities.

(3) **Simultaneous removal of As and Cr**: The formation of a positively charged As-Cr adsorbate complex was effectively demonstrated. The AMPS(Na) gel, enriched with surplus sulfonyl hydroxide groups, demonstrated its proficiency in adsorbing As (V) and Cr (III) through the ion exchange method. This process involved the formation of a positively charged complex comprising As (V) and Cr (III) in a highly acidic

environment, which subsequently exchanged with sodium ions on the AMPS(Na) gel surface. The study also explored the impact of various physicochemical factors on the gel's simultaneous adsorption capabilities. Notably, the AMPS(Na) gel, an anionic hydrogel traditionally limited to adsorbing cations via ion exchange, exhibited the unique ability to adsorb the cationic species Cr (III) as well as remove the anionic species As (V). This adaptability resulted in significantly higher adsorption capacities in binary systems compared to single systems. The stability of the As-Cr complex, although moderate, varied with different pH environments, influencing the gel's adsorption efficiency. Furthermore, the presence of other heavy metal cations, like Fe^{3+}, revealed a decrease in the As-Cr adsorbate complex. These metal ions could form complexes with As, especially at higher concentrations, and be substantially adsorbed, indicating the gel's potential to adsorb not just Cr but also various other metal ions through complex formation. Remarkably, the AMPS(Na) gel demonstrated commendable regeneration performance with Na_2SO_4 (pH 2), underlining its practical application in environmental remediation.

5.3 Novelty

The primary objective of this paper is to harness the unique properties of adsorbates by employing polymer hydrogels as adsorbent materials, thereby facilitating the effective removal of these adsorbates. The paper delves into the dynamics between hydrogels and heavy metal ions, contributing theoretical insights for the deployment of polymer hydrogel adsorbents in treating heavy metal-laden wastewater. Key innovations of this research include:

(1) Polymer hydrogels, enriched with diverse active functional groups, demonstrate superior adsorption capabilities for heavy metals, while also offering the benefit of being cost-effective.

(2) The chemical modification of polymer hydrogels results in a significant

increase in active functional groups, thereby boosting the adsorption efficiency for various adsorbates. Moreover, the hydrogels' intricate three-dimensional network structure securely locks these functional groups inside, minimizing the potential for leakage.

(3) The research meticulously examines the adsorption behaviors of heavy metal ions in both single and dual-component systems, particularly focusing on the co-presence of arsenic and chromium. Through a combination of material characterization methods, the study elucidates the intricate mechanisms of interaction between the hydrogels' active functional groups and the heavy metal ions. This comprehensive analysis provides a solid theoretical foundation for future research in the application of polymer materials for heavy metal adsorption.

5.4 Outlook

In this thesis, a variety of polymer hydrogels have been developed, and their interactions with heavy metal ions have been systematically explored. The findings suggest that polymer hydrogels have considerable potential for heavy metal adsorption, but certain areas necessitate further research:

(1) The study demonstrates that after adsorption, heavy metal ions are distributed quite uniformly throughout the hydrogels. However, understanding the specific diffusion patterns of these ions within the hydrogel structure is an aspect that warrants additional investigation. Future studies could merge experimental data, diffusion models, and characterization methodologies to predict and substantiate the diffusion routes of heavy metal ions in the hydrogels, offering vital theoretical backing for their practical application and design.

(2) Polymer hydrogels are distinguished by high water content, substantial swelling properties, and robust mechanical strength, showcasing their efficiency in heavy metal adsorption. Future research directions could include exploring the

potential of polymer hydrogels in removing organic pollutants from water, such as dyes and antibiotics, thus expanding the range of applications for these hydrogel materials.

(3) The current research reveals that under specific conditions, pentavalent arsenic and trivalent chromium can form a positively charged complex ion, which anionic hydrogels can readily adsorb. Nevertheless, the exact mechanism behind the formation of this As-Cr complex ion remains unclear. Additionally, whether other heavy metal ions can form similar complexes is a crucial area for further exploration. Subsequent research could delve into the foundational principles of As-Cr complex ion formation and develop models to elucidate this mechanism.

List of Publication

(1) Song, Y.; Gotoh, T.; Nakai, S. Hexavalent Chromium Removal by an Ascorbic Acid Functionalized Polymer Hydrogel Adsorbent: the Effect of Physicochemical Factors. *ACS Appl. Polym. Mater.* **2023**, *5* (3), 2105-2112.

(2) Song, Y.; Gotoh, T.; Nakai, S. Synthesis of Oxidant Functionalised Cationic Polymer Hydrogel for Enhanced Removal of Arsenic (III). *Gels* **2021**, *7* (4), 197.

(3) Song, Y.; Gotoh, T.; Nakai, S. Simultaneous Removal of Anionic and Cationic Species by Ionic Hydrogels: Adsorption Mechanism of Arsenic (V) and Chromium (III) to Positively Charged Complex in a Highly Acidic Aqueous Environment. *ACS ES&T Water* (Under Review)

List of Presentation in International/Domestic Conferences

1. 宋　玉，後藤　健彦，中井　智司，酸化剤の担持が高分子吸着剤のヒ素(III)吸着に与える影響，環境科学会 2020 年会，2020 年 9 月 19 日～9 月 20 日，オンライン開催。
2. 宋　玉，後藤　健彦，中井　智司，還元剤の担持が高分子ゲル吸着剤のクロム(VI)吸着に与える影響，環境科学会 2021 年会，2021 年 9 月 10 日～9 月 11 日，オンライン開催。
3. 宋　玉，後藤　健彦，中井　智司，還元剤の担持が高分子ゲル吸着剤のクロム吸着に与える影響，分離技術会年会 2021，2021 年 11 月 4 日～11 月 5 日，オンライン開催。
4. 宋　玉，後藤　健彦，末永 俊和，中井　智司，還元剤のアスコルビン酸を担持した DMAPAA/DMAPAAQ ゲルの作製およびクロム(VI)除去の特性，化学工学会第 87 年会，2022 年 3 月 16 日～3 月 18 日，神戸大学，兵庫県，日本。
5. 宋　玉，後藤　健彦，中井　智司，末永 俊和，イオン性ゲルによる重金属ヒ素(V)とクロム(III)の効率的な同時除去特性，第 35 回日本吸着学会研究発表会，2022 年 11 月 10 日～11 月 11 日，石川県立音楽堂交流ホール，石川県，日本。
6. Yu Song, Takehiko Gotoh, Satoshi, Nakai. “Simultaneous Removal Efficiency of Arsenic (V) and Chromium (III) to a Positively Charged Complex by Ionic Hydrogels”. The 13th SPSJ International Polymer Conference (IPC2023), July 18th-21st **2023**, Sapporo Convention Center, Hokkaido, Japan

7. Yu Song, Takehiko Gotoh, Satoshi, Nakai. “Simultaneous Removal of Anionic and Cationic Species by Ionic Hydrogels: Adsorption Mechanism of Arsenic (V) and Chromium (III) Combining to the Positive-charged Complex at Strong Acidic Aqueous Environment”. The 9th International Conference on Low Carbon Asia (ICLCA), October 16th-19th **2023**, Okayama Convention Centre, Okayama, Japan

Awards and Honors

1. 中国地区化学工学懇話会学生奨励賞　河村祐治記念賞（2021 年 3 月）
2. 広島大学大学院リサーチフェローシップ奨学金（2021 年 4 月）
3. 先進理工系科学研究科学生表彰（2022 年 3 月）

Acknowledgements

Since embarking on my journey as a master's student at Hiroshima University, approximately five years have elapsed, a period marked by perseverance through life's trials and relentless pursuit of research excellence. Despite intermittent moments of struggle and hardship, this period has predominantly been one of profound learning and personal development.

Foremost, my heartfelt gratitude goes to my parents. The decision to advance my studies in Japan was carefully deliberated; however, it was the unwavering support and encouragement from my parents, both materially and emotionally, that fortified my resolve. Amidst the pandemic's three challenging years, despite my frequent yearnings to visit home, their consistent encouragement to prioritize my academics and research, coupled with their comfort during times of discouragement, have been my pillars of strength.

I extend special thanks to my tutor, Takehiko Gotoh. His extensive knowledge and diligent work ethic in the scientific realm have greatly enriched my learning experience. He stands as an exemplar of lifelong learning, guiding me through personal academic research and collaborative projects across disciplines, including medicine, applied chemistry, and agriculture. His amiable nature and thoughtful guidance have nurtured a profound tutor-student relationship.

My sincere appreciation also goes to Professor Satoshi Nakai. His acute academic acumen, stringent scientific methodology, and modest yet open-hearted demeanor have profoundly influenced me. His insightful guidance has been pivotal in both my research endeavors and personal growth, offering invaluable advice and support. Gratitude is also due to Associate Professor Takashi Iizawa, Associate Professor Shin-ichi Kihara, and Assistant Professor Toshiharu Suenaga for their unwavering encouragement, guidance.

I am thankful for the diverse research facilities and laboratory equipment

provided by Hiroshima University. The writing center's constructive feedback and guidance on my academic papers have been invaluable. I extend my heartfelt thanks to Professor Jianghong Shi, Dean of the School of Environmental Science and Engineering at Southern University of Science and Technology, for his invaluable support and guidance during my time there as a visiting student. Furthermore, I am deeply grateful to my friends form the research group of Prof. Shi, Hui Ge, Huanyu Tao, Xin Ji, Yunhe Wang, and Bin Li, for their assistance and mentorship in both academic and personal aspects of my life.

My appreciation extends to Akihiro Sasaya for his assistance with my initial admissions process and for imparting vital experimental techniques. I am grateful to Yoshiki Kimura, Risa Matsumoto, and Masahide Sano for their invaluable suggestions and support in scientific research, as well as their guidance in experimental design. I also express gratitude to my fellow Chinese international students—Feng Wang, Junjie Zhu, Qichen Sun, Jin Huang, Zaichuan Zhang, and Yiyue Li—for their camaraderie and assistance in both daily life and academic pursuits. Lastly, I wish all the seniors who have graduated from our lab continued success and fulfillment in their future paths.

Yu Song

Hiroshima University

18/12/2023